IMPACT OF INJECTION WATER CHEMISTRY ON ZETA POTENTIAL OF CARBONATE ROCKS

BY

AHMED AMARA MUSA KASHA

A Thesis Presented to the

DEANSHIP OF GRADUATE STUDIES

KING FAHD UNIVERSITY OF PETROLEUM & MINERALS

DHAHRAN, SAUDI ARABIA

In Partial Fulfillment of the
Requirements for the Degree of

MASTER OF SCIENCE

In

PETROLEUM ENGINEERING

MAY 2014

KING FAHD UNIVERSITY OF PETROLEUM & MINERALS

DHAHRAN- 31261, SAUDI ARABIA

DEANSHIP OF GRADUATE STUDIES

This thesis, written by **AHMED AMARA MUSA KASHA**, under the direction his thesis advisor and approved by his thesis committee, has been presented and accepted by the Dean of Graduate Studies, in partial fulfillment of the requirements for the degree of **MASTER OF SCIENCE IN PETROLEUM ENGINEERING**.

Dr. Hasan S. Al-Hashim
(Advisor)

Dr. Abdullah S. Sultan
Department Chairman

Dr. Wael A. Abdallah
(Co-Advisor)

Dr. Salam A. Zummo
Dean of Graduate Studies

Dr. Sidqi A. Abu-Khamsin
(Member)

21/9/14
Date

Dr. Hasan Y. Al-Yousef
(Member)

Dr. Mohamed A. Mahmoud
(Member)

This work is dedicated to my family

ACKNOWLEDGMENTS

Glory and praise be to Allah the almighty, first and foremost, for every success I found, and knowledge been developed throughout this work.

Acknowledgement is due to King Fahd University of petroleum & minerals for the scholarship I have been given to complete my master degree in petroleum engineering.

My sincere gratitude goes to my thesis advisor, Dr. Hasan Salman Al-Hashim, for allowing me to join his research activities and for the trust he put on me, and for his professional guidance during the course of my thesis work. I would like to extend my thanks to all of my committee members for their valuable comments and contributions.

I would like to thank the department of petroleum engineering represented by the chairman, Dr. Abdullah Sultan, for allowing me to use the department's laboratories and equipment to perform my work. I would also like to thank to Dr. Abdullah Sultan for his valuable support during ordering of the consumables and materials for my thesis work through the Center for Petroleum & Minerals of the Research Institute.

I'm very grateful for Schlumberger Dhahran Carbonate Research Center (SDCR), represent by my thesis co-advisor Dr. Wael Abdullah. I would like to thank him for the supply of materials that I used in my study and for allowing me to use SDCR's equipment on my samples as well as his help and support during the thesis work. In SDCR, I'm quite thankful for Dr. Reza Taherian for his valuable comments and notes. I would like to express my special thanks to Dr. Bastian Sauerer for the precious time he spent with me on the

AFM machine and for the professional comments he made on my laboratory experiments and the review of results.

In KFUPM, I would like to thank Dr. Ahmet Dogan, professor at the Earth Science Department, for his help in preparing the calcite and dolomite chips which I used in my study. I would also like to thank Dr. Hassan Eltom who was very helpful in clarifying every geological aspect I needed. I would like to thank him also for his help in characterizing of the thin sections of my samples. My sincere thanks go to Mr. Abdalgafar Osman from the Chemistry Department at KFUPM for his help during preparation of the model oil and for Mr. Hatim Dafallah from the Center for Engineering and Research for the time he spent with me on the SEM and EDS machine.

TABLE OF CONTENTS

LIST OF TABLES

LIST OF FIGURES

LIST OF ABBREVIATIONS

AFM	:	Atomic Force Microscopy
AGSW	:	Arabian Gulf Sea Water
EDS	:	Energy Dispersed Spectroscopy
ELS	:	Electrophoretic Light Scattering
MEC	:	Middle East Carbonate
MO	:	Model Oil
PALS	:	Phase Analysis Light Scattering
PDIs	:	Potential Determining Ions
PPM	:	Parts Per Million
SEM	:	Scanning Electron Microscopy
SWCT	:	Single Well Chemical Tracer
TAN	:	Total Acid Number
TDS	:	Total Dissolved Solids
WBEOR	:	Water Based Enhanced Oil Recovery

ABSTRACT

Full Name : Ahmed Amara Musa Kasha

Thesis Title : Impact of Injection Water Chemistry on Zeta Potential of Carbonate Rocks

Major Field : Petroleum Engineering

Date of Degree : May 2014

Although wettability alteration is believed to be responsible for oil recovery during smart water flooding in carbonate oil reservoirs, the exact mechanisms behind altering the wettability is not fully understood.

The ultimate objective of the current study was to raise the level of understanding about the mechanisms by which adsorbed oil phase is released from carbonate surfaces during smart water flooding. Microscopic investigation was conducted on calcite and dolomite crystals in addition to a carbonate rock sample from a Middle East oil field (MEC) using zeta potential measurements coupled with Atomic Force Microscopy (AFM), Scanning Electron Microscopy (SEM) and Energy Dispersed Spectroscopy (EDS). Model oil made of stearic acid was used to represent oil phase and to prepare oil wet samples, and synthetically prepared aqueous brines with wide variety of ionic compositions were prepared to represent modified versions of AGSW (AGSW) which is the main source of water for injection in Middle East oil reservoirs. In deionized water and NaCL brine, calcite and MEC samples possessed negative surface charges due to the preferential dissolution of calcium ions from both samples' surfaces. In the dolomite, positive surface charges were found which are attributed to the high concentration of cations on the rock lattice.

Adsorption of negatively charged carboxylic materials on carbonates surfaces increased the magnitude of the original negative surface charges of calcite and MEC and decreased the magnitude of the original positive surface charges of the dolomite. Increasing the concentration of SO_4^{2-} ions increased the original negative surface charges of calcite and MEC and completely altered the surface charges of dolomite from positive to negative which indicates the high affinity of SO_4^{2-} ions to adsorb on carbonates surfaces. On the other hand, increasing the concentration of Ca^{2+} and Mg^{2+} ions increased the magnitude of positive surface charges of dolomite and altered the original negative surface charges of calcite and MEC. The individual effect of PDIs was suppressed by the presence of another PDI in the same brine as a result of the competition between these ions towards the carbonate surface. The magnitude of developed surface charges for all samples was higher in the original AGSW compared to 50% diluted AGSW due to the high concentration of PDIs in the undiluted AGSW. However, the efficiency of 50% diluted AGSW as wettability modifier, can be improved either by increasing the concentration of sulfate and magnesium, which will enhance the adsorption of SO_4^{2-}, or by using the 50% diluted AGSW after primary injection of original AGSW, and in this case, developed surface charges will be attributed to the induced surface dissolution rather than adsorption of PDIs from the injected water.

Based on the interpretation of zeta potential measurements, it is concluded that adsorbed oil phase can be released from carbonate surface by the reactions caused by the adsorbed PDIs from the injected water and/or microscopic dissolution of the carbonate rock surface on which oil phase is located, and by both mechanisms, wettability will be altered towards more water wet.

ملخص الرسالة

الاسم الكامل: أحمد عماره موسى كاشا

عنوان الرسالة: تأثير كيمياء مياه الحقن على جهد زيتا للصخور الكربونية

التخصص: هندسة البترول

تاريخ الدرجة العلمية: مايو 2014

على الرغم من أن تغيير التبلل الصخري يعتبر هو العامل الاساس المسؤول عن استخلاص الزيت من المكامن الكربونية خلال عمليات الغمر بالماء الذكي، إلا أن الآليات المسببة لتغير التبلل الصخري غير مفهومة بعد بصورة واضحة.

تهدف الدراسة الحالية الى زيادة المعرفة المتعلقة بآليات تحرير الزيت من على أسطح الصخور الكربونية وذلك بإجراء تجارب مجهرية لقياس الجهد الكهرو-حركي، أو ما يصطلح على تسميته بجهد زيتا، على بلورات الكالسايت والدولومايت إضافة الى عينة صخرية من أحد حقول النفط في الشرق الأوسط. لإضافة الى ذلك، تم مسح أسطح هذه العينات باستخدام مجهر القوة الذرية والمجهر الإلكتروني الى جانب تشتت الطاقة الطيفي لتحليل التركيب الأيوني لأسطح هذه العينات. تم تحضير زيت نموذجي لاستخدامه بدلاً عن الزيت الخام الطبيعي وذلك باستخدام حمض الإستياريك المذاب في التولوين. تم تحضير محاليل مائية تحتوي على تراكيز مختلفة من الايونات الفاعلة للجهد (الكالسيوم، الماغنيسيوم الكبريتات) الموجودة في مياه الخليج العربي والتي تعتبر المصدر الأساس لمياه الحقن في الشرق الأوسط. في المياه منزوعة الايونات ومحلول كلوريد الصوديوم وُجد أن بلورات الكالسايت والعينة الكربونية تحملان شحنات سطح سالبة ناتجة من تحلل ايونات الكالسيوم من أسطح هذه العينات، أما في بلورات الدولومايت فقد وُجد انها تحمل شحنات موجبة وهو ما يعزى الى التركيز العالي للأيونات الموجبة في هذه العينة. امتزاز حمض الاستياريك على سطح عينة الكالسايت والعينة الصخرية أدى الى زيادة الشحنات السالبة على أسطح هذه العينات، أما في عينة الدولومايت، فقد أدى ذلك الى تقليل الشحنات الموجبة الموجودة على السطح. أدت زيادة تركيز ايونات

الكالسيوم والماغنيسيوم الى زيادة الشحنات الموجبة في عينة الدولومايت فيما أدت الى تغيير شحنات السطح السالبة الموجودة على عينة الكالسايت والعينة الكربونية الي شحنات موجبة. في المقابل، أدت زيادة ايونات الكبريتات الى زيادة الشحنات السالبة على سطح عينة الكالسايت والعينة الصخرية فيما أدت الى تغيير شحنات السطح على عينة الدولومايت الموجبة الى سالبة. وجود هذه الأيونات الثلاث مجتمعة في نفس المحلول أدى الى تقليل الفعالية النسبية لكل أيون وهو ما يعزي الى التنافس بين هذه الأيونات على الأسطح الكربونية. عندما استخدمت مياه الخليج العربي المخففة بنسبة 50%، وجد أن شحنات السطح للعينات الثلاث اقل منها فيما لو استخدمت مياه الخليج العربي بدون تخفيف، وذلك نتيجة للتركيز العالي للأيونات الفاعلة للجهد في المياه غير المخففة. لزيادة كفاءة مياه الخليج العربي المخففة، يمكن زيادة تركيز أيوني الماغنيسيوم الكبريتات لزيادة امتزازهما على الأسطح الكربونية، أو باستخدام المياه المخففة بالتعاقب بعد استخدام مياه الخليج العربي غير المخففة، وفي هذه الحالة، يكون التغير في شحنات السطح ناتج عن تحلل الايونات من الاسطح الكربونية وليس نتيجة لامتزاز الايونات الفاعلة من مياه الحقن.

بناءً على تحليل قياسات جهد زيتا، فقد خلصت هذه الراسة الى أن عملية إزاحة الزيت الملتصق على الاسطح الكربونية تتم أما بواسطة التفاعلات الناتجة عن امتزاز الأيونات الفاعلة للجهد من مياه الحقن، أو عن طريق التحلل المجهري للأسطح الكربونية المحتوية على الزيت الملتصق، وفي كلتا الحاليتين يؤدي ذلك الى تغير التبلل الصخري من زيتي الى مائي التبلل.

CHAPTER 1

INTRODUCTION

1.1 Overview of the Water Based Enhanced Oil Recovery

Carbonate reservoirs are very heterogeneous in terms of mineralogy and petro-physical properties and they contain about 60% of the world's oil reserves. [1, 2] Due to this heterogeneity, oil recovery from carbonate reservoirs is very low compared to sandstone reservoirs with 30% being the world wide average oil recovery for carbonates so far. [3, 4]Capillary, viscous and gravity forces control the fluid flow during water flooding with capillary forces being the most crucial and dominant forces for defining the residual oil saturation. [5] In naturally fractured carbonate reservoirs displacement of oil by water is governed by spontaneous imbibition of water from fractures into the matrix blocks which is strongly related to the capillary forces and wettability nature of the reservoir. Most of the carbonate reservoirs are classified as mixed-wet or preferentially oil-wet. [6, 7] At such wettability, no spontaneous imbibition of water is expected, and due to which, most of the conventional water flooding projects in carbonate reservoirs were not successful and low oil recoveries were always recorded due to the high residual oil saturation retained by wettability and capillarity. [4, 8, 9]

Carbonate rocks are positively charged in high salinity formation water which has high concentration of cations. [10] The mixed-wet or preferentially oil-wet condition of carbonate rocks is caused by the adsorption of the negatively charged polar components in the crude oil on positively charged areas in the rock surface. [7] Thomas et al 1993 [11] mentioned that 80 – 84 % of the crude oils make carbonates oil-wet and it was experimentally verified that medium-to-long chain fatty acids and carboxylate polymers which are present in crude oils have strong affinity to adsorb on carbonate minerals due to availability of the carboxylic groups in these components which ionize and act similar to the carbonate anions of the mineral lattice. The carboxylate materials present in the crude oil are very important wetting parameter. [4] As the acid number of the crude oil increases, the oil-wetness increases .[12] However, it was found that structure and type of the carboxylic materials might be more important than concentrations of these materials in the crude oil. [6] Stability of the water film around the rock surface, which is bound between the solid/brine interface and brine/oil interface, will prevent adsorption of the active polar components from the crude oil on the rock surface and only the collapse of these stable films will alter the wettability. [13] Existence of stable water films in a range of 1 to 100 nm thickness depends on the presence of electrical double-layer repulsion that results from surface charges at the solid/water and water/oil interfaces being of the same sign. [14, 15] Stability of the water film has always been discussed in terms of the disjoining pressure [16] which is defined as the changes in energy per unit area as a function of the distance of two interfaces as they approach each other. In order to mobilize the retained oil by wettability and capillarity, capillary forces which are function of fluid-fluid and fluid-rock interactions

must be reduced. [5] Increasing water wetness of the rock and reducing the IFT will help in overcoming the forces that retain the oil. [8]

Recently, Water-Based Enhanced Oil Recovery (WBEOR) has been evolved as a promising mean of oil recovery by reducing the salinity and or changing the ionic composition of the injected water which was able to mobilize some of the residual oil. Historically, improving the quality of the injected water was mainly aimed to avoid corrosion, plugging or formation damage problems rather than improving the oil recovery. [17] During the last decade, water based enhanced oil recovery received considerable attention due to the positive results evolved out from different formats of laboratory studies on improving oil recovery from sandstone and carbonate reservoirs. Small scale field trials, mainly in producing wells, were conducted to evaluate the ability of this method in reducing the residual oil saturation. Some of these trials were conducted in sandstone reservoirs using log-inject-log and Single Well Chemical Tracer (SWCT) techniques to quantify the change in residual oil saturation. [18-21] The first ever field trial in carbonate was conducted in Saudi Arabia using SWCT. [22] Results from these small scale field trails confirmed that WBEOR is a very promising method that helps reducing the residual oil saturation and improving oil recovery. Despite all these positive results from laboratories and field trials, this mean of recovery has not been implemented in a large scale due to lack of understanding the exact mechanism behind the observed oil recovery.[14] Improved/Enhanced oil recovery by this method is controlled by crude oil/water/rock chemical interactions which can significantly influence the microscopic displacement efficiency and lead to desorption of crude oil components from the rock surface. The efficiency of this process is influenced by several critical parameters including ionic

composition of the injected brine, chemistry of crude oil, temperature, mineralogy of the rock surface and wetting state before injection. [7, 17] The recovery mechanism during smart water flooding is completely different for sandstones and carbonates. In sandstone, it is generally accepted that presence of clay in sandstone is very important for improving oil recovery during low salinity water flooding. [17, 23] Various recovery mechanisms have been proposed for sandstones, such as migration of fines, impact of alkaline flooding, multicomponent ion exchange, microscopically diverted flow and double layer expansion. [24] In carbonate reservoirs, some mechanisms are proposed such as wettability alteration as a result of interactions between potential determining ions (PDIs) present in the injected water with the rock surface and the adsorbed polar materials material (carboxylic acids, resins, asphaltene, etc.) or by alternating the wettability by optimizing the salinity and ionic strength of the injected water. Dissolution of rock minerals and dissolution of anhydrite present in the rock are also suggested as possible recovery mechanisms in carbonates. [5, 9, 12, 13, 16, 25] Zhang et al. [26] showed that PDIs (Ca^{2+}, Mg^{2+} and SO_4^{2-}) which are present in injected water from the North sea are able to influence surface charges of the chalk and alter the wettability of the rock and help displacing more oil. A chemical mechanism was suggested for the interplay between those ions. Sulfate from the injected water will adsorb on the positive sites of the chalk and will lower the positive surface charges, and due to less electrostatic repulsion, more calcium ions will adsorb on the chalk surface. Eventually, these ions will react with the adsorbed carboxylic materials of the crude oil on the rock and release some of them. At high temperature, magnesium ions can substitute calcium ions on the chalk surface as well as those linked to the carboxylic groups.

The effect of charges at oil/brine and rock/brine interfaces on wettability, which directly affects the oil recovery, can be studied using zeta potential technique whose value and sign can dictate the nature of the wettability. [12, 14]

Electrokinetic (zeta) potential measures the difference in electrical charge between the dense layer of ions surrounding the particle and the charge of the bulk of the suspended fluid surrounding the particles. [10, 16] It usually refers to the electric potential at the outer limit of the boundary layer, often called shear plane of slipping plane whose location in the electric double layer is difficult to be defined precisely. This makes zeta potential an ambiguous measure of the potential at the surface of the particle. [27, 28] Several methods are used to measure zeta potential, such as electrophoresis, electro-osmosis, streaming potential or sedimentation potential. [29] Mathematical models have also been used to predict and calculate the zeta potential by applying several assumption. [13] However, they are questionable when applied to describe extremely dynamic interfaces. [30]

1.2 Thesis Objective

It is commonly agreed that the chemistry of the injection water has significant impact on oil recovery from carbonate rocks as proved by different laboratory experiments. From most of the recently released studies in carbonates, three interrelated mechanisms have been proposed for the observed oil recovery. The first and the most favored mechanism is wettability alteration from oil wet towards more water wet as a result of interactions between the injected water, rock surface and adsorbed carboxylic materials which is mainly caused by the PDIs present in the injected water.

In order to understand the potential mechanisms for oil recovery by water-based enhanced oil recovery it is important to conduct a comprehensive study in microscopic level in order to develop fundamental understanding of any mechanism. In a microscopic level, the wettability of the rock is directly related to surface charges. Any interaction at the oil/brine and brine/rock interfaces that might result in changing the surface charges will directly alter the wettability of that surface. As mentioned earlier, zeta potential measurements can be used to study rock-surface/fluid interactions more directly compared to imbibition and core flooding experiments.

The ultimate objective of the current study was to develop a fundamental understanding about the individual and relative effects of the main PDIS which are present the Arabian Gulf Seawater (AGSW) on the surface charges of typical carbonate minerals. Zeta potential measurement was conducted as the main technique to accomplish this objective by varying some of the critical controlling factors such concentration of the PDIs, wetting state of the

rock particles, temperature and the pH value. Several studies suggested that during this type of recovery the carbonate surface will exhibit structural changes as a result of the brine/rock/oil interactions which may lead to leaching or replacement of ions from the rock lattice. To study the possible changes in the rock surface morphology, microscopic imaging was conducted to investigate possible structural changes which could be directly correlated to the measured zeta potential values. For this part, optical microscope and high resolution Atomic Force Microscopy (AFM) were used. On each detected deposit or structural changes by the optical microscope, Energy Dispersed Spectroscopy (EDS) coupled with Scanning Electron Microscopy (SEM) were used to determine the type of elements present on the modified rock surfaces.

1.3 Thesis Organization

In addition to the current chapter, this thesis consists of another six chapters. In chapter two, detailed literature review is given for major research on zeta potential and other means of microscopic surface characterization conducted to investigate oil recovery by smart water flooding. Chapter three summarizes all materials used in the current study are summarized in addition to a detailed description of all experimental procedures followed to achieve the objectives of the thesis. In chapters four, five and six, results are summarized and discussed in details. In chapter 7, an attempt is made to explain reported results from core flooding experiment on smart water flooding in carbonates, based on the findings of the current study. Chapter seven summarizes our conclusions. All measured zeta potential values in the current study are tabulated in Appendix A.

CHAPTER 2

LITERATURE REVIEW

Measuring zeta potential needs conducting special procedures for preparing stable colloid suspension. Measured zeta potential values are strongly affected by brines compositions, pH, temperature, etc. As a result, contradictions in literature are sometimes expected, even for the same particles and dispersion mediums. As mentioned earlier, the value and the sign of the zeta potential have been used to indicate the possible mechanisms of wettability alteration towards more water wet by modifying the surface charges as concluded by several researchers after conducting some basic experiments, such as core flooding, contact angle measurements, interfacial tension measurements, etc. In all of the major studies, zeta potential measurements had a profound usage in the interpretation of the observed incremental recoveries in terms of wettability alteration by desorbing the oil phase. In this chapter, major studies concerned with the use of zeta potential to investigate the possible mechanisms during smart/low salinity water flooding are reviewed starting with a review of some very basic and fundamental electrokinetic studies which are very important to interpret the obtained results in the current study.

In addition to zeta potential studies, highlights of the major research on the application of microscopic surface characterization, mainly by AFM, are summarized.

2.1 Major Research on Zeta Potential for Water Based EOR

Buckely et al. [15] Measured electrophoretic motilities for emulsions of three different crude oils at room temperature as a function of pH and concentration of sodium ions of NaCl solutions. For all samples, the magnitude of the negative charges increased as the concentration of the sodium ions in the solution decreased. Measured zeta potentials were matched by the Ionisable Surface Group (ISG) model which predicts the zeta potential based on some material constants that are related to the acidic, basic and amphoteric species present in the crude oil. From the matching parameters, it was concluded that sufficient surfactants are present in the crude oil to saturate the oil interface.

Cicerone et al. [30] studied the effect of different ion species on surface charges of the calcite/water interface. Zeta potential was calculated from the electrophoretic motility of calcite particles immersed in saturated solutions with a wide range of Ca^{2+}, Mg^{2+} and dodecyl sulfate anions. Increasing calcium ions' concentration shifted zeta potential toward more positive values while the effect of pH was negligible for constant concentration of calcium ions. It was found that the effect of magnesium ions on zeta potential is heavily dependent on the pH and the aging time. The negative surface charges of the calcite particles were reverted above certain pH value. They also found that the dodecyl sulfate ions had very strong affinity towards calcite surfaces and their adsorption changed surface charges from positive to negative. From zeta potential values, it was concluded that Ca^{2+} and CO_3^{2-} are the only PDIs for calcite. However for a magnesium bearing calcite, Mg^{2+} became another PDI.

Pierre et al. [31] studied the effect of pH and concentration of different ions (Na^+, Ca^{2+}, Cl^- ,SO_4^{2-}) on the electrophoretic motilities of natural and synthetic calcite suspension at room temperature. For different ionic strengths of NaCl solutions, the mobility became negative for high pH value while the isoelectric pH was the same for all cases. Decrease in mobility at constant pH as ionic strength increased was explained by the decrease in the thickness of the diffusive layer around the particles. It was found that at constant pH and ionic strength of NaCl solution, surface charges of natural calcite particles became negative when small amount of divalent cations were added. As the concentration of these cations increased, the electrophoretic mobility became positive and remained constant for high concentration. The effect of sulfate ions was found to be insignificant compared to the effect of the divalent cations. From this work, it was concluded that Ca^{2+} is considered as a PDI in the calcite/water interface while NaCl acted as indifferent salt towards $CaCO_3$(s).

Legens et al. [32] measured the electrophoretic motilities of synthetic calcite powder as function of pH in different salinity brines. For all solutions, measured zeta potentials were always positive. For NaCl solutions, zeta potential values decreased as the concentration of the solution increased due to compression of the electric double layer.

Hirasaki and Zhang [8] studied the use of sodium carbonate and anionic surfactant to alter the wettability of carbonate rocks to more water wet and to reduce the IFT to ultralow values. Zeta potential was measured for the oil/brine interface and the calcite/brine interface as function of pH. Zeta potential values for the oil/brine interface was negative for pH greater than 3 while values for the brine/calcite interface were only negative for pH greater than 9 when the only electrolytes are 0.2 M NaCl and NaOH or HCl to adjust the pH. They mentioned that this opposite charges between the two interfaces will cause

electrostatic attraction between mineral/brine and brine/oil interfaces which will collapse the water films' stability and bring oil to the mineral surface. If the two surfaces are both negatively charged, an electric repulsion will be developed between them which will stabilize the water films between the two interfaces. It was concluded that Ca^{2+}, CO_3^{2-} and HCO_3^- are PDIs for the calcite surface and a system with carbonate/bicarbonate ions may be expected to have a preference to be water wet.

Gomari et al. [33] studied the interaction between brines with different concentrations of Mg^{2+} and SO_4^{2-} ions and a modified calcite surface with a model oil made of stearic acid using zeta potential and contact angle measurements. It was found that Mg^{2+} ions were able to alter calcite wettability towards more water wet compared to SO_4^{2-} ions and this was attributed to the high affinity of both ions to adsorb on calcite surface.

Zhang and Austad [16] investigated the effect of Ca^{2+} and SO_4^{2-} ions on the zeta potential of a chalk suspension in a NaCl solution. It was found that small amount of Ca^{2+} increased the zeta potential towards more positive and the positive value of zeta potential increased linearly with increased concentration the Ca^{2+}. On the other hand, SO_4^{2-} shifted zeta potential to negative and as the concentration increased, the zeta potential increased linearly. To account for the degree of mixing during injection, they studied the relative effect of Ca^{2+} and SO_4^{2-} by keeping the concentration of one ion constant while varying the concentration of the other ions and measure the zeta potential at different concentration ratio. They noticed that zeta potential is close to zero when the concentration ratio between SO_4^{2-} and Ca^{2+} ions is about 1 and it became positive when Ca^{2+} is in excess of SO_4^{2-} and negative when SO_4^{2-} is in excess of Ca^{2+}. From zeta potential measurements, they concluded that injected seawater that contains Ca^{2+} and SO_4^{2-} can increase the water

wetness of chalk and when those ions are present the zeta potential will be dictated by the concentration ratio SO_4^{2-} /Ca^{2+}. From spontaneous imbibition tests, it was found that oil recovery increased significantly when concentration of sulfate was increased in the imbibing fluid and the efficiency of this wettability alteration process increased as the temperature increased.

Rodríguez and Araujo [29] studied the effect of temperature and pressure on zeta potential of typical reservoir minerals (quartz, kaolinite and calcite). They found that the zeta potential decreased with temperature at a rate of -2.3 mV/ºC, -0.96 mV/ºC and -2.1 mV/ºC for quartz, kaolinite and calcite particles respectively for pressure less than 45 psi. For the pressure effect, a systematic increase in zeta potential with pressure for quartz was observed for all pH values, while a monotonic decrease with pressure was found for the kaolinite. For the calcite, the response was variable with the pressure. They concluded that the behavior of zeta potential of calcite in respect to temperature depends mainly on Ca^{2+} and CO_3^{2-} available in the solution. At high temperatures, solubility of Ca^{2+} will increase and this will force calcium ions to leave the lattice of the calcite, thus, more negative charges will be created at the calcite surface. The pressure response of the calcite particles was explained by the slight increase in solubility of calcite with pressure, which is accompanied by an increase in Ca^{2+} concentration at the surface, thus, the surface charges will be less negative and the zeta potential will decrease.

Zhang el al. [9] studied the symbiotic effect of Ca^{2+} and SO_4^{2-} on improving oil recovery from moderate water-wet chalk. It was found that the zeta potential increased towards more positive as the concentration of the Ca^{2+} increased while presence of SO_4^{2-} decreased the value of the zeta potential. In a subsequent study [26] the effect of Mg^{2+} on the zeta potential

of a chalk suspension was investigated by gradually adding $MgCl_2$ solution to the chalk suspension that has the same pH and ionic strength of the previous study. They found that positive charges on the chalk surface increased as the concentration of the Mg^{2+} increased. From zeta potential measurements in the both studies, as well as other experiments, they concluded that the relative concentration of Ca^{2+} and SO_4^{2-} appeared to dictate the surface charges on chalk and that Ca^{2+} ions appeared to have a similar effect as SO_4^{2-} ions to promote enhanced spontaneous imbibition of water. It was also found that Ca^{2+} ions together with SO_4^{2-} ions play a crucial role in the process of wettability alteration. From the second study, they have experimentally verified that Mg^{2+} ions are strong PDIs towards chalk surface and they can increase the positive charges on the chalk surface. At high temperature, Mg^{2+} ions can substitute Ca^{2+} ions from the chalk surface though a dolomitization process and the degree of substitution increased with temperature. The main outcome of these studies was a proposed chemical mechanism that explains the interplay between the PDIs , the chalk surface and the crude oil which lead to a release of some of the adsorbed crude oil carboxylic materials from the chalk surface.

Hiorth et al. [13] developed a geochemical model that couples bulk aqueous and surface chemistry and used it to investigate how the water chemistry affects the surface charges and minerals dissolution in pure calcium carbonate rock. To develop this model, they assumed that the dominant mineral is calcium carbonate and the thermodynamic equilibrium constants at the surface have the same temperature dependence as the equilibrium constants in the aqueous phase. The developed model was used to analyze some of the experimentally measured zeta potentials available in the literature. The model was able to provide good matching. From the comparison, they found that change in

solution chemistry does not change the surface charges of the carbonate in a way that supports the observed oil recovery during spontaneous imbibition experiments. The only possible mechanism is carbonate dissolution. They mentioned that at high temperature, calcium in the injected water will react with the rock minerals and the aqueous phase will lose calcium which will then be supplied from the calcite surface. If the calcite dissolution takes place where oil is adsorbed, then oil can be liberated from the rock.

Alotaibi et al. [10] conducted zeta potential experiments to characterize electrokinetics of limestone and dolomite rock particles in different synthetic brines that represent the Middle East reservoirs. For pH equal to 7, they found that zeta potential for the limestone particle is positive in AGSW (54,680 ppm TDS) which was due to the weak electrostatic repulsion caused by compression of the electric double layer. In aquifer water (5436 ppm TDS), the zeta potential was always negative as a result of expanding the thickness of the electric double layer. Lack of Na^+ and other cations in the aquifer water increased the magnitude of the negative charges. The magnitude of the negative charges also increased as the aquifer water was diluted. In aquifer water, zeta potential had an ascending trend with pH. They found that increasing the temperature to 50 ^oC results in more negative charges for the limestone particles immersed in aquifer water which was attributed to the increased solubility of calcium ions which will preferentially leave the calcite lattice and create more negative charges. For the dolomite particles, presence of Mg^{2+} in the particles lattice created different interactions. From this study, they concluded that low salinity water creates more negative charges on limestone and dolomite particles by expanding the thickness of the electric double layer and increasing the temperature will significantly decrease the zeta potential.

Alotaibi and Nasr-El-Din, in a later study [34], investigated surface charges of crude oil and limestone particles at 50 ºC and pH 8 in different aqueous solutions. Crude oil emulsions in the Arabian Gulf Seawater (AGSW) and low salinity aquifer water were prepared to study surface charges at oil/water interface. In all measurements, zeta potential was negative, except for particles treated with the formation water. They found that the magnitude of zeta potential at the oil/water interface increased when the salinity decreased and when adding more sulfate or removing divalent cations from the water. Water wet limestone particles had positive charges due to excess of divalent cations in the formation water while the zeta potential was negative for oil-wet and intermediate-wet particles. The effect of the ionic strength was more pronounced in the oil-wet limestone particles than the others.

Yousef et al. [5] measured zeta potential of a Middle East carbonate rock suspension on diluted versions of AGSW. At 40 ºC zeta potentials were negative at 50% diluted AGSW and as the salinity decreased the absolute value of negative charges increased. Increasing the temperature to 60 ºC increased the magnitude of the negative charge for all versions of diluted AGSW which was attributed to the increased reactivity of SO_4^{2-} and Ca^{2+} ions as well as the increased solubility of Ca^{2+} ions which will force Ca^{2+} to leave the carbonate lattice, Thus, more negative charges are created. From zeta potential measurements as well as previously released NMR and rock wettability results , authors concluded that injecting diluted AGSW as in the described manner is able to change the surface charges of carbonate rocks toward more negative which will lead to more interactions with water molecules, and eventually, alter rock wettability.

2.2 Major Research on Atomic Force Microscopy for Water Based EOR

Basu and Sharma [35] investigated the role of crude-oil polar fractions on wettability alteration by studying surface forces on glass micro-slides in different salinity and pH using AFM. It was concluded that for resins and asphaltene, the critical disjoining pressure increases with decrease in salinity and increase in pH which indicates more stable water films.

Kummar et al. [36] used AFM to study the nature of adsorbed components of the crude oil as well as the wettability alteration of oil-treated Mica and Silica surfaces using anionic and cationic surfactants. Measurements of adhesion forces indicate that the adsorbed materials from the used crude oil is asphaltenic in nature. Anionic surfactant was found to be more effective in removing adsorbed oil molecules than the cationic surfactants.

Karoussi and Hamouda [37] studied wettability alteration of oil-wet calcite surface treated with stearic acid in presence of sulfate and magnesium ions using AFM and contact angle measurements. The individual effect of magnesium and sulfate ions on desorbing carboxylic groups was not fully distinguished using AFM topology images. However the adhesion force measurements were found to be in-line with the contact angle measurements which showed that magnesium ions were able to alter the wettability of the modified calcite towards more water wet compared to sulfate ions.

CHAPTER 3

MATERIALS AND METHODOLOGY

3.1 Materials

3.1.1 Rock Samples

In the current study, calcite and dolomite crystals were used in addition to a real sample from a Middle East oil field. These samples were characterized by several methods as summarized in the following subsections and in Table 3.1.

I. Calcite

Var. Iceland spar calcite crystals from Creel, Chihuahua Mexico, were used in the current study and were supplied by WARD'S Natural Science. Characterization of the sample shows that this sample is almost 100 % calcium carbonate. Fine powder of the crushed crystals was analyzed by X-Ray Diffraction (XRD). The result is shown in Figure 3.1. The sample was also characterized by Scanning Electron Microscopy (SEM) and Energy Dispersed Spectroscopy (EDS) on small chips. Conductive coating with gold was first done for tested chips to prevent affecting the SEM images by the sample's charging. Figure 3.2 shows two sites on the tested chip. Thin section was also prepared from the calcite crystal and examined under an optical microscope to visualize the crystals arrangement. The result is shown in Figure 3.3.

II. Dolomite

Dolomite crystals from Butte, Montana, supplied by WARD'S Natural Science were used in the current study. From the XRD analyses of the prepared powder, 1.9 % wt. of Quartz, were detected as shown in Figure 3.1. As done on calcite chips, dolomite chips were first coated by gold before SEM and EDS tests. From SEM and EDS results shown in Figure 3.2 no elements other than those present in the dolomite crystal were detected. From the thin section, very clear rhombohedral crystals were seen under the optical microscope as shown in Figure 3.3. In general, the used crystal is mainly dolomite [$CaMg(CO_3)_2$] with impurities less than 2 wt. %. From EDS spectra, as it will be shown in chapter 6, traces of Fe^{3+}, Mn^{2+} ions were detected which indicate that small amount of ankerite [$Ca(Fe,Mg,Mn)(CO_3)_2$] is presented in this crystal.

III. Middle East Carbonate (MEC)

Slabs from a real Middle East carbonate field were used in the current study. Slabs were first cleaned by immersing them in toluene which was changed every 24 hours till no change in the toluene color was noticed. From XRD (Figure 3.1) SEM and EDS (Figure 3.2) and Raman shift (Figure 3.4) it was found that this sample is mainly calcite.

Table 3.1: Summary of rock samples' characterization

Sample	Mineralogical composition as detected by the XRD	Elemental composition as detected by the EDS
Calcite	Calcite, $CaCO_3$ ~100%	Elemental Wt.% O 43 Ca 42 C 15
Dolomite	Dolomite, $CaMg(CO_3)_2$ ~ 97% Other impurities: Quartz, SiO_2 < 2%. Ankerite, $Ca(FeMgMn)(CO_3)_2$ < 1%.	Element Wt.% O 34 C 32 Ca 22 Mg 12
Middle East Carbonate (MEC)	Calcite, $CaCO_3$ ~100%	Element Wt.% O 40 Ca 40 C 20

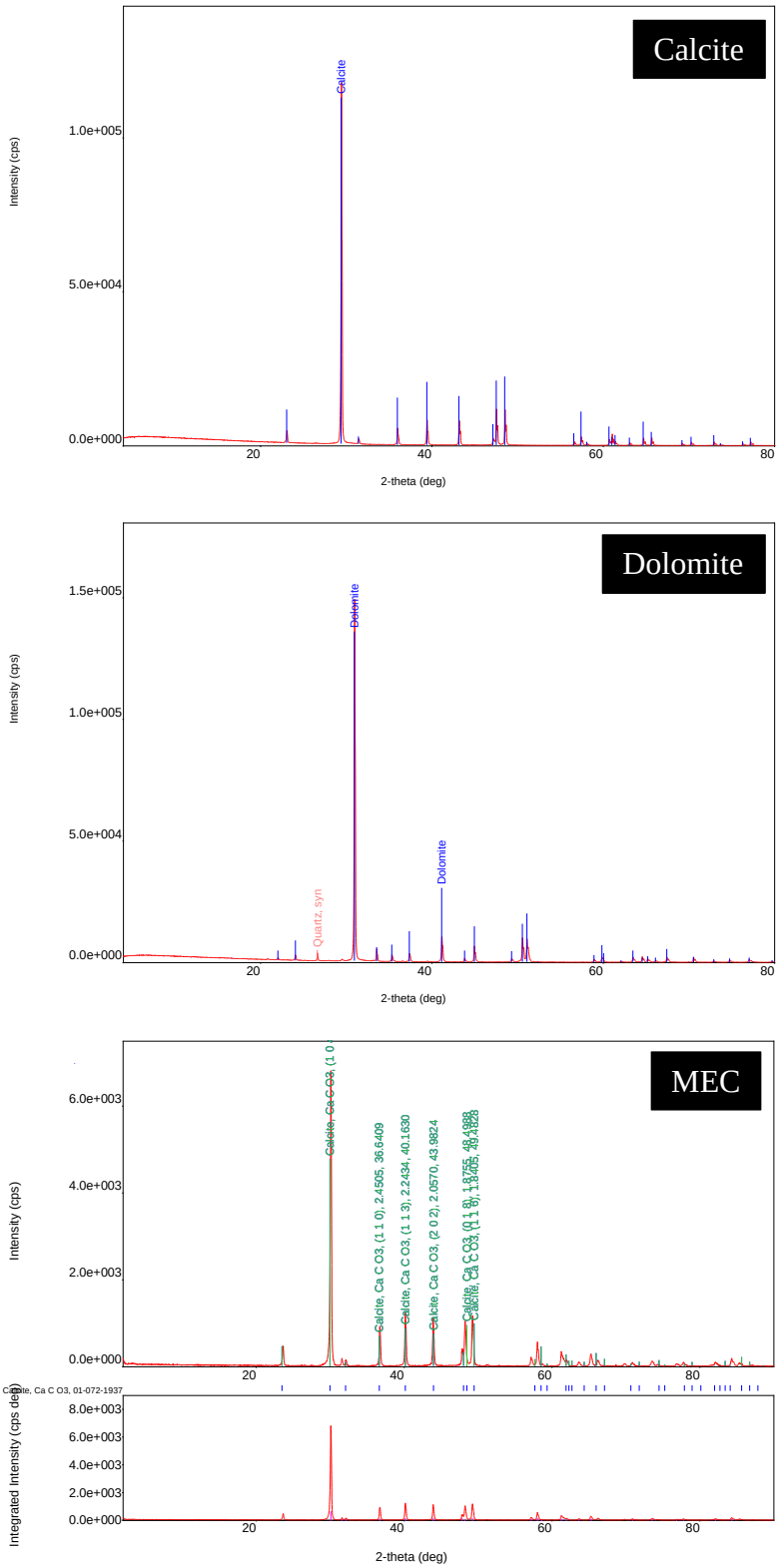

Figure 3.1: XRD of the calcite (top) the dolomite (mid) and the Middle East Carbonate (bottom) powders.

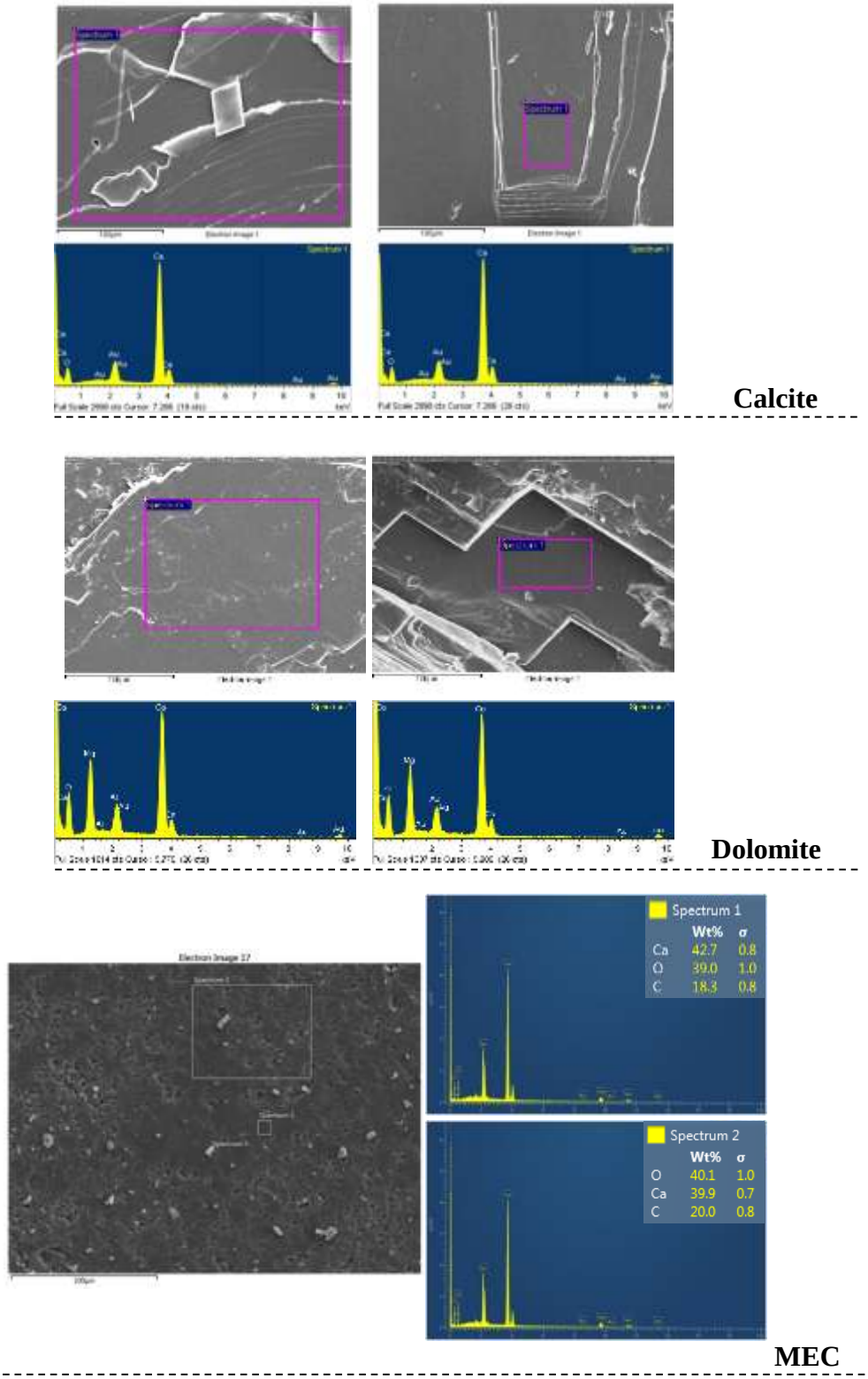

Figure 3.2: SEM images and EDS spectra of different locations on the calcite (top), the dolomite (mid) and the Middle East Carbonate (bottom) chips.

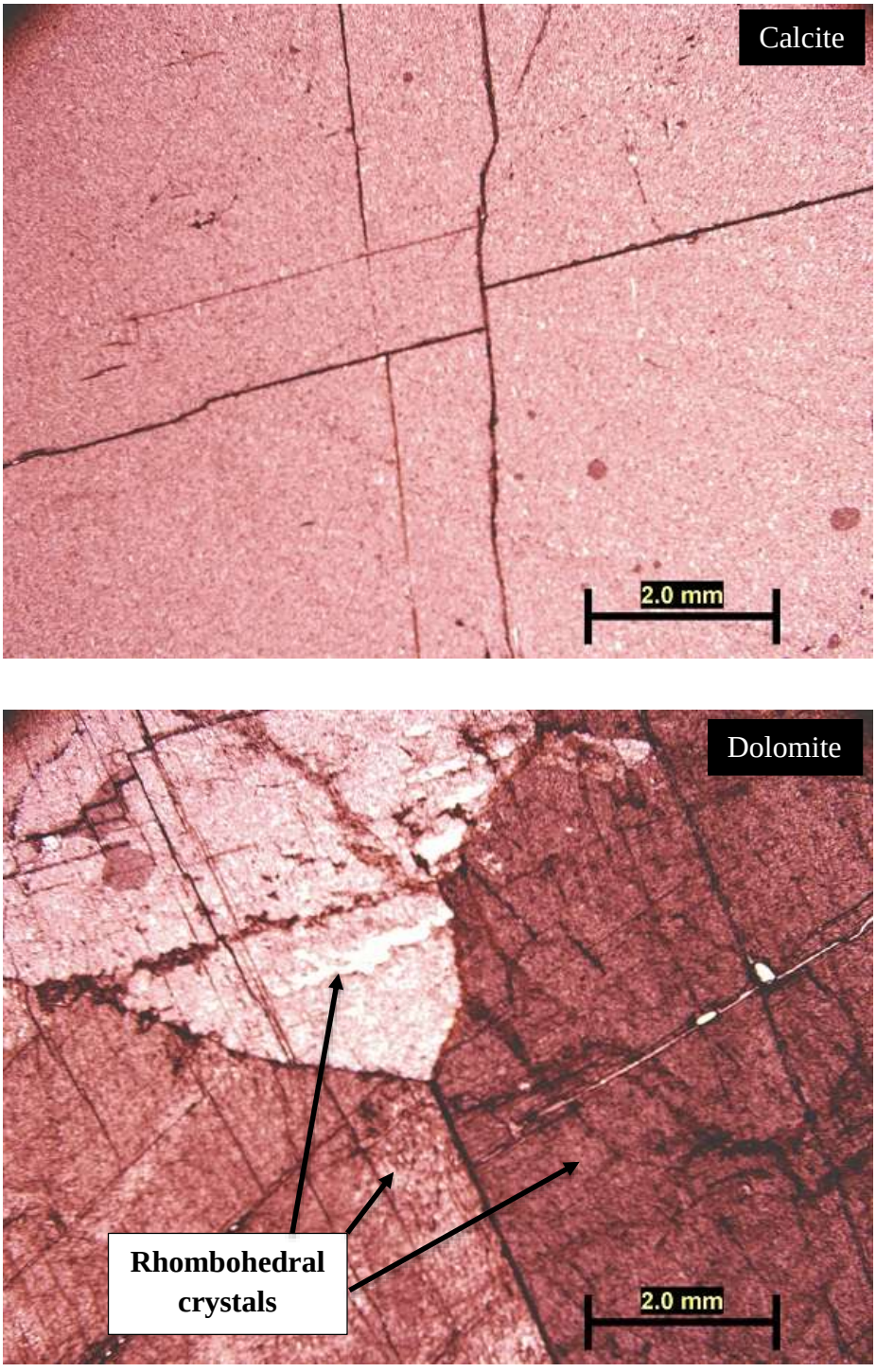

Figure 3.3: Thin section of the calcite (top) and the dolomite (bottom).

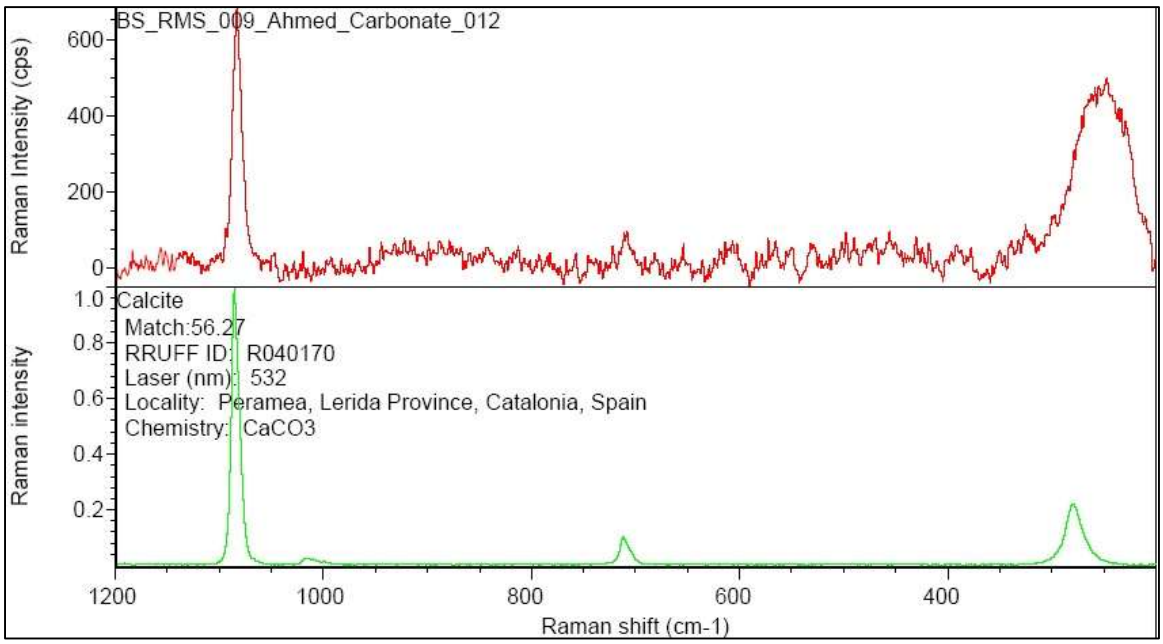

Figure 3.4: Raman shift of the Middle East Carbonate powder.

3.1.2 Model Oil

A model oil, made of stearic acid and toluene was used for all experiments in the current study to represent oil phase. Stearic acid and toluene were supplied by Sigma-Aldrich with specifications shown in Table 3.2 Stearic acid was dissolved in toluene in specific ratios as shown in Table 3.3 to develop a model oil with total acid number (TAN) of 2.0 mg KOH/g. From visual investigation of the final mixture, all stearic acid powder has perfectly dissolved is toluene, which is in line with reported observations which found that stearic acid is more soluble in non-polar organic solvent than polar organic solvents [38].

Table 3.2: Chemical properties of stearic acid and toluene used to prepare model oil

Stearic Acid, Grade 1 [$CH_3(CH_2)_{16}COOH$] • Purity: >98.5 %. • Molecular Weight: 284.48 grams/mole.
Toluene, anhydrous[$C_6H_5CH_3$] • Purity: 99.8 %. • Molecular Weight: 92.14 grams/mole.

Table 3.3: Weights of model oil components

Model Oil with TAN = 2 mg KOH/g	
Stearic Acid	1.00 gram
Toluene	97.60 grams
Final Mixture	98.60 grams

Total acid number of an oil sample is defined as the amount of potassium hydroxide in milligrams that is needed to neutralize the acids in one gram of oil. From this definition, TAN of the prepared model oil can be calculated from the weight ratios of acid to toluene as shown in below steps:

1. Fraction of acid in the mixture:

$$\text{Acid Fraction} = \frac{\text{Acid Weitgh}}{\text{Mixture Weigth}} = \frac{1.0\ [\text{g}]}{98.60\ [\text{g}]} = 0.010142$$

2. Number of moles of dissolved acid:

$$\text{Number of moles} = \frac{\text{Acid fraction}}{\text{Acid molecular weight}} = \frac{0.010142}{284.48\ [\text{g/mol}]}$$

$$= 3.5651\text{E} - 05\ \left[\frac{mol}{g}\right]$$

3. Milligrams of potassium hydroxide to equilibrate dissolved acid (TAN):

$$\text{mg of KOH} = \text{KOH molecular weigh} * \text{moles of dissolved acid} * 1000$$

$$= 56.1\ \left[\frac{\text{g}}{\text{mol}}\right] * 3.5651\text{E} - 05[\frac{\text{mol}}{\text{g}}] * 1000 = 2.0\ \text{mg KOH/g}$$

From the above three steps, and using excel solver, data point were generated for the required weights from stearic acid and toluene to be mixed in order to develop a model oil with TAN = 2.0 mg KOH/g. A plot of the generated data is shown in Figure 3.5.

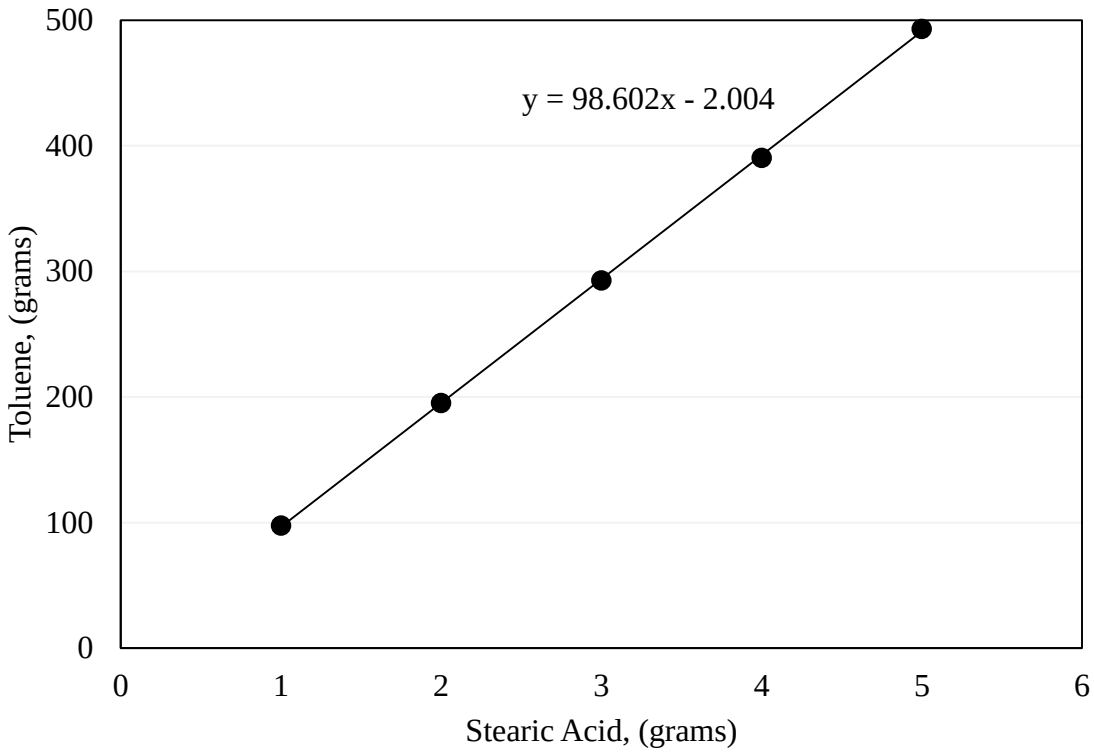

Figure 3.5: Weights of stearic acid and toluene to develop a model oil with TAN = 2.0 mg KOH/g

Calculated TAN was experimentally verified using ASTM Standard D974-12 [39]. In summary, weighted amount from the prepared model oil was dissolved in a titration solvent which was made of toluene, water and anhydrous isopropyl alcohol in a ratio of 100:1:99 respectively. The resulting single phase solution was titrated at room temperature with standard alcoholic base solution to the end point indicated by the color change of the added phenolphthalein solution drops. A brief summary of each step followed during the test is discussed in the next two subsections.

I. Preparation of Standard Alcoholic Solution

Six (6) grams of potassium hydroxide were first dissolved in 6 ml of deionized water and the resulting solution was added to approximately one liter of anhydrous isopropyl alcohol (propanol) in a two liters flask. The mixture was boiled at 80 ^{o}C and stirred for 15 minutes. One gram of a calcium hydroxide was dissolved in 2 ml of deionized water and then added to the mixture, which was stirred again at 80 ^{o}C for another 15 minutes. The final homogeneous mixture was allowed to stand for cooling at room temperature overnight before the resulting supernatant was filtered through 0.45 µm filter paper.

The final filtered mixture was standardized using potassium acid phthalate for molarity determination. Few drops of phenolphthalein indicator were added to a solution that consists of a precisely weighted 0.200 grams of potassium acid phthalate which was dissolved in 40 ml of deionized water. This solution was titrated with the prepared standard alcoholic solution which was dispensed from a 50 ml burette until the end point. The end point is defined by the appearance of permanent pink color. The net volume of dispensed standard alcoholic solution at the end point was recorded. This process was conducted

twice after which a blank titration with the de-ionized water which was used for dissolving the potassium acid phthalate was also conducted. Net volumes recorded at the end of the three titration tests are shown in Table 3.4.

Table 3.4: Titration of the standard alcoholic solution

Titration #	Net Volume of Standard Alcoholic solution at the end point (ml)
1	12.2
2	12.2
Avg.	12.2
Volume of standard alcoholic solution used to titrate the deionized water = 0.1 ml	

Molarity of the standard alcoholic solution was calculated using the following equation:

$$\text{Molarity} = \frac{W_p}{204.23} * \frac{1000}{V - V_b}$$

Where:

- W_p = weight of the potassium acid phthalate (0.2 g),
- 204.23 = molecular weight of the potassium acid phthalate,
- V = volume of titrant (standard Alcoholic Solution) used to titrate the salt to the specific end point, (12.2 ml), and
- V_b = Volume of titrant used to titrate the de-ionized water (0.1 ml).

Using above equationa and recorded volumes, molarity of the standard alcoholic solution was determined:

$$\text{Molarity} = \frac{0.2}{204.23} * \frac{1000}{12.2 - 0.1} = \mathbf{0.0809\ M}$$

II. Procedures for acid number determination

Into 100 ml of the prepared titration solvent, 20 grams from the model oil was dissolved, and the mixture was stirred for few minutes, after which, six drops of phenolphthalein indicator were added. The final mixture, which is color-less, was titrated with the standard alcoholic solution, whose standardized molarity was found to be 0.0809, until a permanent pink color appeared. This process was repeated twice, and then followed by another titration for the titration solvent itself. Table 3.5 summarizes the net volumes recorded.

Table 3.5: Titration of the model oil

Titration #	Net Volume of Standard Alcoholic solution at the end point (ml)
1	9.00
2	8.90
Avg.	*8.95*
Volume of Standard Alcoholic solution used to titrate the titration solvent = 0.35 ml	

Total Acid number was calculated using the following equation:

$$\text{Total Acid Number (mg KOH/g)} = \frac{[(\text{A} - \text{B})\text{M} * 56.1]}{\text{W}}$$

Where:

- A = volume of standard alcoholic solution required for titration of the sample (ml),
- B = volume of standard alcoholic solution required for titration of the blank (titration solvent) (ml),
- M = molarity of the standard alcoholic solution, and
- W = weight of model oil used in titration, g.

Using the above equation and volumes recorded in Table 3.5, total acid number of the model oil was calculated as shown below:

$$\text{Total Acid Number (TAN)} = \frac{[(8.95 - 0.35) * 0.0809 * 56.1]}{20}$$

$$= \mathbf{1.952}\ \text{mg KOH/g}$$

The above calculated value from the titration test is very close to the theoretically calculated value considering possible experimental errors.

3.1.3 Brines

Synthetic aqueous brines were prepared using high purity salts (> 99.5% wt.) and ultra-pure deionized water. Listed salts in Table 3.6 were supplied by Panreac Spain. Deionized water with a resistivity of 18.2 MΩ-cm at room temperature was produced by Barnstead Ultrapure Water System manufactured by Thermo Scientific.

Prepared brines were formulated in a way that enables studying the individual and relative effect of potential determining ions present in the Arabian Gulf Seawater. Due to the salinity limits of the zeta potential analyzer used in the current study, all brines were prepared at constant ionic strength level equal to 50% diluted AGSW (0.574 M) and this was achieved by manipulating the concentration of NaCl salt. Ionic composition of AGSW is shown in Table 3.7 as reported by Lindlof and Stoffor. [40] Zeta potential of the three rock samples in AGSW was measured only one time to make reference data points for comparison purposes. Figure 3.6 is a flow chart showing a summary of brines used in the current study.

Table 3.6: Salts used to prepare aqueous brines

Salt	Molecular Weight (grams/mole)
NaCl	58.44
$NaHCO_3$	84.01
Na_2SO_4	142.04
$CaCl_2.2H_2O$	147.02
$MgCl_2.6H_2O$	203.30

Table 3.7: Ionic composition of the Arabian Gulf Seawater

Ion	Concentration (ppm)
Na^+	18,043
Ca^{2+}	652
Mg^{2+}	2,159
Cl^-	31,808
SO_4^{2-}	4,450
HCO_3^-	173
TDS (ppm)	57,285
Ionic Strength (M)	1.15

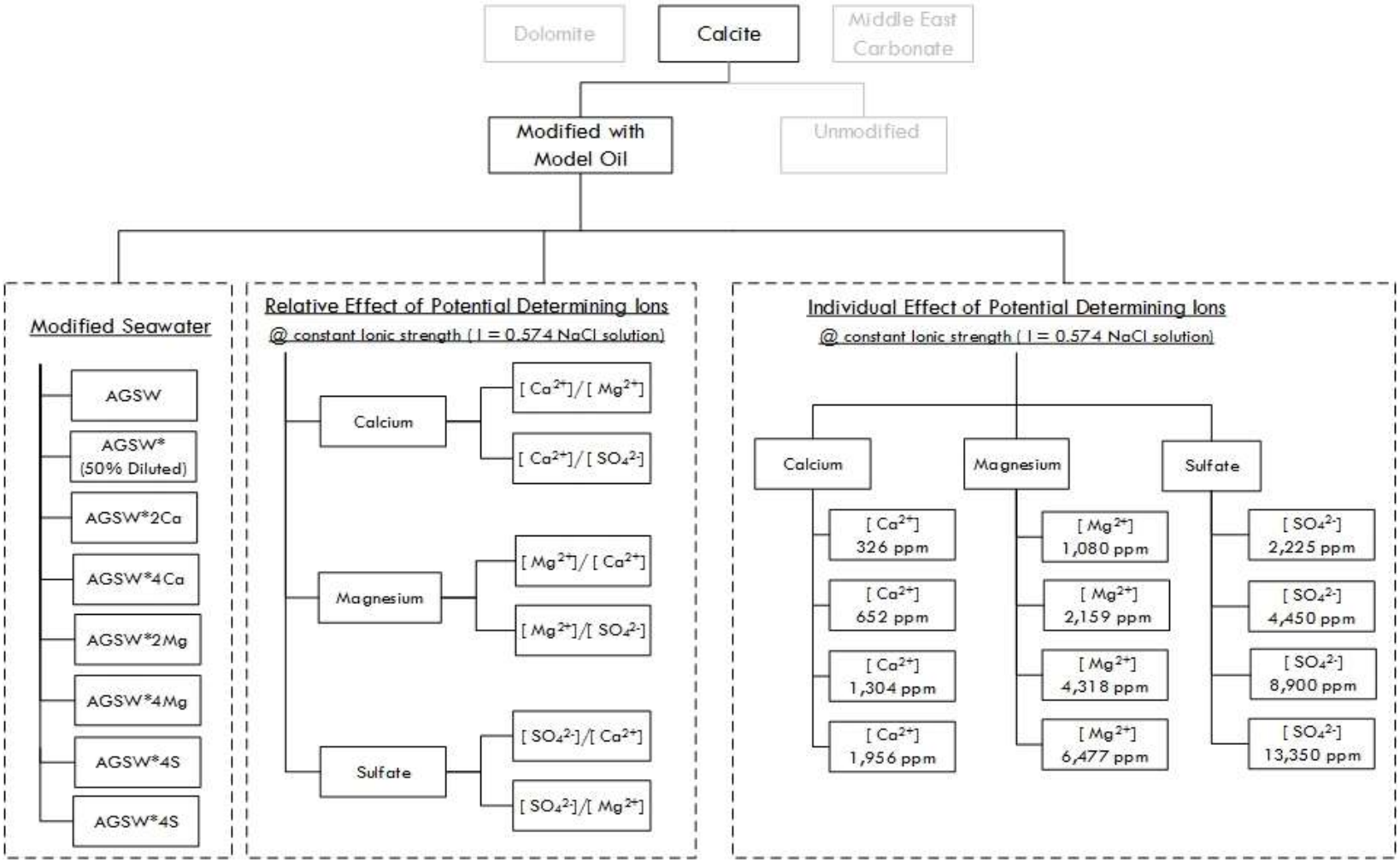

Figure 3.6: Flow chart of the formulated brines.

3.2 Methodology

3.2.1 Procedures for Preparing and Running Samples on the Zeta Potential Analyzer

Calcite, dolomite and MEC rock samples were crushed by a ROCKLAB crushing machine which produced very fine powder. To avoid contaminations, no sieves were used to determine the size of produced powders. From each rock, unmodified powder (not contacted with model oil) and powder modified with model oil were both considered for zeta potential measurements.

At reservoir conditions, formation water was in contact with reservoir rock surface before oil came in. To check the possibility of mimicking this condition when preparing oil-wet samples for the current study, calcite powder was first soaked in high salinity Middle East formation water (Table 3.8) [41] for 24 hours before the powder was filtered and allowed to dry in oven at 90 ^{o}C overnight. Dry powder was then mixed with distilled water in 0.5% solid-to-liquid ratio and conditioned on multi-writ shaker at room temperature for 24 hours. The conditioned mixture was filtered through 5.0 µm syringe filter to prepare the final suspension. Another calcite suspension was prepared using the same procedures without soaking the powder in formation water. For the two suspensions, electric conductance was measured by Brookhaven ZetaPALS which is the machine used in the current study for zeta potential measurement and discussed later in this subsection. Electric conductance of the colloid suspension, which is reported in MicroSiemens (µS) in this machine, is a useful and direct measure of free salt ions' concentration. [42] From measured values of electric

conductance shown in Table 3.9 it can be clearly seen that there is high concentration of free salt ion in the case of soaked calcite powder in formation water. Typical values of conductance for aqueous suspension to be used in Brookhaven ZetaPALS have a range from 30 µS to 30,000 µS. From the measured value in Table 3.9 it was concluded that soaking carbonate powders in formation water will produce suspensions beyond the machine's specifications. Due to this constrain, oil wet sample for the current study were prepared without initial soaking in formation water.

Table 3.8: Ionic composition of Middle East high salinity formation water

Ion	Concentration (ppm)
Na^+	51,187
Ca^{2+}	29,760
Mg^{2+}	4,264
Ba^{2+}	10
Sr^{2+}	1,035
Cl^-	143,285
SO_4^{2-}	108
HCO_3^-	351
TDS	230,000

Table 3.9: Effect of formation water on calcite suspension in distilled water

Sample #	Description	Electric conductance
1	Calcite soaking in formation water and conditioned in distilled water	43,876 µS
2	Calcite conditioned in distilled water without initial soaking in formation water.	601 µS

Similar preparation procedures used by Gomari et al [33] for preparation of calcite powder with adsorbed model oil were followed in the current study. In summary, 100 ml of prepared oil was added to 10 grams of each sample's powder in a closed jar. Mixtures were then stirred at low speed for 24 hours at room temperature, after which, conditioned mixtures were filtered through 0.45 µm filter paper using a vacuum pump, glass funnel and a flask. Modified powders were then allowed to dry at room temperature for another 24 hours. Simple floatation tests were conducted to check the degree of particles' coating with model oil. 0.5 grams of modified powder from each rock was added to 10 ml of distilled water in a test tube. In another test tube, equal amounts of unmodified powder from the same rock was added to 10 ml of deionized water. Unmodified powder of calcite and dolomite immediately settled down at bottom of the tube. On the other hand, modified powders of all rocks perfectly floated on top of the deionized water and almost no particles settled down for a duration of one week when tubes were allowed to stand at room temperature. For the MEC, it was noticed that both modified and unmodified powders floated on top of the water which indicates that some hydrophobic materials are still adsorbed on the powders' surfaces. This floatation test is shown in Figure 3.7.

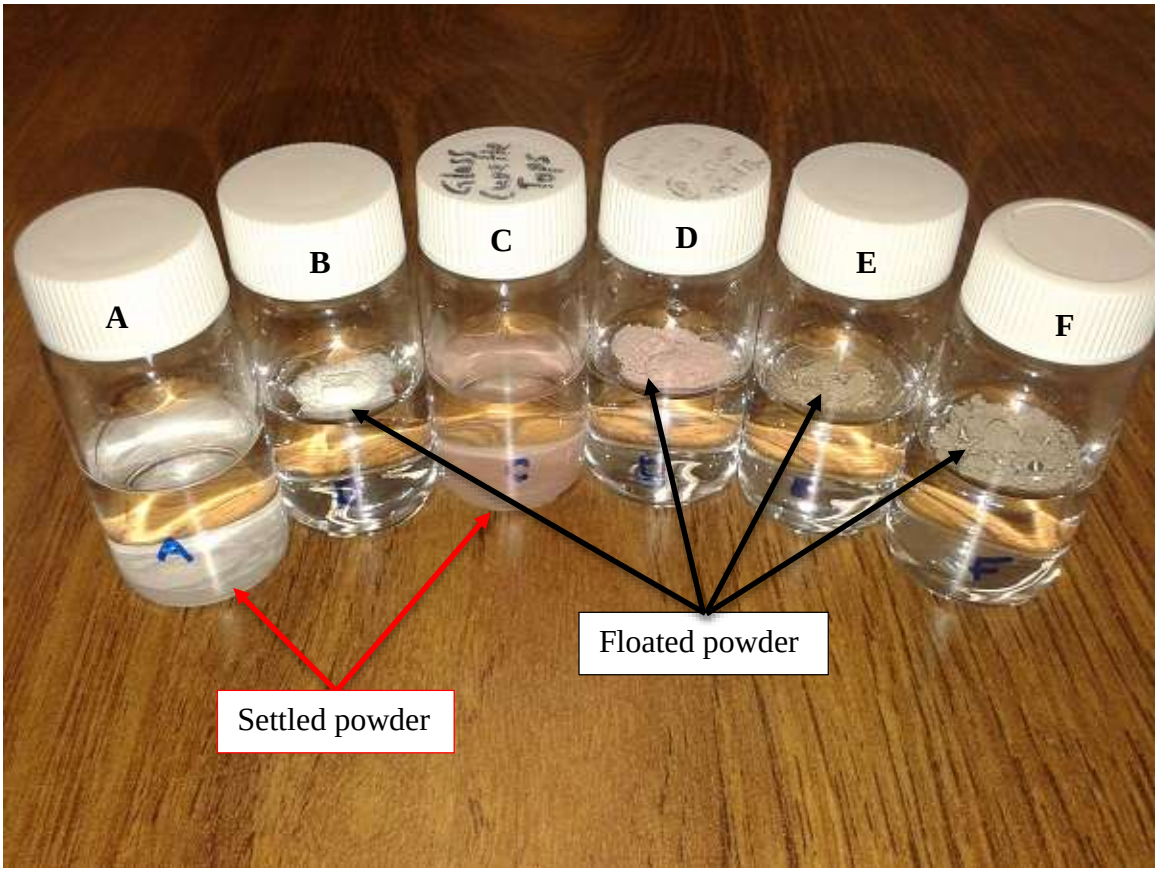

Figure 3.7: Flotation test for (A) unmodified calcite, (B) modified calcite with the model oil, (C) unmodified dolomite, (D) modified dolomite in the model oil, (E) unmodified Middle East Carbonate and (F) modified Middle East Carbonate with the model oil

The first step in preparing the final suspension for zeta potential measurements was to condition the modified and unmodified powders of each rock with each of the formulated brines as well as with deionized water as a reference point. For each rock, powder was added to a brine in a solid to liquid ratio of 0.5 wt. % which was achieved by adding 0.15 gram of powder to 29.85 ml of brine in 40 ml test tube. The mixture was then allowed to condition at room temperature on a multi-wrist shaker for 24 hours. The second step was to prepare good suspension from conditioned mixture to be used according to the specifications of zeta potential analyzer mainly in terms of particle size and particles concentration. To do this step, conditioned mixture was filtered through 5.0 µm aqueous hydrophobic syringe filter and transferred to a clean vial and the resultant suspension was directly used into the machine.

ZetaPALS zeta potential analyzer, manufactured by Brookhaven Instruments Cooperation was used for zeta potential measurements. It calculates zeta potential of suspended particles in electrolytes solutions using Phase Analysis Light Scattering (PALS). About 1.5 ml of the final filtered suspension was poured in 4 ml transparent plastic square cuvette and an assembly of two palladium electrodes was immersed in the sample. Regarding the principle of work for this machine, an electric field is generated across the sample by applying alternating current through the two electrodes which force charged particles to move. At the same time, a laser beam is passed through the sample and the moving particles will scatter the applied laser beam. From the recorded shift of the phase, an electrophoretic mobility of particles will be measured which has a unit of (micron/second)/ (volt/cm). From measured electrophoretic mobility, the zeta potential will be calculated using

Smoluchowski model for aqueous suspension or the Huckel model for particles suspended in solvents. [42]

After conducting preliminary experiments on this machine it was found that when running high salt concentration suspensions using the machine's default settings, the tested sample were always contaminated with a brownish substance at the end of the measurement. This contamination is probably coming from the palladium electrodes. To overcome this problem, the effect of voltage and frequency on development of this brownish substance was investigated by changing the value of one parameter while keeping the second fixed, and then, making zeta potential measurements on calcite suspension in 0.5M NaCl brine using a single run that consists of 100 cycles and between each 5 cycles the run was stopped and the sample was checked for contamination. It was found that when specifying 20 Hz for the frequency while keeping the voltage at auto mode, no brownish substance was developed. This adjusted frequency value was used for all zeta potential measurements in the current study. Regarding the measurement parameters, a single run that consists of 100 cycles was specified. During the run, all reported data on the screen was monitored, especially, the value and the sign of displayed mobility in addition to the relative residual and phase shape. This process was repeated at least four times, while cleaning and conditioning the electrodes after each two runs until a good mobility was observed. This good mobility is defined as the average mobility from a range that has very close and stable values, stable sign and has good phase shape. To condition the electrodes, zeta potential measurement on pure original brine (with no particles) was conducted using 10 continuous runs, each one consists of 15 cycles.

3.2.2 Procedures for Preparing and Characterizing Samples Using Optical and Atomic Force Microscopy

Microscopic surface images and morphology images were taken on small chips from the three rock samples using an optical microscope and AFM. The optical microscope used was manufactured by Leica-Microsystem and has high magnification set of lenses. The AFM machine used is MultiMode 5.0 which was manufactured by Bruker Cooperation.

From calcite and dolomite crystals, small chips were produced by scratching along the crystal's cleavage directions using a sharp scalpel to produce an average approximate sizes of 4mm x 4mm x 2mm from each sample. For the Middle East carbonate, 0.5 cm diameter disks were prepared by cutting small disks from cleaned slabs which were then grinded, ultrasonically re-cleaned and extremely polished to produce flat and smooth surfaces suitable for AFM scanning. In this part, only modified AGSW solutions were considered in addition to deionized water and 0.574 M NaCl.

To modify a sample with a fluid, a chip was immersed in that fluid in a small test tube for 24 hours at room temperature and then taken out and allowed to dry for 24 hours. For optical microscope imaging, the dried chip was put on a clean glass plate and high resolution surface images were directly taken at different location on the chip at room conditions. For the AFM, dry chips were carefully glued on a metal plate on one side to avoid movement when scanning and then scanned on the other side by a silicon nitride tip under contact mode at 23 ^{o}C fixed temperature.

To test and visualize the adsorption of stearic acid from model oil on carbonate surface, microscopic images were first taken from pure stearic acid powder. Three calcite chips

were then selected and blown-off by a flow of dry air to remove possible dust from the surface. One chip was directly imaged by the optical microscope to establish the original condition of the surface. The second chips was immersed in 10 ml of pure toluene and the third chip was immersed in 10 ml of the model oil, both for 24 hours, and then they were taken out and allowed to dry for 24 hours at room temperature. Microscopic images were then taken for both samples. Results of this test is shown in Figure 3.8 and as it can be seen, no surface changes from the original condition were noticed on the calcite chip immersed in toluene only while very clear deposits with different sizes were found on the chip immersed in model oil. This results clearly show that stearic acid which is dissolved in toluene has adsorbed on the calcite surface. Topology of the adsorbed deposits are quite similar to the pure stearic acid crystals. From this test, as well as the previous floatation tests on samples' powder, it was concluded that the aforementioned preparation procedure is able to develop acceptable oil wet conditions on powders and chips, and thus, it was applied for all three samples.

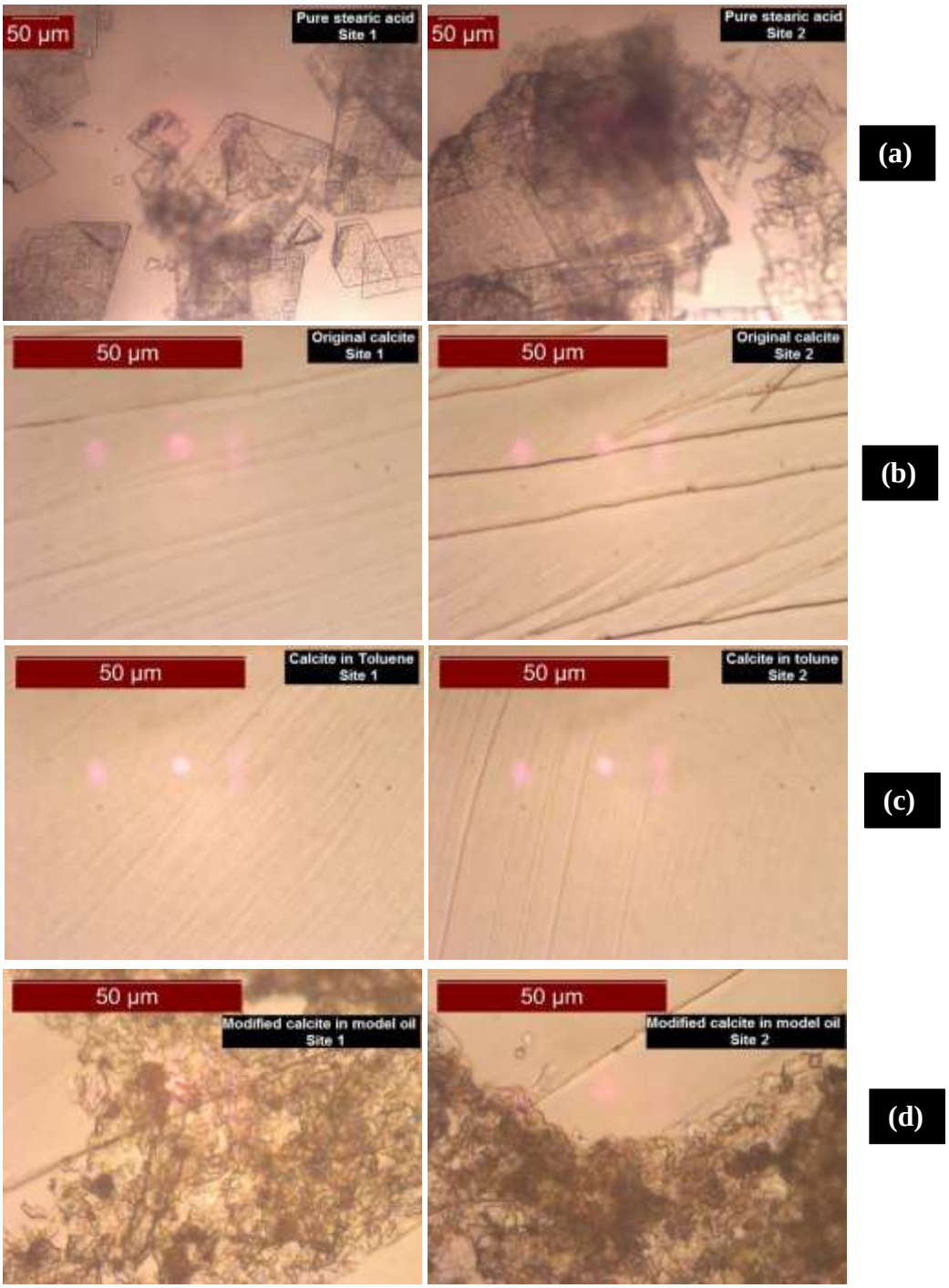

Figure 3.8: Microscopic images for stearic acid crystals (a), pure calcite chip (b), calcite chip immersed in toluene (c) and calcite chip immersed in the model oil (d).

3.2.3 Variable and Fixed Parameters during Experiments

Several experimental parameters can affect the value and the sign of zeta potential. In the current study, the brine's pH and the concentration of PDIs were the only parameters to be changed while other parameters were kept fixed in order to accurately define the role of each PDI on alteration of sample surface charges. Fixed parameters in the current study are summarized in Table 3.10.

Table 3.10: Fixed parameters during experiments

Fixed experimental parameters:

- Temperature (all phases): 25 ^{o}C.
- Pressure (all phases): Ambient pressure (1 atm.).
- Oil: Model oil made of stearic acid and toluene with TAN = 2.0 mg KOH/g.
- Brines' ionic strength: 0.574 M.
- Solid-to-liquid ratio for zeta potential experiments: 0.5% wt.
- Conditioning time on shaker for zeta potential experiments: 24 hours.
- Syringe filter size for zeta potential experiments: 5 µm.
- pH adjustment solutions: 0.1 M HCl and 0.1 M NaOH.
- Conditioning time of chips in model oil and brines for AFM and microscopic imaging: 24 hours.
- Scan size for AFM experiments: 15 µm.
- Scan speed for AFM experiments: 1.43 Hz.

3.2.4 Particles Sizing and Polydispersity

In addition to zeta potential measurements, the zeta potential analyzer comes with an option for suspended particles' sizing which enables measuring the hydrodynamic diameter and the polydispersity of the tested sample. The hydrodynamic diameter, expressed in nanometers (nm), is defined as the particle diameter plus the double layer thickness. The Polydispersity is a measure of non-uniformities that exists in the particles size distribution. The Polydispersity has no units. It is close to zero (0.00 to 0.020) for monodisperse or nearly monodisperse samples, small (0.020 to 0.080) for narrow distribution, and larger for broader distributions (instruction manuals for Brookhaven Zeta Potential Analyzer).

For all suspension used in the current study, the effective diameter and the polydispersity were measured. Figure 3.9 to Figure 3.11 show the histograms of the measured values for calcite, dolomite and MEC suspensions. For the effective diameters, an average values of 2,104 nm, 677 nm and 994 nm were measured for the calcite, dolomite and MEC suspensions respectively. Histograms of polydispersity indicate that most of the suspensions monodisperse to narrow disperse particles. These results indicate that the preparation procedure used in the current study develops homogenous suspensions.

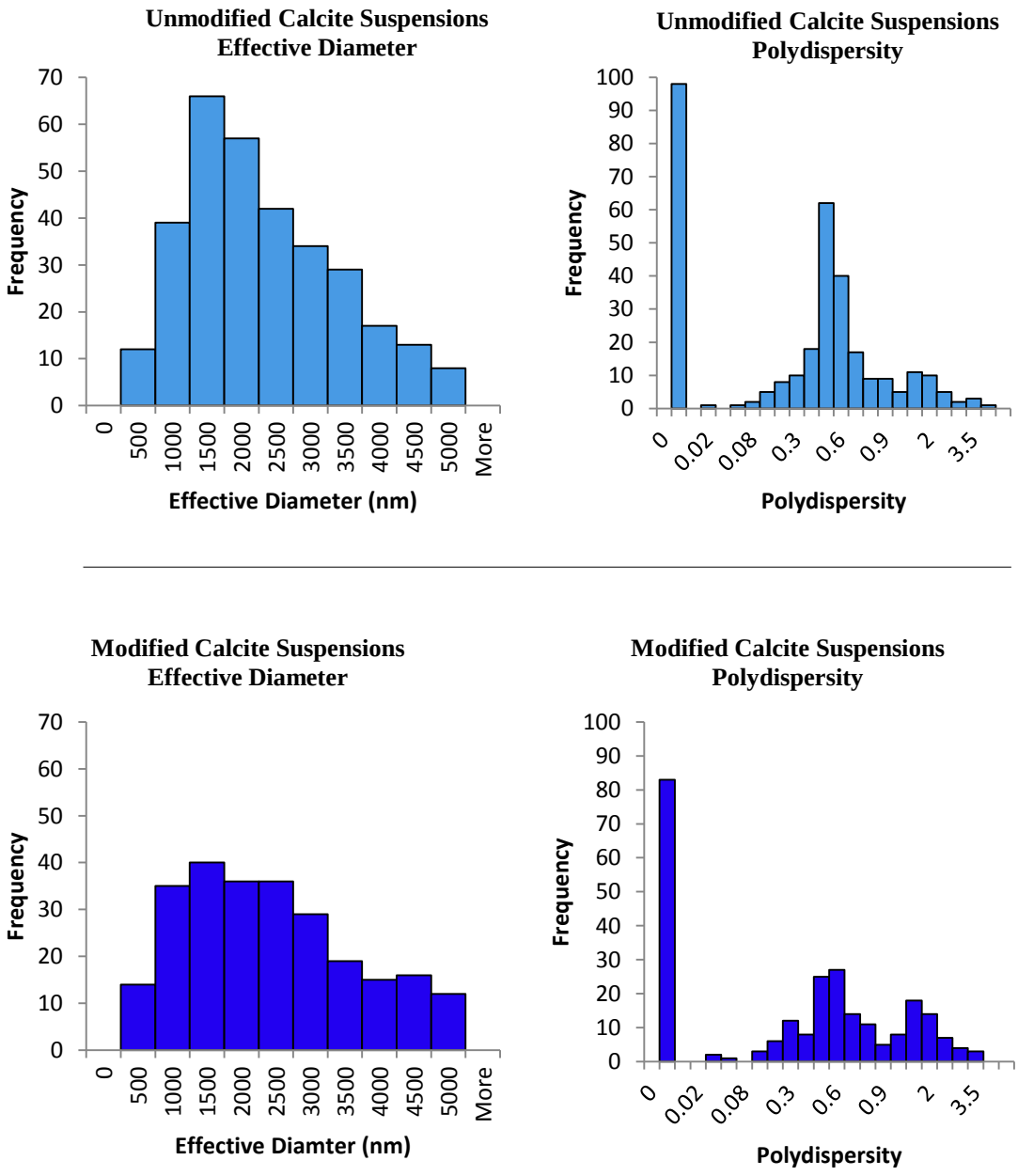

Figure 3.9: Histograms of effective diameters and polydispersity for unmodified calcite suspensions (top) and modified calcite suspensions (bottom).

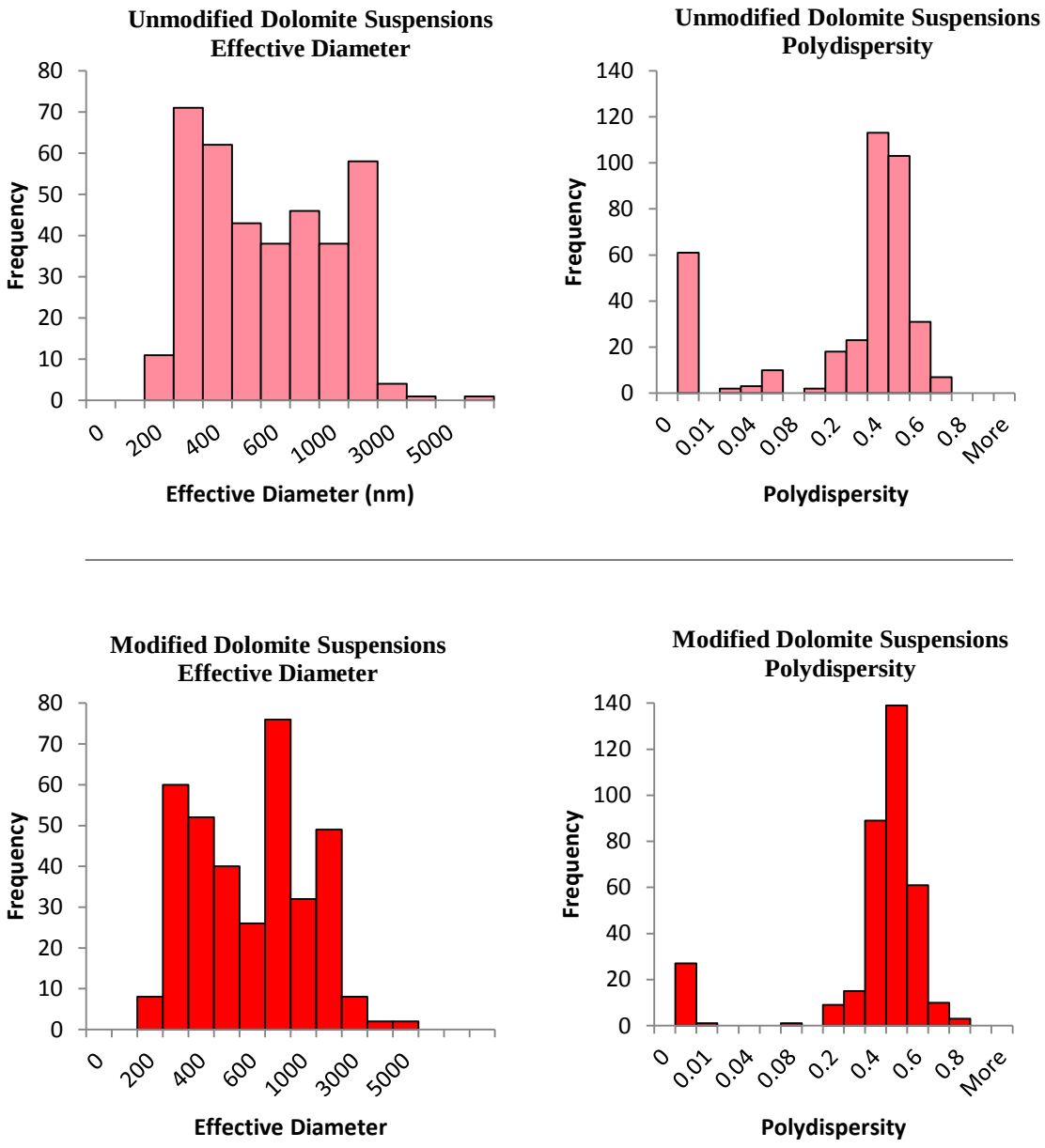

Figure 3.10: Histograms of effective diameters and polydispersity for unmodified dolomite suspensions (top) and modified dolomite suspensions (bottom).

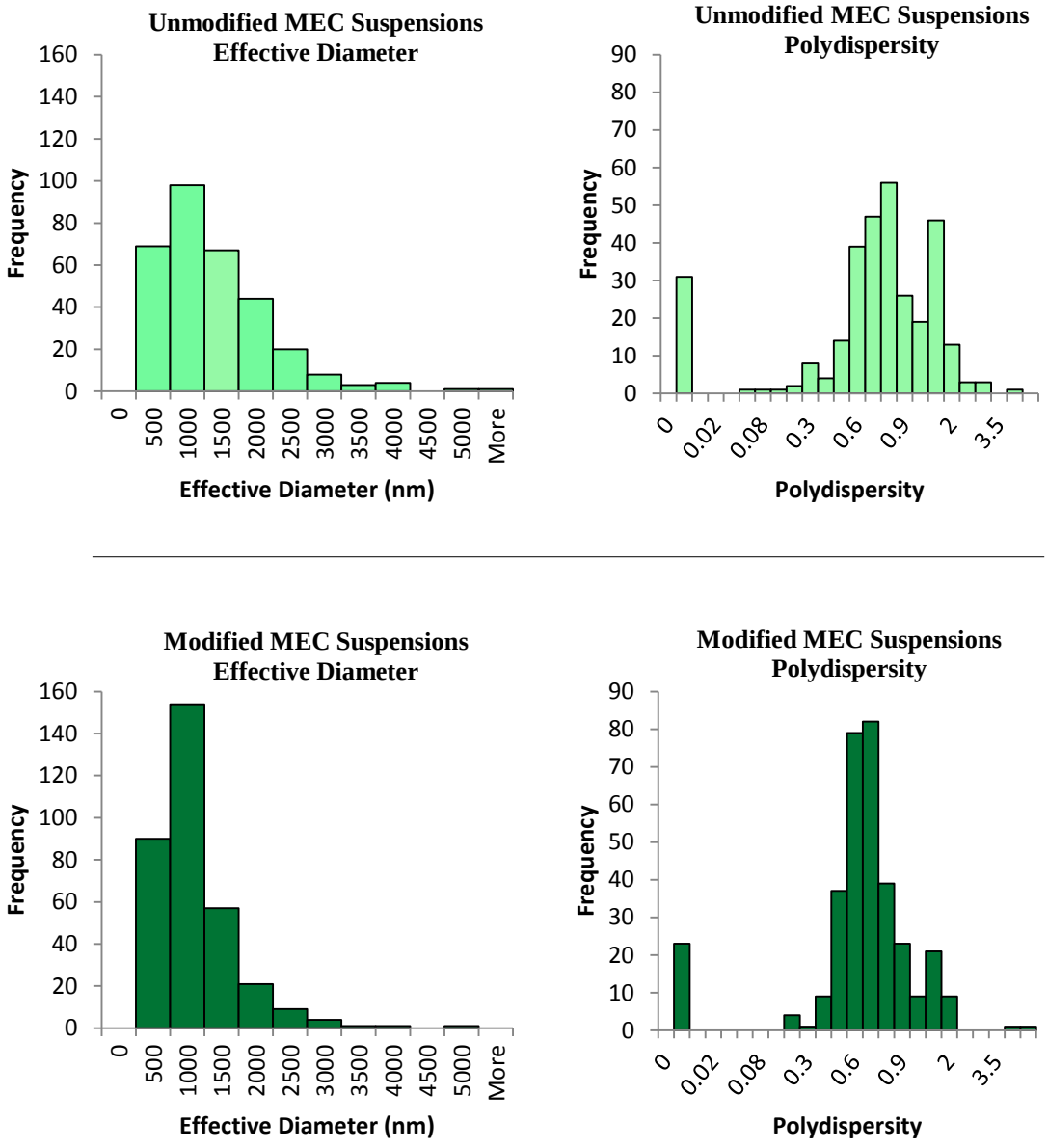

Figure 3.11: Histograms of effective diameters and polydispersity for unmodified Middle East Carbonate suspensions (top) and modified Middle East Carbonate suspensions (bottom).

CHAPTER 4

EFFECT OF SURFACE DISSOLUTION AND CONCENTRATION OF INDIVIDUAL POTENTIAL DETERMINING IONS

4.1 Dissolution of Carbonate Surfaces in Deionized Water

Zeta potential of each sample was first measured in deionized water at varied pH to locate the isoelectric point of each sample. This point is defined as the pH value at which the sample surface carries no net electric charges. [27] Zeta potential as function of pH for unmodified and modified powders in deionized water at 25^{o}C for the three samples is shown in Figure 4.1.

For each of the three rock samples, microscopic and surface morphology images were taken using optical microscope and AFM to see how the sample surface would change when it comes in contact with deionized water and model oil. Four chips from each rock sample were first blown off by a flow of dry air to remove possible dust from their surfaces. One chip was then directly used under the optical microscope and the AFM to establish initial surface conditions before the rock is contacted by any fluid. To investigate the effect of deionized water and model oil on the surface of the rock sample, one of three chips was immersed in deionized water and the other two were immersed in model oil, all for 24 hours at room temperature. After that, the chip which was immersed in deionized water

and one of the two other chips which were immersed in model oil were both taken out and allowed to dry at room temperature for 24 hours. The second chip in the model oil was taken out and directly immersed in deionized water for another 24 hours, after which, it was taken out of the deionized water and dried at room temperature. For the three dried chips, in addition to the first pure one, optical microscope and AFM images were taken.

The results of the aforementioned tests are shown in Figure 4.2 and Figure 4.5 for calcite using optical microscope and AFM respectively. Same tests on dolomite chips are shown in Figure 4.3 and Figure 4.6 for using the optical microscope and AFM respectively. For the MEC sample, only microscopic images were taken by the optical microscope of the AFM as shown in Figure 4.4. No AFM images were recorded for the MEC chips, because they were found to be very rough despite the extreme polishing during the initial chips preparation.

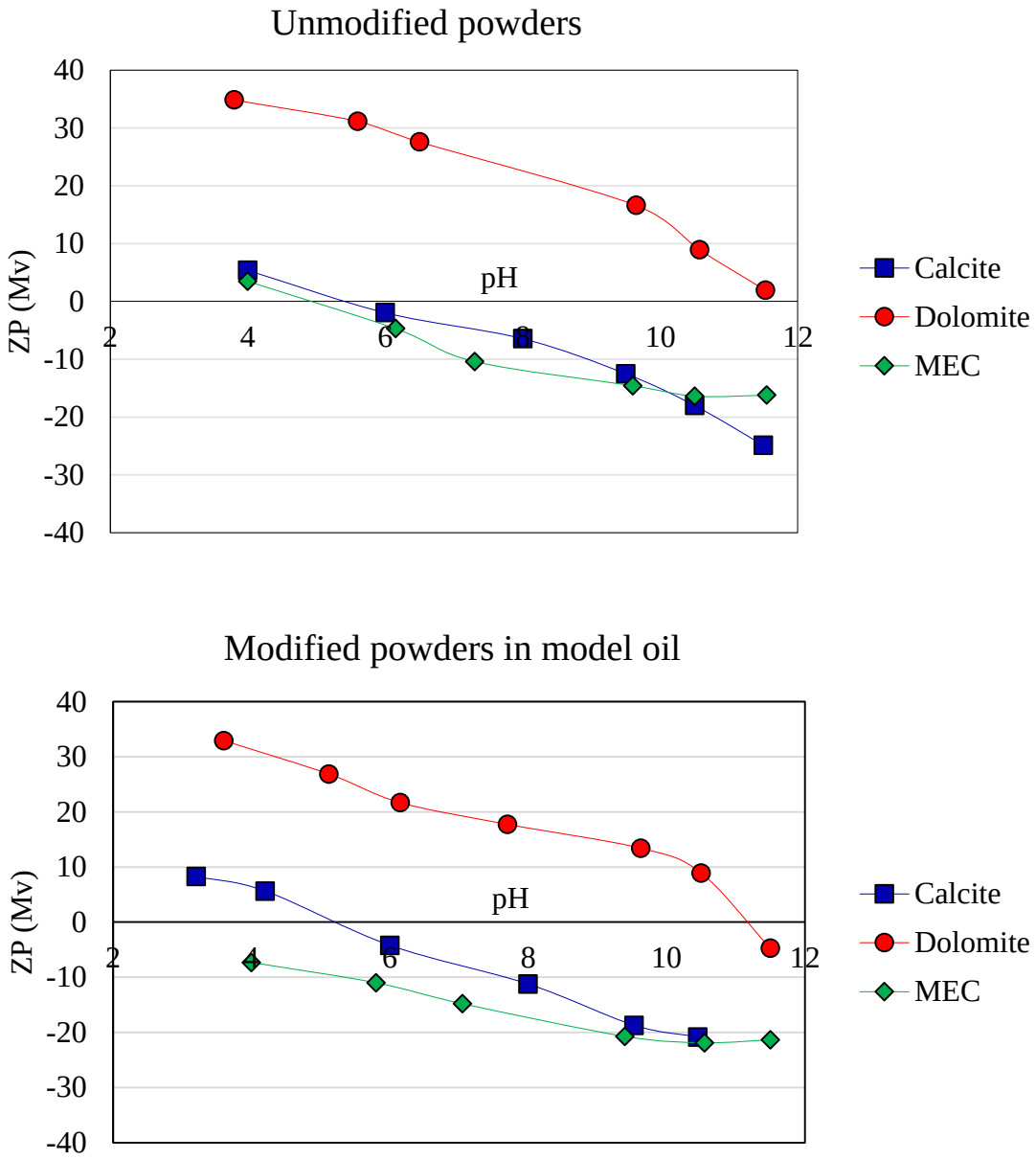

Figure 4.1: Zeta potential of unmodified (top) and modified (bottom) calcite, dolomite and Middle East Carbonate powders in deionized water as function of pH at 25 ºC.

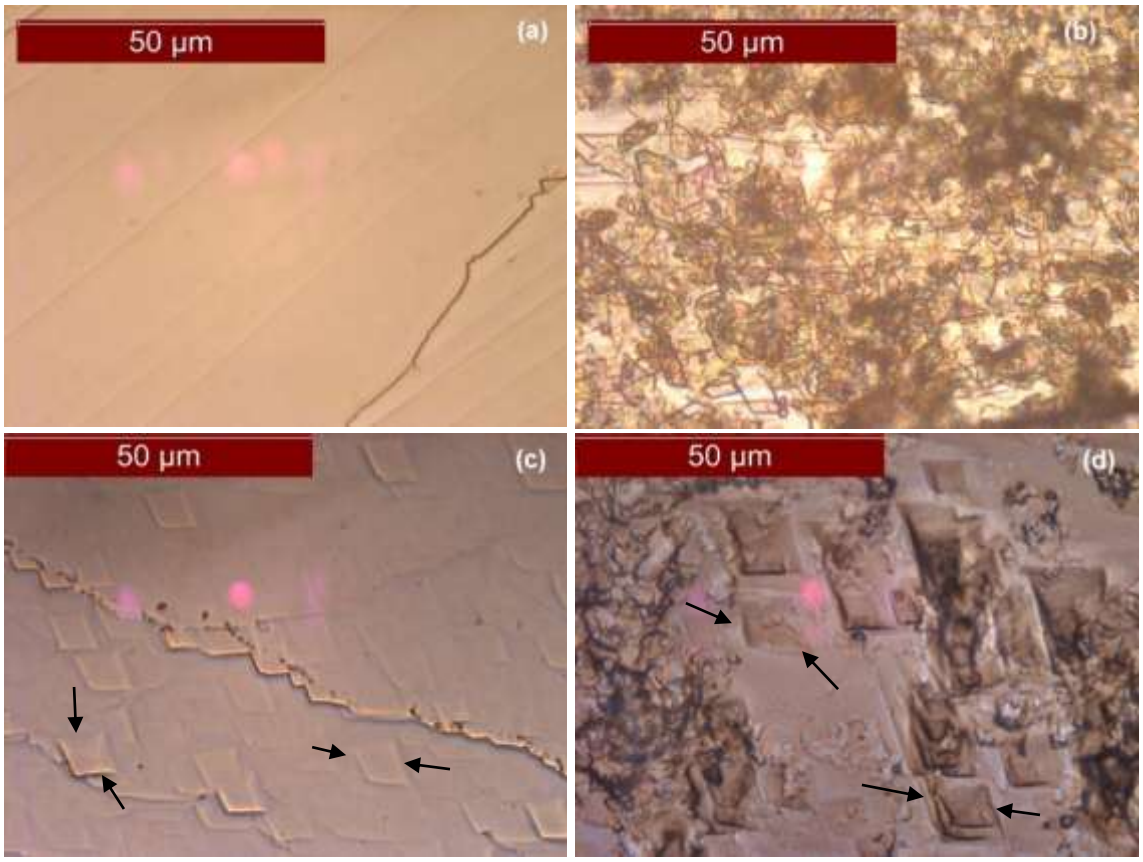

Figure 4.2: Microscopic surface images of a calcite chip not contacted with any fluid (a), a calcite chip immersed model oil (b), a calcite chip immersed in deionized water (c) and a calcite chip immersed in model oil then deionized water (e).

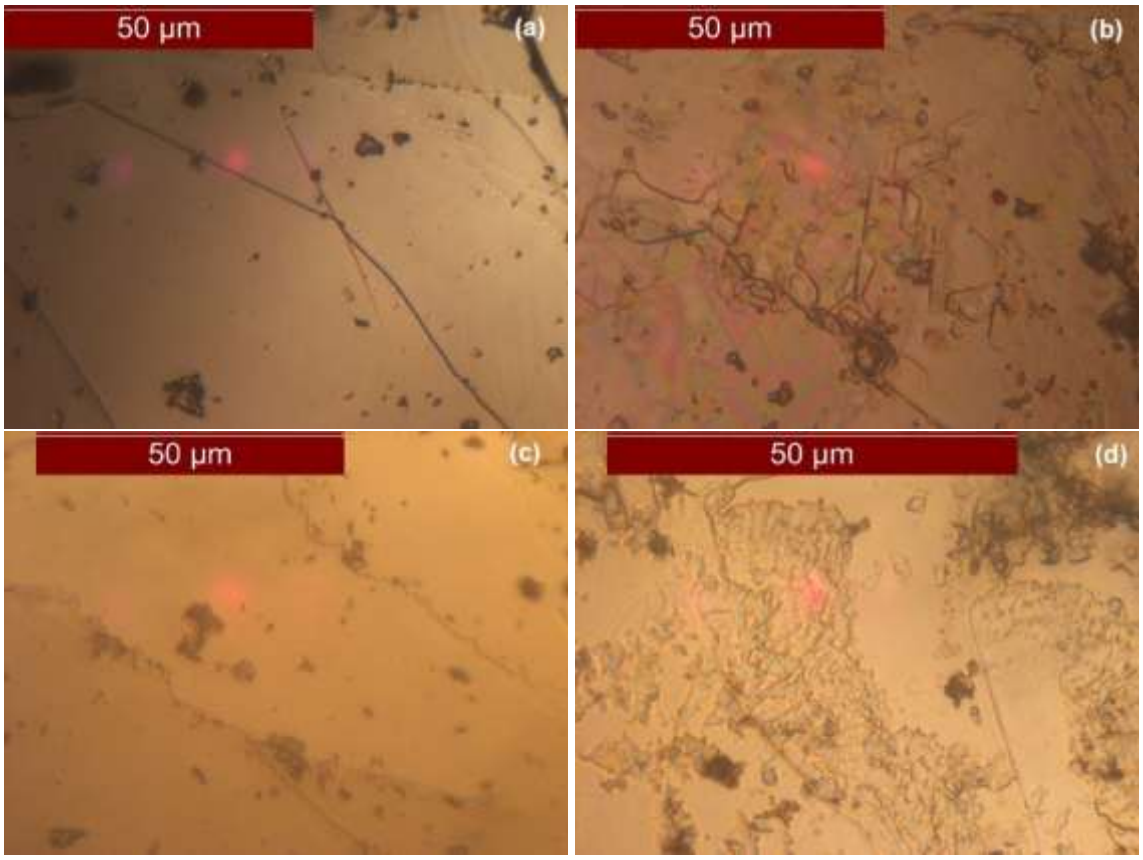

Figure 4.3: Microscopic surface images of a dolomite chip not contacted with any fluid (a), a dolomite chip immersed the model oil (b), a dolomite chip immersed in deionized water (c) and a dolomite chip immersed in the model oil , then in deionized water (e).

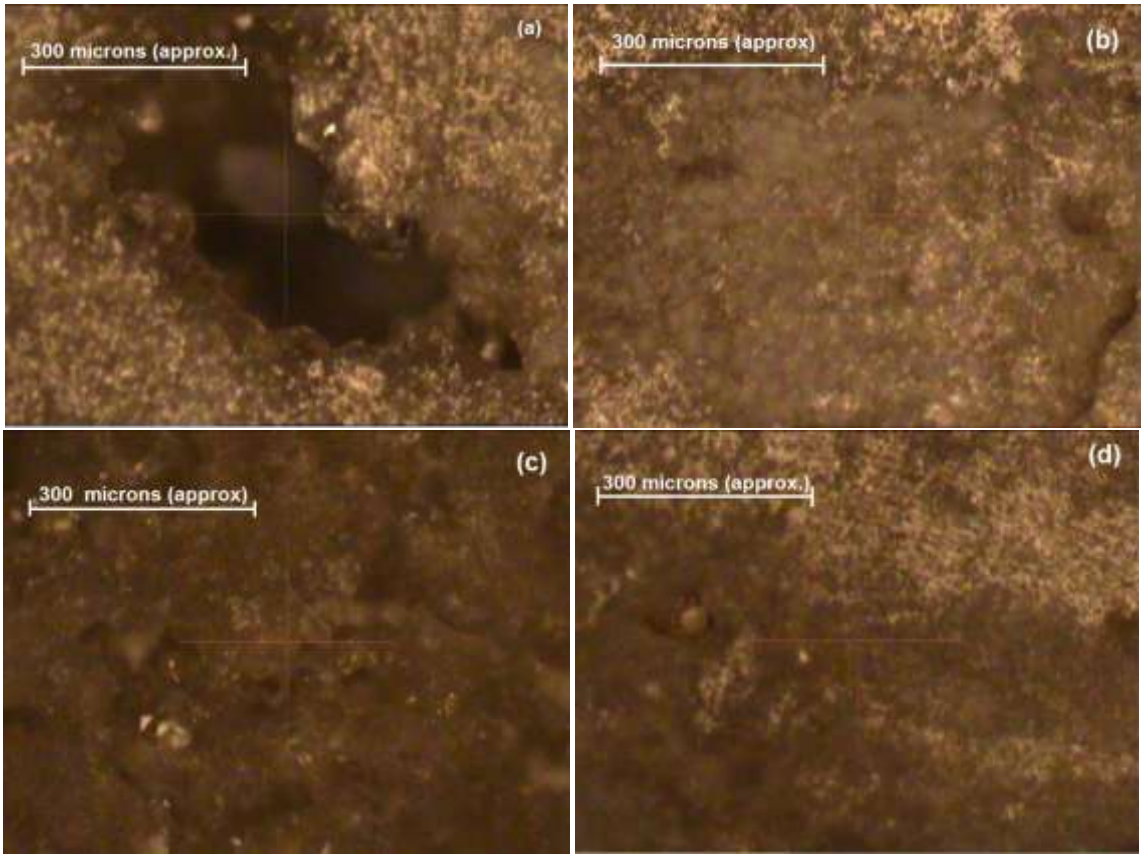

Figure 4.4: Microscopic surface images of Middle East Carbonate chip not contacted with any fluid (a), Middle East Carbonate chip immersed the model oil (b), Middle East Carbonate chip immersed in deionized water (c) and Middle East Carbonate chip immersed in the model oil, then in deionized water (e).

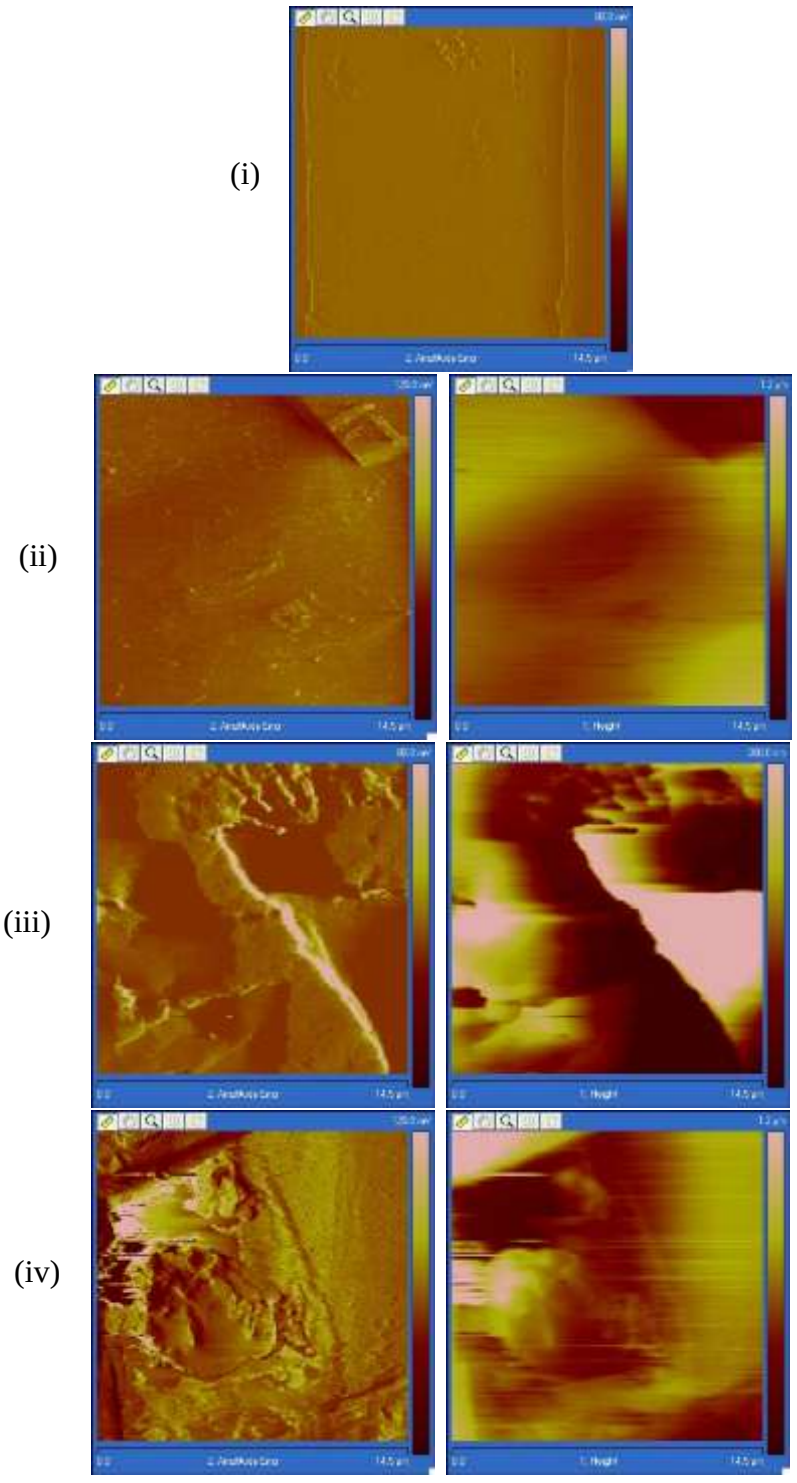

Figure 4.5: AFM deflection (a) and height images (b) for a calcite chip not contacted with any fluid (i), a calcite chip immersed in deionized water (ii), a calcite chip immersed in the model oil (iii) and a calcite chip immersed in the model oil then, then in deionized water (iv).

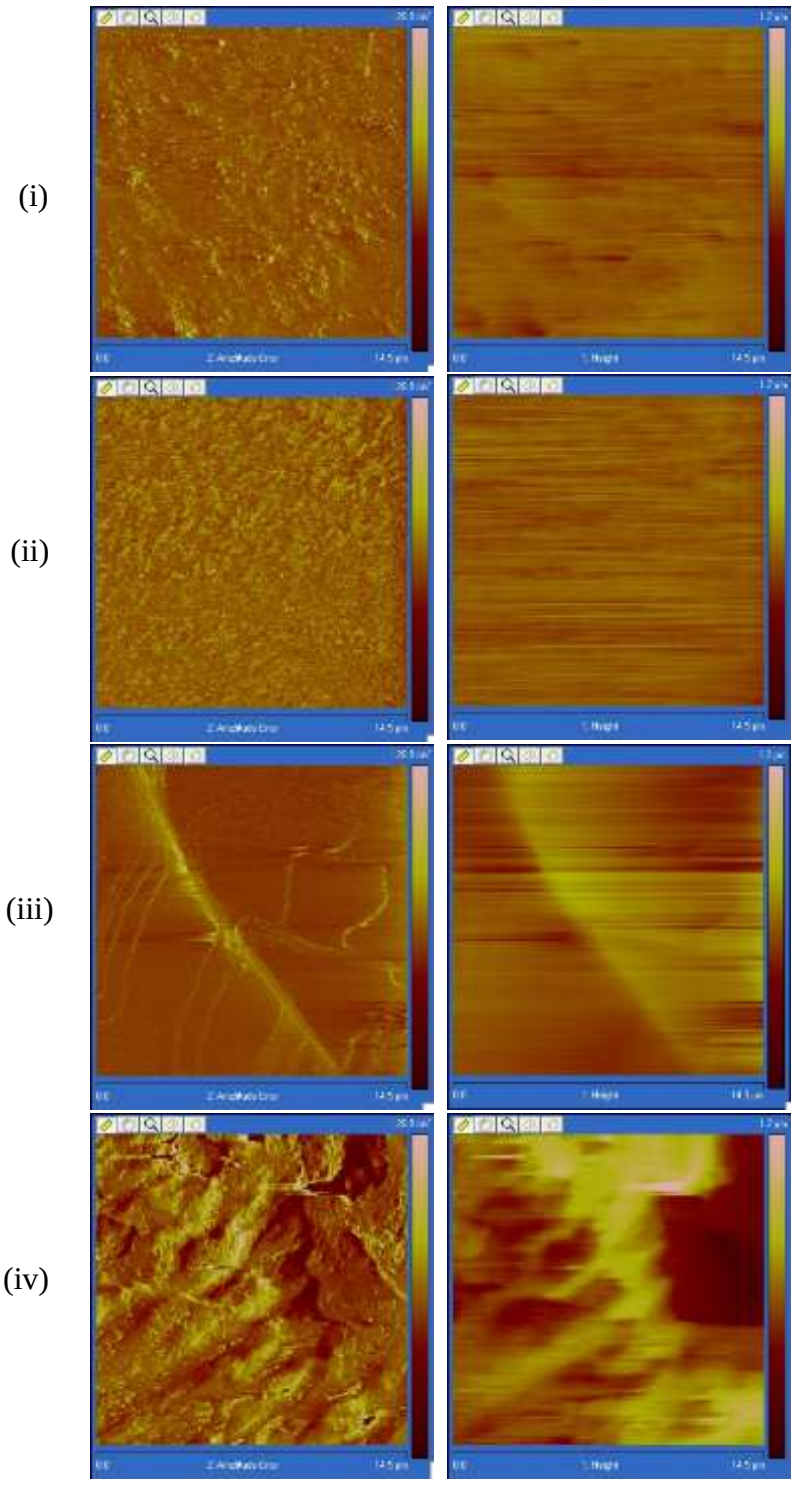

Figure 4.6: AFM deflection (a) and height images (b) for a dolomite chip not contacted with any fluid (i), a dolomite chip immersed in deionized water (ii), a dolomite chip immersed in the model oil (iii) and a dolomite chip immersed in the model oil, then in deionized water (iv).

In deionized water, the initial pH of unmodified and modified suspensions of all three samples without adding NaOH or HCl had a range of 9.4 to 9.6. At this pH, the zeta potential was negative for calcite and MEC while for dolomite it was positive for modified and unmodified suspension as shown in Figure 4.1.

When the calcite and MEC samples come in contact with deionized water, calcium ions will preferentially leave the surface and this will make the surface negatively charged. When pH of the solution is increased, more calcium ions will leave the surface and this will increase the magnitude of negative zeta potential of calcite. This phenomenon of calcite surface hydrolysis and dissolution has been widely discussed for calcite suspensions in water. [31, 43-45] Dissolution of calcite surface is very important when explaining the measured values of zeta potential in modified and unmodified suspensions. When the sample's powder was soaked in model oil, negatively charged carboxylic groups from the model oil adsorbed on the particles surface. When the modified powder was mixed with water, some of the surface calcium icon, most likely with attached carboxylic materials, preferentially left the surface. Adsorbed carboxylic materials left on the surface at the end of the hydrolysis process are believed to be the reason behind the slight difference in zeta potential between modified and unmodified powders. This explanation is in line with what was found by Hiorth et al 2010 [13] who claimed that carbonate dissolution is the mechanism responsible for the observed incremental recovery from spontaneous imbibition tests on Stevns Klint outcrop chalk.

Current finding on calcite dissolution is further supported by microscopic and AFM images shown in Figure 4.2 and Figure 4.5 respectively. From Figure 4.2c and Figure 4.2d, very clear rhombohedral shapes can be seen on the calcite chip immersed in deionized water as

well as the calcite chip immersed in model oil then in deionized water. These structures are deeper than the original surface as shown from AFM images in Figure 4.5. These shapes were not found on the pure calcite chip, or the calcite chip immersed in model oil. Therefore they are most likely created by dissolution of calcite surface. Another important observation from the optical microscope images is that the rhombohedral shapes on the chip immersed in model oil then in deionized water are deeper than the chip immersed in deionized water only. This can only happen when more calcium ions leave the calcite surface and it will increase the magnitude of negative surface charges. From this observation, it can be pointed out that adsorption of carboxylic materials on the calcite surface will enhance the dissolution of the calcite surface when contacted by water.

Very similar rhombohedral shapes which are caused by calcite dissolution were reported by Karoussi et al [37, 46] using AFM height and topology images of modified calcite chips on stearic acid which were exposed to deionized water. Smith et al [47] reported similar rhombohedral shapes caused by calcite dissolution when exposed to NaCl solutions. Very recently, Wael Abdallah and Ahmed Gmira [48] reported a rapid development of rhombohedral structures on Iceland spar calcite chips saturated in deionized water and NaCl brines using AFM.

Unmodified dolomite suspensions in deionized water had positive zeta potential at all pH values while it became negative on modified powder only at pH values higher than 11 as shown in Figure 4.1. These positive zeta potential values are due to the high concentration of divalent cations in the dolomite lattice. The effect of adsorbed carboxylic material on decreasing the magnitude of positive surface charges can be clearly seen by comparing zeta potential values of modified and unmodified suspensions. In some studies, the isoelectric

point of dolomite suspensions in aqueous solutions was found in ranges of pH 7 to pH 8, and this was attributed to dissolution of dolomite. [49, 50] In an old study, the zeta potential of dolomite suspensions in water was found to be positive for all pH values [51] . No significant surface dissolution was seen on the dolomite sample used in the current study as shown in the optical microscope (Figure 4.3) and AFM topographic images (Figure 4.6). This would explain the positive zeta potential values of unmodified dolomite. In the case of modified dolomite, the magnitude of the positive zeta potential has decreased and this can be only attributed to adsorption of carboxylic material from the model oil on dolomite surface.

Zeta potential values of unmodified MEC suspensions were all negative and they only became positive when the solution's pH decreased below pH 5. Negative surface charges in this case can be attributed to the possible presence of organic deposits on the MEC surfaces. In modified suspensions, zeta potential was negative for all pH values and the magnitude of values is higher than those found in unmodified suspensions. This is caused by adsorbed carboxylic materials from the model oil. From the microscopic images shown in Figure 4.4, some modifications occurred on the MEC surface when immersed in deionized water and model oil. However, due to the high roughness of the chips no solid conclusion can be made in regards to surface dissolution.

To investigate the effect of the brines' ionic strength on zeta potential of calcite, dolomite and MEC, a 0.574 M NaCl brine was prepared by dissolving 33.54 grams of NaCl in 1 liter of deionized water. Zeta potential measurements were conducted on modified powders of each sample. Comparison between zeta potential values in NaCl brine and deionized water is shown in Figure 4.7 at initial unadjusted pH values which had a very close range of 9.4

to 9.6. To check the effect of the 0.574 M NaCl brine on the surface structure of the three carbonates, a chip from each sample was first blown off by dry air then immersed in model oil for 24 hours. It was then immediately immersed in the NaCl brine for 24 hours, then the chips was taken out of the brine and allowed to dry at room temperature for 24 hours. Microscopic surface images for dried chips are shown in Figure 4.8.

From comparison of zeta potential values in Figure 4.7, some decrease in the magnitude of negative zeta potentials of modified calcite and MEC carbonates was noticed. In dolomite, very slight increase was noticed on the NaCl case. Very interesting results were found from the microscopic surface images on modified calcite shown in Figure 4.8b. Similar rhombohedral shape caused by calcite surface dissolution when immersed in deionized water (Figure 4.2d) were also seen on NaCl brine, but in the case of NaCl, surface dissolution was deeper than what was seen in the deionized water. In the case of NaCl brine, more calcium ions are expected to be released from the calcite surface in order to cause deeper rhombohedral shapes than those found on calcite chip immersed in deionized water. Based on the depth of the developed rhombohedral shapes in the calcite chip which was immersed in NaCl, higher zeta potential value was expected compared to the case of calcite suspension in deionized water. However, from Figure 4.7 it can be seen that in deionized water, the measured zeta potential was higher than the value found on calcite suspension in NaCl. The only explanation would be that such higher negative zeta potential values were suppressed by compression of electric double layer of ions atmosphere around charged particles caused by the high concentration of free salt ions present in the NaCl solution. [27]

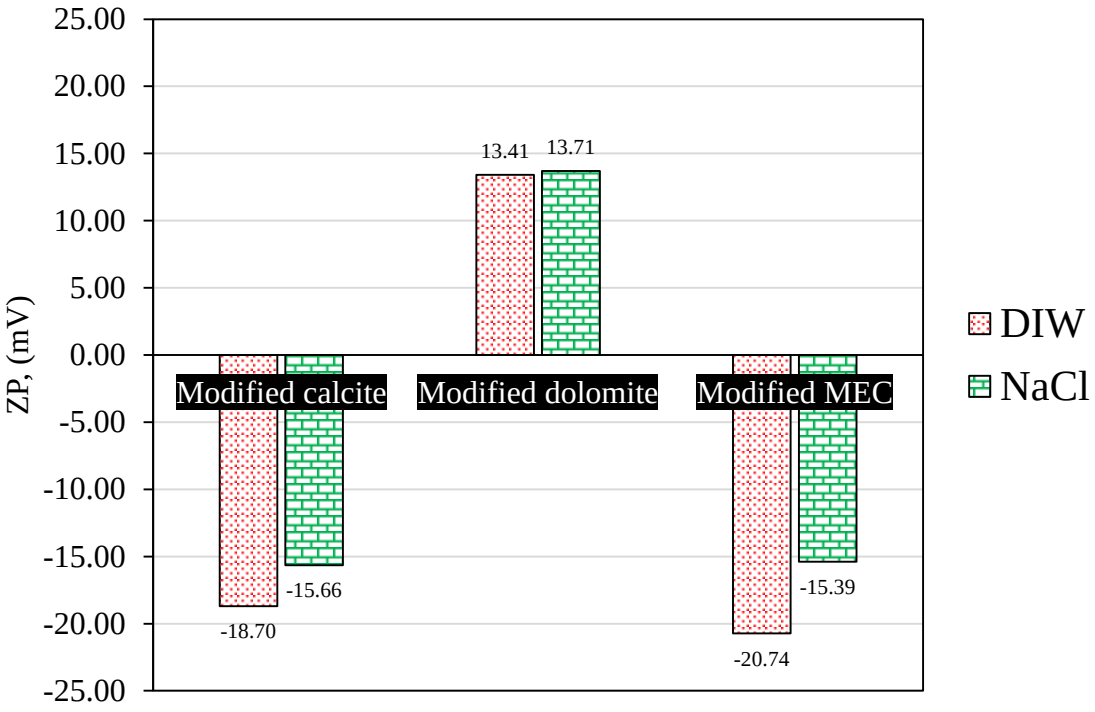

Figure 4.7: Comparison between zeta potential in deionized water and NaCl for modified calcite powder at initial pH 9.5 at 25 ºC.

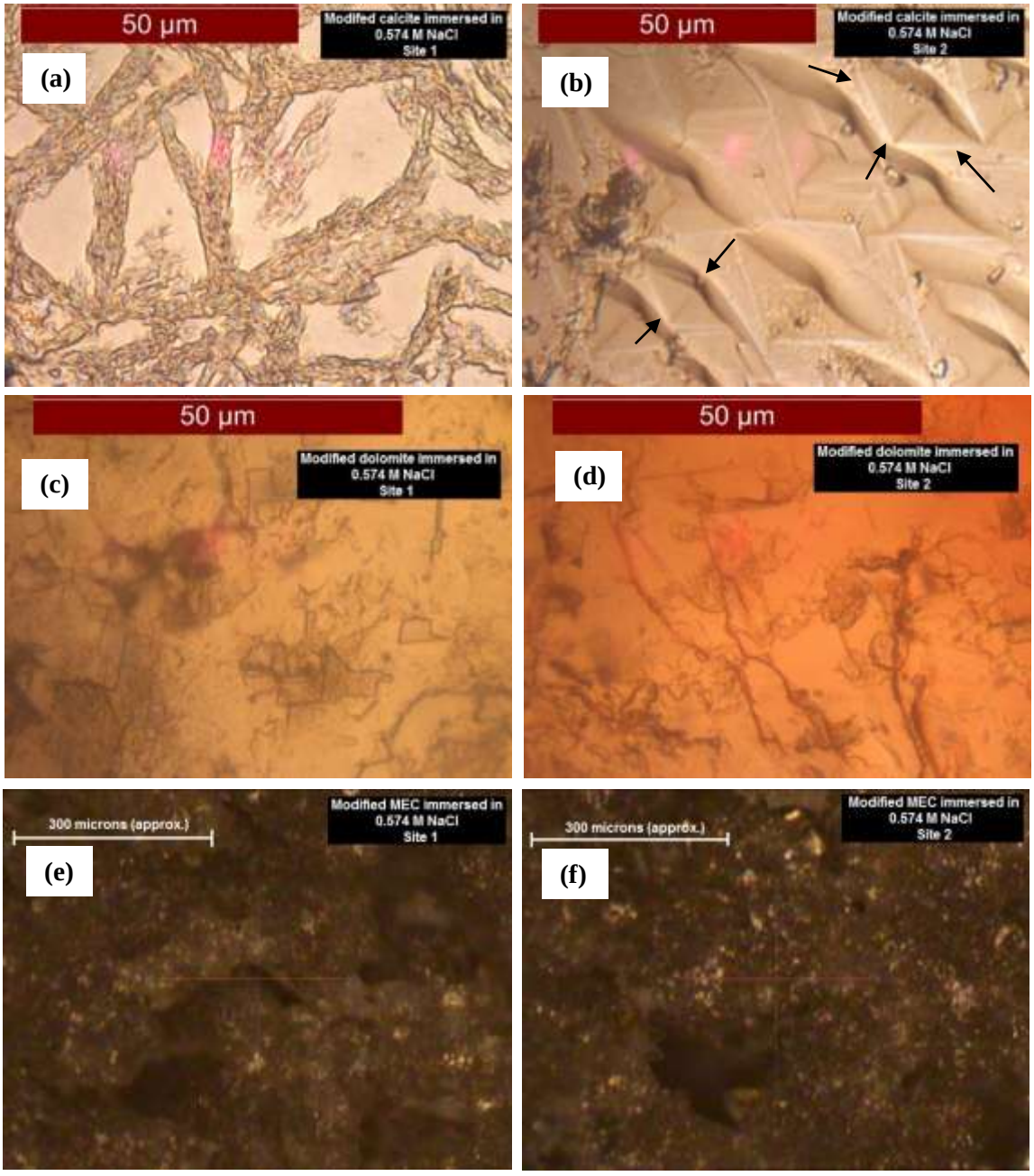

Figure 4.8: Microscopic surface images for a modified calcite chip (a & b), a modified dolomite chip (c & d) and a modified Middle East Carbonate chip (e & f), all immersed in 0.574 M NaCl.

4.2 Individual Effect of Potential Determining Ions

To evaluate the individual effect of Ca^{2+}, Mg^{2+} and SO_4^{2-} ions on the zeta potential of calcite, dolomite and MEC samples, with and without model oil, the concentration of each ion was individually increased starting from 50% AGSW and up to three times AGSW salinity levels. All brines were prepared in solutions of manipulated concentration of NaCl salt to have fixed ionic strength of 0.574 M as shown in Table 4.1. Zeta potential measurements for modified and unmodified powders of the three rock samples were conducted at initial unadjusted pH of conditioned mixtures in addition to pH 6 and pH 10. The same zeta potential trend with respect to pH, which was observed in deionized water (Figure 4.1) was also found in all brines used in this part. Zeta potential results presented in the rest of this chapter are only for initial unadjusted pH values.

The effect of increasing calcium ions' concentration on zeta potential of unmodified and modified powders of the three rock samples is shown in Figure 4.9. The effect of increasing magnesium ions' concentration is shown in Figure 4.10 for unmodified and modified powders of the three samples, and the effect of increasing sulfate ions' concentration is shown in Figure 4.11 for unmodified and modified powders of the three rock samples. Average values of pH 8.0, pH 8.7 and pH 9.4 were measured when increasing calcium, magnesium and sulfate ions respectively.

Table 4.1: Formulated brines for the individual effect of Ca^{2+}, Mg^{2+} and SO_4^{2-} ions

	Individual effect of calcium ions				Individual effect of magnesium ions				Individual effect of sulfate ions			
	Ca_0.5SW	Ca_SW	Ca_2SW	Ca_3SW	Mg_0.5SW	Mg_SW	Mg_2SW	Mg_3SW	SO_0.5SW	SO_SW	SO_2SW	SO_3SW
	ppm	ppm	ppm	ppm	ppm	ppm	ppm	ppm	ppm	ppm	ppm	ppm
Na^+	15,649	15,121	14,831	13,788	13,688	11,134	6,153	1,164	14,847	13,691	10,929	8,305
Cl^-	15,421	15,079	13,215	12,511	13,297	10,938	6,016	1,106	14,530	13,029	10,719	8,198
Ca^{2+}	326	652	1,304	1,956	-	-	-	-	-	-	-	-
Mg^{2+}	-	-	-	-	1,080	2,159	4,318	6,477	-	-	-	-
SO_4^{2-}	-	-	-	-	-	-	-	-	2,225	4,450	8,900	13,350
Ionic Strength	0.574	0.574	0.574	0.574	0.574	0.574	0.574	0.574	0.574	0.574	0.574	0.574

	Salts used (g/L)											
Na_2SO_4	0.00	0.00	0.00	0.00	0.00	0.00	0.00	0.00	3.29	6.58	13.15	19.73
NaCl	39.77	38.43	35.75	35.04	33.80	26.49	15.64	2.96	34.59	28.08	15.05	4.87
$CaCl_2.2H_2O$	1.20	2.39	4.79	7.18	0.00	0.00	0.00	0.00	0.00	0.00	0.00	0.00
$MgCl_2.6H_2O$	0.00	0.00	0.00	0.00	9.03	18.05	36.11	54.16	0.00	0.00	0.00	0.00
TDS (g/L)	40.97	40.82	40.53	42.22	42.83	44.54	51.74	57.12	37.88	34.65	28.20	24.59

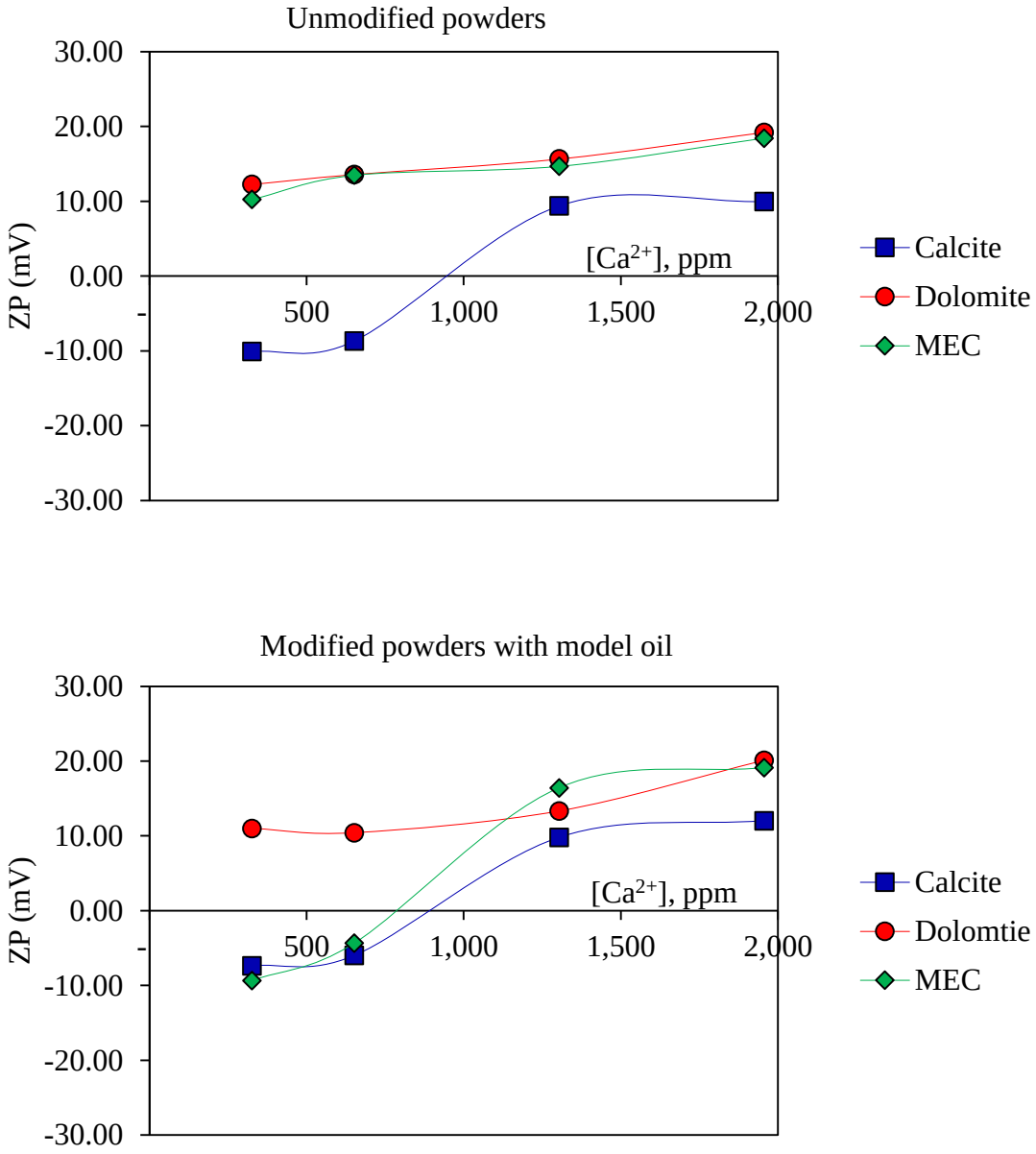

Figure 4.9: Effect of Ca^{2+} ions' concentration on the zeta potential of unmodified (top) and modified (bottom) calcite, dolomite and Middle East Carbonate powders at an average unadjusted system pH=8.0, at 25 ºC and 0.574 M constant ionic strength brine.

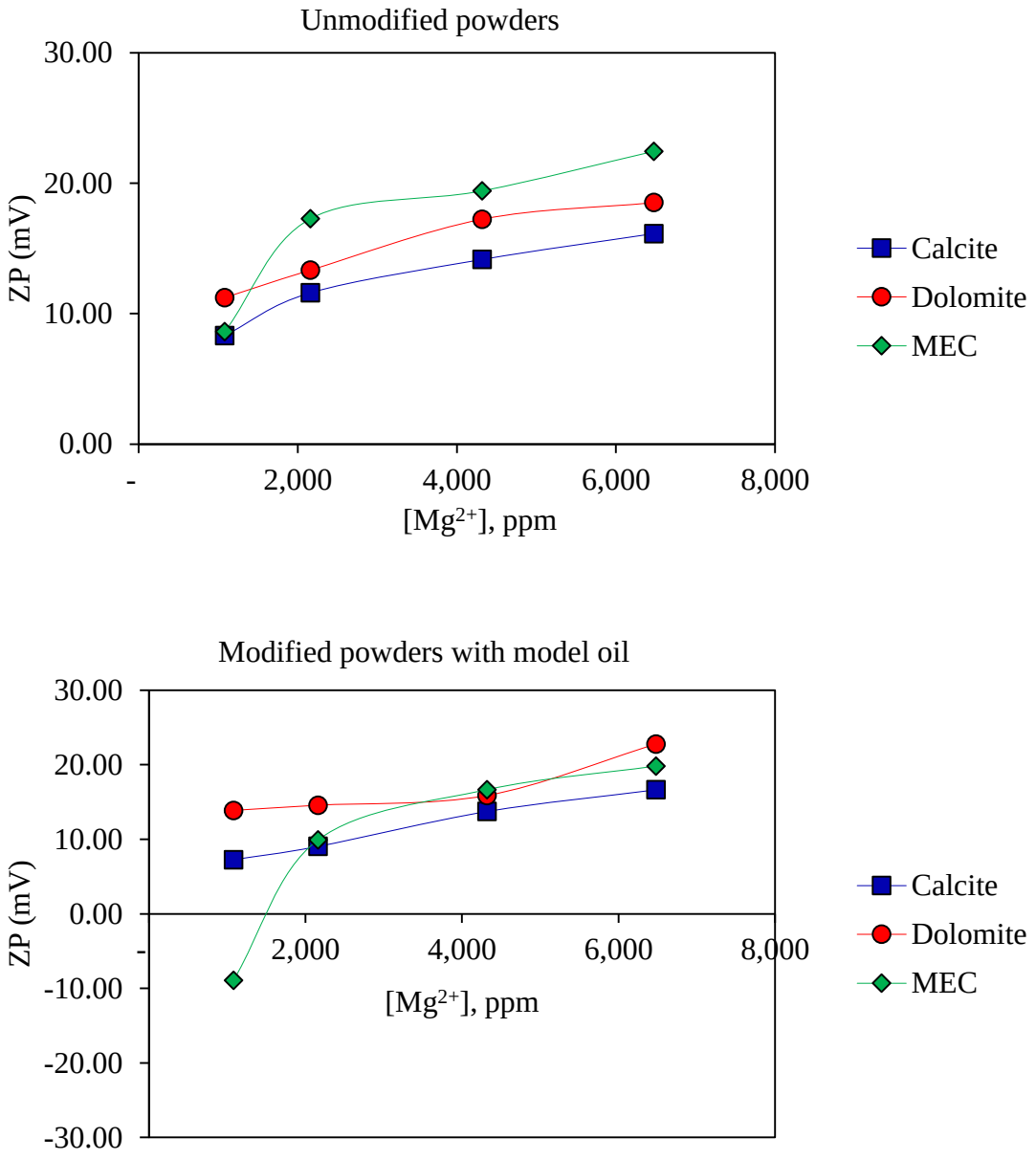

Figure 4.10: Effect of Mg^{2+}ions concentration on zeta potential of unmodified (top) and modified (bottom) calcite, dolomite and Middle East Carbonate powders at an average unadjusted system pH=8.7, at 25 ºC and 0.574 M constant ionic strength brine

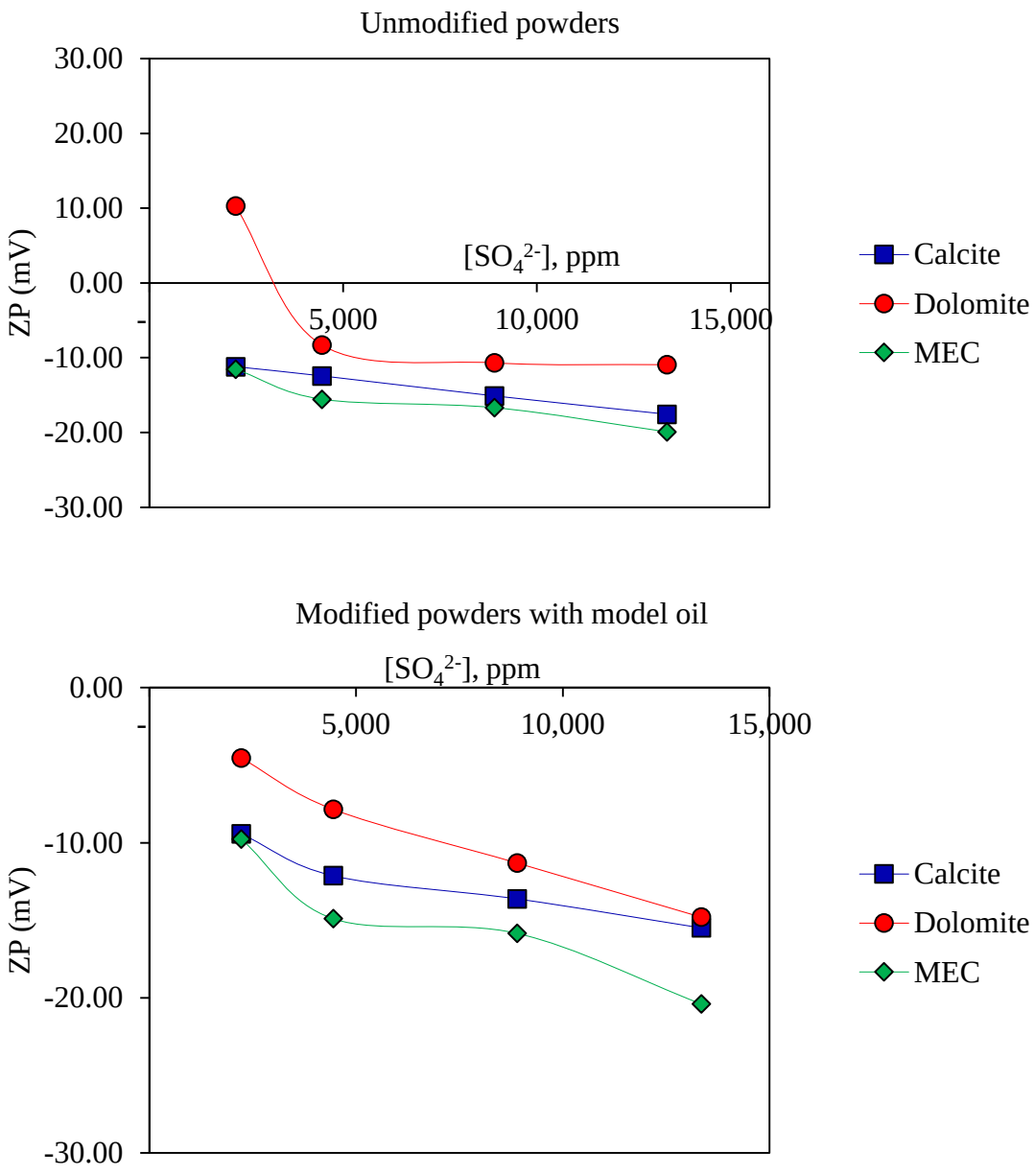

Figure 4.11: Effect of SO_4^{2-} ions' concentration on zeta potential of unmodified (top) and modified (bottom) calcite, dolomite and Middle East Carbonate powders at an average unadjusted system pH=9.4, at 25 ºC and 0.574 M constant ionic strength brine.

From the zeta potential trend shown in Figure 4.9, it can be clearly seen that increasing calcium ions' concentration will add more positive charges to all samples surface. In both samples of calcite, as well as modified MEC, calcium ions were able to completely alter the surface charges of these samples' suspensions when its concentration was increased more than AGSW salinity level. A plateau +10 mV surface charges was reached when calcium ions' concentration was increased more than two times AGSW salinity level, which can be considered as a saturation level of calcite from calcium ions. This observed influence of calcium ions' concentration towards calcium carbonate surfaces has been commonly reported in zeta potential studies which confirmed the ability of calcium ions to affect calcite surface charges. [30, 31] In chalk samples, it was found that increasing calcium ions' concentration increased the positive charges of unmodified powders. [9, 16]

On the other hand, magnesium had a very significant effect in changing surface charges of calcite and MEC suspensions from negative to positive and the magnitude of these positive charges increases as the concentration of magnesium ions increases as shown in Figure 4.10. Some studies showed that magnesium ions were found to have high affinity towards calcite surfaces based on zeta potential measurements and it was concluded that magnesium ions are able to displace calcium ions from calcite surface which might have attached oil phase. [26, 33]

The profound effect of sulfate ions on surface charges of carbonates can be sensed from its ability to change the surface charge of the strongly positive dolomite used in the current study to negative as shown in Figure 4.11. This super effect of the sulfate ions was the main finding of almost all studies investigating the ability of sulfate ions to alter the wettability of carbonates towards more water wet as discussed earlier in chapter 1. Similar

trends of zeta potential as a function of sulfate ions' concentration was reported for calcite samples, and in cases of oil wet calcite, it was concluded that adsorption of sulfate ions is able to displace negatively charged carboxylic materials. [4, 16, 30, 52]

From all experiments shown in this chapter, it was concluded that adsorption of negatively charged carboxylic material on calcite, dolomite and MEC surfaces will have a direct impact on surface charges of these rocks. The main mechanisms which are strongly believed to be responsible for removing these carboxylic materials are either the preferential dissolution of surface ions on which carboxylic materials are attached or displacement of adsorbed carboxylic material or surface ions with attached carboxylic materials by other potential determining ions present in the injection water, such as magnesium and sulfate, or a combination of these two possible mechanisms. It was also found that NaCl has an effect on calcite surface charges based on zeta potential measurements and microscopic surface images which in contradiction to the reported postulations on the innocent effect of NaCl salt on calcite surface.

CHAPTER 5

RELATIVE EFFECT OF POTENTIAL DETERMINING IONS

In presence of more than one PDI in the injected water, the individual effect of each ion will be affected. The difference between zeta potential measurements in the previous chapter and this chapter is that the zeta potential of calcite, dolomite and the MEC samples is evaluated as function of varied PDIs concentration while keeping the concentration of another PDI fixed at 50 % diluted AGSW level.

Very few papers addressed the relative effect of PDIs on the zeta potential of carbonate rocks considering only the relative effects of Ca^{2+} and SO_4^{2-} ions. [4, 9, 16] In the current study, a comprehensive evaluation of the effect of $Ca^{2+,}$ Mg^{2+} and SO_4^{2-} on each other is considered.

5.1 Relative Effect of Ca^{2+} Ions in Presence of Mg^{2+} and SO_4^{2-} Ions

Formulated brines for this part are shown in Table 5.1. For each brine, zeta potential measurements were conducted on unmodified and modified powder with model oil at initial unadjusted pH, pH 6 and pH 10 for calcite and dolomite powders, while in MEC, zeta potential was measured at initial unadjusted pH only. The same trend of zeta potential as function of pH which was noticed in deionized water (Figure 4.1) was also found for

most of the tested calcite and dolomite suspensions. For comparison purposes, only zeta potential results at initial unadjusted pH will be reported for all samples. The relative effect of calcium to magnesium and calcium to sulfate is shown in Figure 5.1 and Figure 5.2 respectively for unmodified and modified powders of calcite, dolomite and MEC.

In the case of calcite, when no magnesium ions were in the solution (Figure 4.9) surface charges were altered from negative to positive when calcium ions' concentration exceeds its level in AGSW. However, when magnesium ions were present (Figure 5.1), immediate alteration of negative surface charges took place at the lowest concentration of calcium ions in unmodified and modified conditions. Explanation of this should be made in light of the individual effect of magnesium ion shown in Figure 4.10, in which, it was found that magnesium ions alone were able to alter calcite surface charges from negative to positive. These results confirm the individual and relative effect of calcium and magnesium ions in altering calcite surface charges with stronger effect of magnesium than calcium. The magnesium ions are believed to be able to replace calcium ions from the calcite surface with attached carboxylic materials. [26] From zeta potential measurements, possible adsorption of magnesium ions on calcite can be endorsed based on the increase of positive surface charges. However, no similar basis can be made to explain the possible removal of adsorbed oil phase from zeta potential values only. On dolomite samples, no pronounced changes were found when comparing effect of increased calcium ions' concentration when magnesium ions are either present or not. This might be attributed to the original strong positive charges of dolomite (Figure 4.1) with which, the effect of increasing calcium ions' concentration will be masked and removing strongly adsorbed polar species will be difficult by only increasing calcium or magnesium ions' concentration. On the MEC

sample, the effect of altering surface charges by calcium ions in the presence of magnesium was more pronounced than what was found on the calcite sample, especially in modified MEC with model oil. This can be explained by the higher affinity of calcium and magnesium ions on the MEC surface. Based on the theory of surface dissolution of calcium carbonate surfaces, more carboxylic materials are expected to be released from the MEC sample than the calcite.

In presence of sulfate, (Figure 5.2) the magnitude of the developed positive surface charges by calcium ions has decreased compared to when no sulfate ions were in the solution. However, for MEC, sulfate ions were able to keep the negative surface charges state, even at high concentration of calcium ions. This indicates that adsorption of calcium ions decreases in presence of sulfate. Similar trends of the zeta potentials as function of the concentration ratio between calcium and sulfate ions were reported for chalk suspensions. [4, 9, 16]

Table 5.1: Formulated brines for the relative effect Mg^{2+} and SO_4^{2-} on Ca^{2+} ions

	$[Ca^{2+}]/[Mg^{2+}]$, $[Mg^{2+}]$ = 1080 ppm				$[Ca^{2+}]/[SO_4^{2-}]$, $[SO_4^{2-}]$ = 8900 ppm			
	Ca/Mg_B1	Ca/Mg_B2	Ca_Mg_B3	Ca_Mg_B3	Ca_SO_B1	Ca_SO_B2	Ca_SO_B3	Ca_SO_B4
	ppm	ppm	ppm	ppm	ppm	ppm	ppm	ppm
Na^+	13,092	12,793	11,978	10,923	14,370	14,239	13,344	12,449
Cl^-	13,060	12,366	11,310	10,625	14,110	13,155	12,223	11,291
Ca^{2+}	326	652	1,304	1,956	326	652	1,304	1,956
Mg^{2+}	1,080	1,080	1,080	1,080	-	-	-	-
SO_4^{2-}	-	-	-	-	2,225	2,225	2,225	2,225
$[Ca^{2+}]/[Mg^{2+}]$, $[Ca^{2+}]/[SO_4^{2-}]$ Ratio	0.30	0.60	1.21	1.81	0.15	0.29	0.59	0.88
Ionic Strength	0.574	0.574	0.574	0.574	0.574	0.574	0.574	0.574
	Salts needed (g/L)							
Na_2SO_4	-	-	-	-	3.29	3.29	3.29	3.29
NaCl	33.27	32.51	30.44	27.76	33.81	33.48	31.21	28.93
$CaCl_2.2H_2O$	1.20	2.39	4.79	7.18	1.20	2.39	4.79	7.18
$MgCl_2.6H_2O$	9.03	9.03	9.03	9.03	-	-	-	-
TDS (g/L)	43.50	43.94	44.26	43.97	38.29	39.16	39.28	39.40

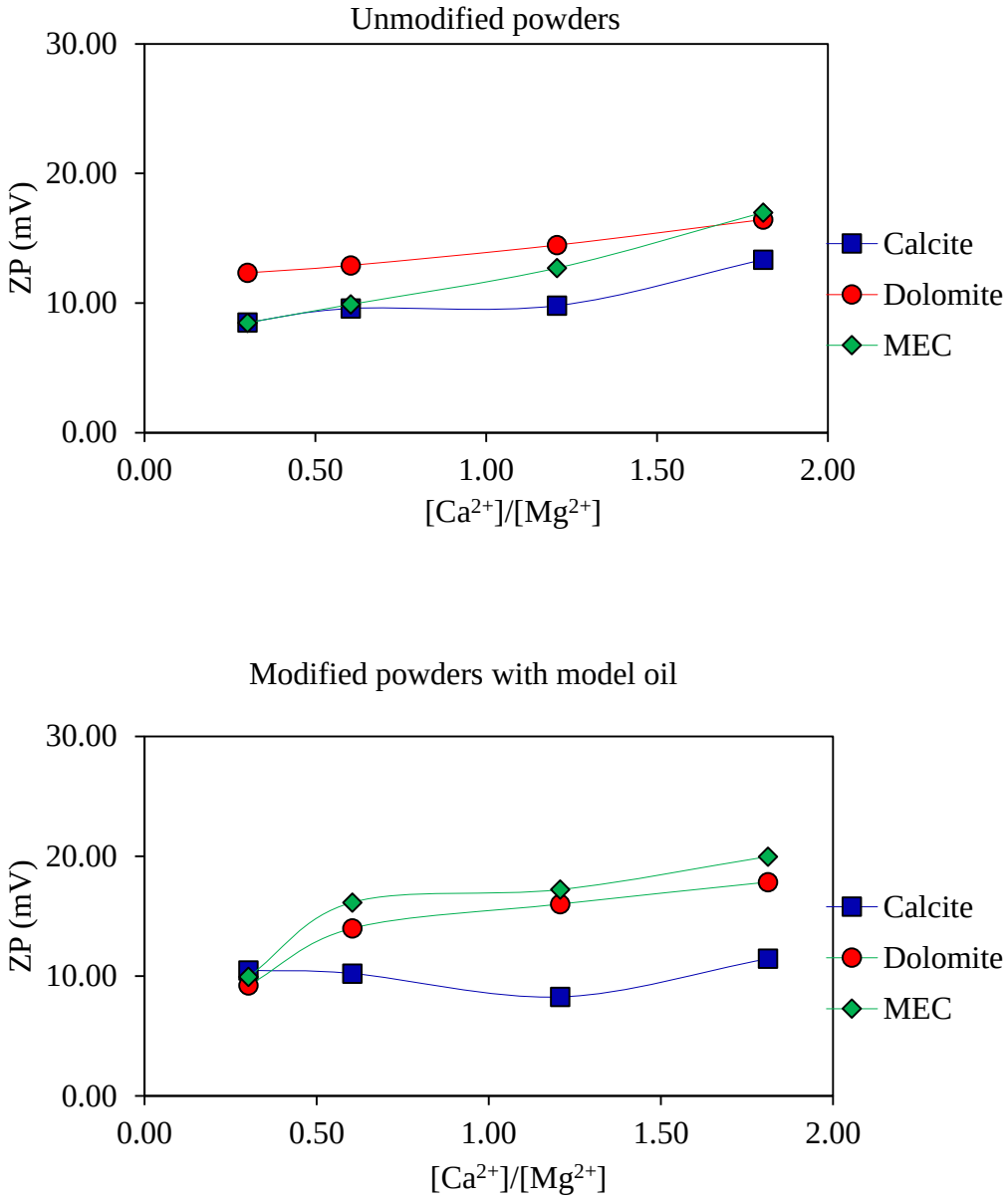

Figure 5.1: Relative effect of Ca^{2+} ions in presence of Mg^{2+} ions on the zeta potential of unmodified (top) and modified (bottom) calcite, dolomite and Middle East Carbonate powders at an average unadjusted system pH=8.2, at 25 ºC and at 0.574 M constant ionic strength brine.

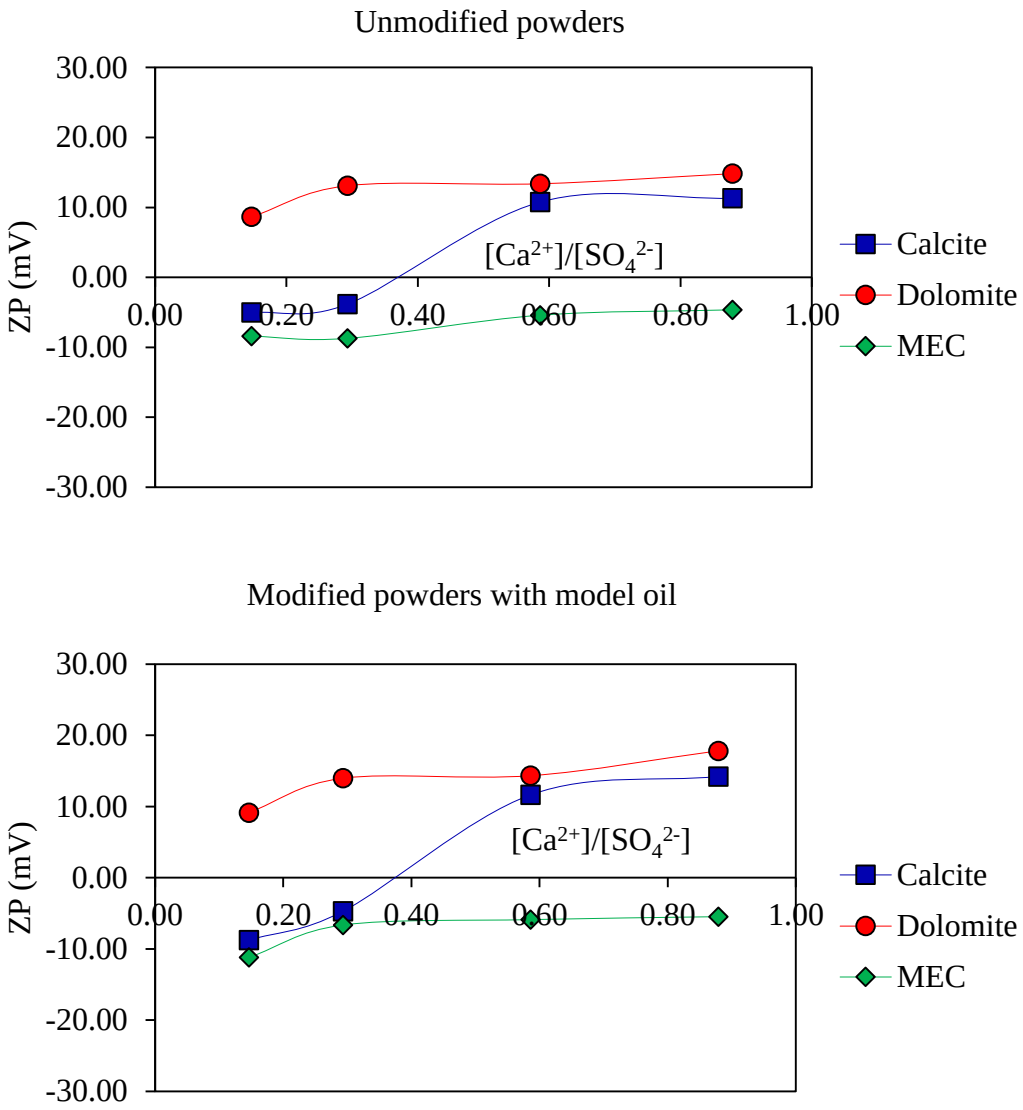

Figure 5.2: Relative effect ofCa^{2+} ions in presence of SO_4^{2-} ions on the zeta potential of unmodified (top) and modified (bottom) calcite, dolomite and Middle East Carbonate powders at an average unadjusted system pH=8.2, at 25 ºC and at 0.574 M constant ionic strength brine.

5.2 Relative Effect of Mg^{2+} Ions in Presence of Ca^{2+} and SO_4^{2-} Ions

Effect of increasing magnesium ions' concentration on zeta potential of unmodified and modified powders of calcite, dolomite and MEC is shown in Figure 5.3 when calcium is present at a fixed concentration, and in Figure 5.4, when sulfate is present at a fixed concentration.

In presence of calcium ions (Figure 5.3) it was interestingly found that the individual effect of the magnesium ions on adding more positive charges on the three carbonate samples has slightly decreased compared to when the magnesium ions were alone in the solution (Figure 4.10). This indicates that the affinity of magnesium ions to adsorb on carbonate surfaces decreases in presence of calcium. At ambient temperature, as in our current case, it was reported that the calcium ions are better wettability modifier than the magnesium ions. [26] A similar effect was noticed when sulfate ions were present as shown in Figure 5.4. In MEC sample, the developed positive surface charges by magnesium ions (Figure 4.10) have been completely altered to be negative as a result of the present of sulfate, and only at very high concentration of magnesium ions positive charges were re-developed.

From these results, it can be concluded that the reported ability of magnesium ions to replace calcium ions from carbonate surfaces, with possible attached carboxylic material, can be affected by the presence of calcium and sulfate ions in solution.

Table 5.2: Formulated brine for the relative effect of Ca^{2+} and SO_4^{2-} on Mg^{2+} ions

	$[Mg^{2+}]/[Ca^{2+}]$, $[Ca^{2+}]$ = 326 ppm				$[Mg^{2+}]/[SO_4^{2-}]$, $[SO_4^{2-}]$ = 8900 ppm		
	Mg/Ca_B1	Mg/Ca_B2	Mg/Ca_B3	Mg/Ca_B4	Mg/SO_B1	Mg/SO_B2	Mg/SO_B3
	ppm	ppm	ppm	ppm	ppm	ppm	ppm
Na^+	13,092	10,698	6,427	730	12,738	10,023	5,529
Cl^-	13,060	10,453	4,438	620	11,479	9,366	3,694
Ca^{2+}	326	326	326	326	-	-	-
Mg^{2+}	1,080	2,159	4,318	6,477	1,080	1,080	1,080
SO_4^{2-}	-	-	-	-	2,225	2,225	2,225
$[Mg^{2+}]/[Ca^{2+}]$, $[Mg^{2+}]/[SO_4^{2-}]$ Ratio	3.31	6.62	13.25	19.87	0.49	0.97	1.94
Ionic Strength	0.574	0.574	0.574	0.574	0.574	0.574	0.574

	Salts needed (g/L)						
Na_2SO_4	-	-	-	-	3.29	3.29	3.29
NaCl	34.49	27.19	16.33	1.86	29.66	22.77	11.34
$CaCl_2.2H_2O$	1.20	1.20	1.20	1.20	-	-	-
$MgCl_2.6H_2O$	9.03	18.05	36.11	54.16	9.03	18.05	36.11
TDS (g/L)	44.72	46.44	53.64	57.21	41.98	44.11	50.74

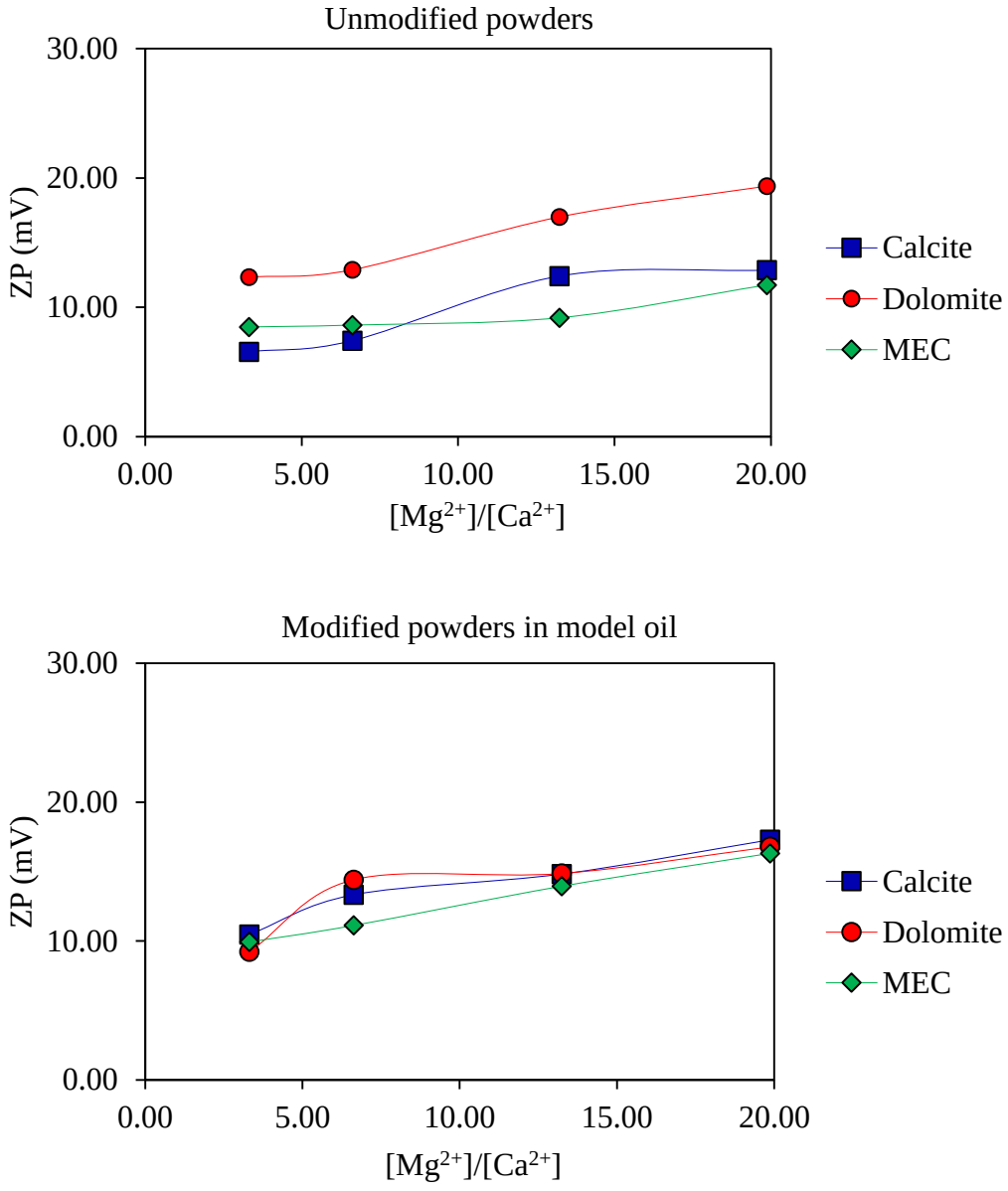

Figure 5.3: Relative effect of Mg^{2+} ions in presence of Ca^{2+} ions on the zeta potential of unmodified (top) and modified (bottom) calcite, dolomite and Middle East Carbonate powders at an average unadjusted system pH=8.4 and at 25 ºC and at 0.574 M constant ionic strength brine.

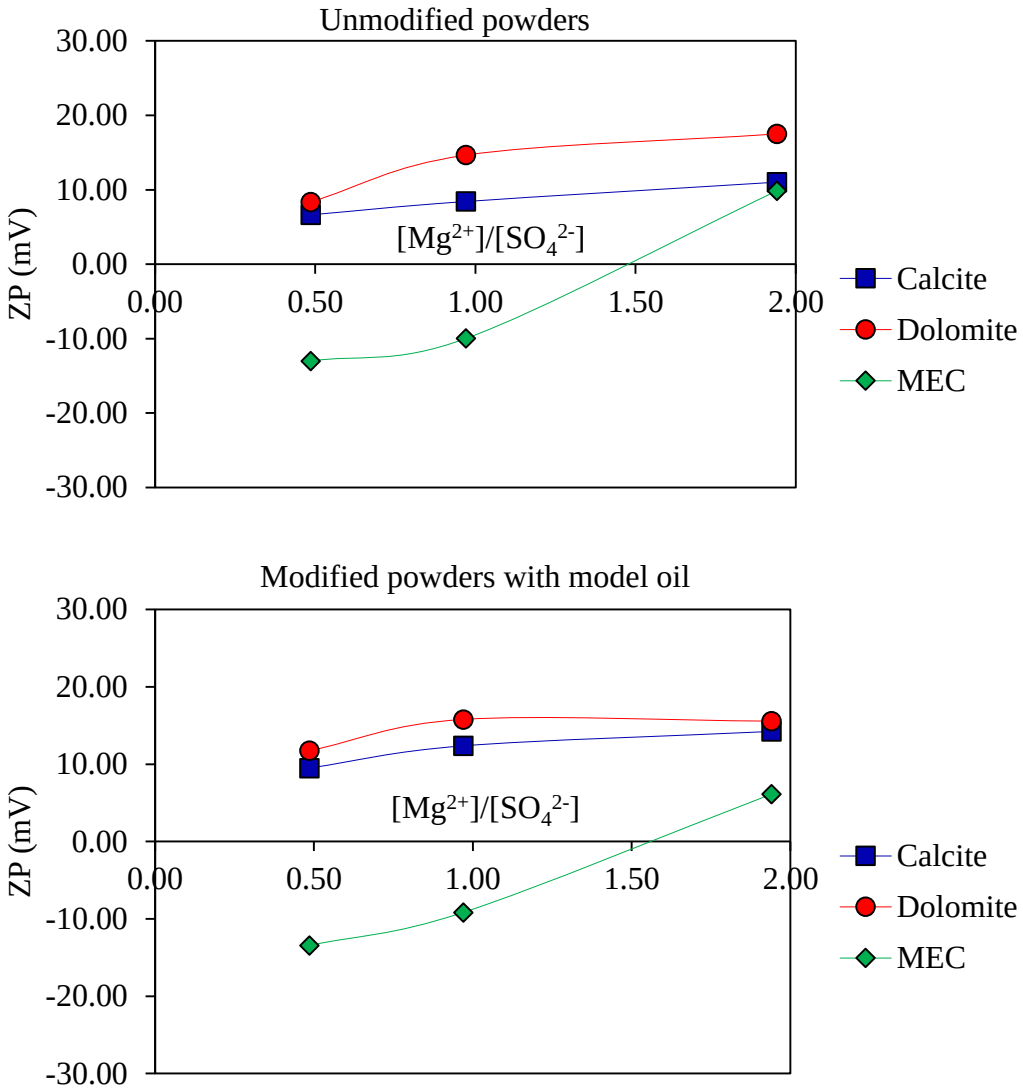

Figure 5.4: Relative effect of Mg^{2+} ions to in presence of SO_4^{2-} ions on the zeta potential of unmodified (top) and modified (bottom) calcite, dolomite and Middle East Carbonate powders, at an average unadjusted system pH=8.9, at 25 ºC and at 0.574 M constant ionic strength brine.

5.3 Relative Effect of SO_4^{2-} Ions in Presence of Ca^{2+} and Mg^{2+} Ions

To evaluate the effect of Ca^{2+} and Mg^{2+} ions on the developed surface charges by SO_4^{2-} ions, the concentration of SO_4^{2-} ions was gradually increased starting from 50% diluted AGSW and up to 3 times AGSW salinity level while keeping the concentration of Ca^{2+} and Mg^{2+} ions fixed at 50% diluted AGSW salinity levels. Formulated brines are shown in Table 5.3. Figure 5.5 shows the results when Ca^{2+} ions are present while Figure 5.6 shows the results when Mg^{2+} ions are present.

In the presence of Ca^{2+} ions, slight decrease in the magnitude of the negative zeta potential of unmodified calcite, dolomite and MEC, was found as compared to the individual effect of sulfate shown in Figure 4.11 while no significant changes were found in modified samples as shown in Figure 5.5. This indicates that Ca^{2+} ions at 50% diluted AGSW concentration would have negligible effect on the affinity of sulfate towards carbonate surfaces. Zhang and Austad [16] found that adsorption of calcium ions can enhance the adsorption of sulfate based on zeta potential and adsorption studies on chalk powder. This conclusion was not observed on the measured zeta potential of calcite, dolomite and MEC samples used in our study. On the other hand, in the presence of magnesium ions was, the generated negative surface charges on calcite and dolomite powders by sulfate ions (Figure 4.11) were altered from negative to positive and only re-developed at very high concentration of sulfate ion (Figure 5.6). In MEC, however, no such effect was found on zeta potential values compared to the individual effect of sulfate ions.

Table 5.3: Formulated brine for the relative effect of Ca^{2+} and Mg^{2+} on SO_4^{2-} ions

	$[SO_4^{2-}]/[Ca^{2+}]$, $[Ca^{2+}]$ = 326 ppm				$[SO_4^{2-}]/[Mg^{2+}]$, $[Mg^{2+}]$ = 1080 ppm		
	SO_Ca_B1	SO_Ca_B2	SO_Ca_B3	SO_Ca_B4	SO_Mg_B1	SO_Mg_B2	SO_Mg_B3
	ppm	ppm	ppm	ppm	ppm	ppm	ppm
Na^+	14,370	13,132	10,455	7,930	12,738	10,942	8,425
Cl^-	14,110	12,734	10,295	7,620	11,479	10,963	8,276
Ca^{2+}	326	326	326	326	-	-	-
Mg^{2+}	-	-	-	-	1,080	1,080	1,080
SO_4^{2-}	2,225	4,450	8,900	13,350	2,225	4,450	8,900
$[SO_4^{2-}]/[Ca^{2+}]$, $[SO_4^{2-}]/[Mg^{2+}]$, Ratio	0.15	13.65	27.30	40.95	2.06	4.12	8.24
Ionic Strength	0.574	0.574	0.574	0.574	0.574	0.574	0.574
	Salts needed (g/L)						
Na_2SO_4	3.29	6.58	13.15	19.73	3.29	6.58	13.15
NaCl	33.81	27.96	15.74	3.91	29.66	22.39	10.59
$CaCl_2.2H_2O$	1.20	1.20	1.20	1.20	-	-	-
$MgCl_2.6H_2O$	-	-	-	-	9.03	9.03	9.03
TDS (g/L)	38.29	35.73	30.09	24.84	41.98	38.00	32.77

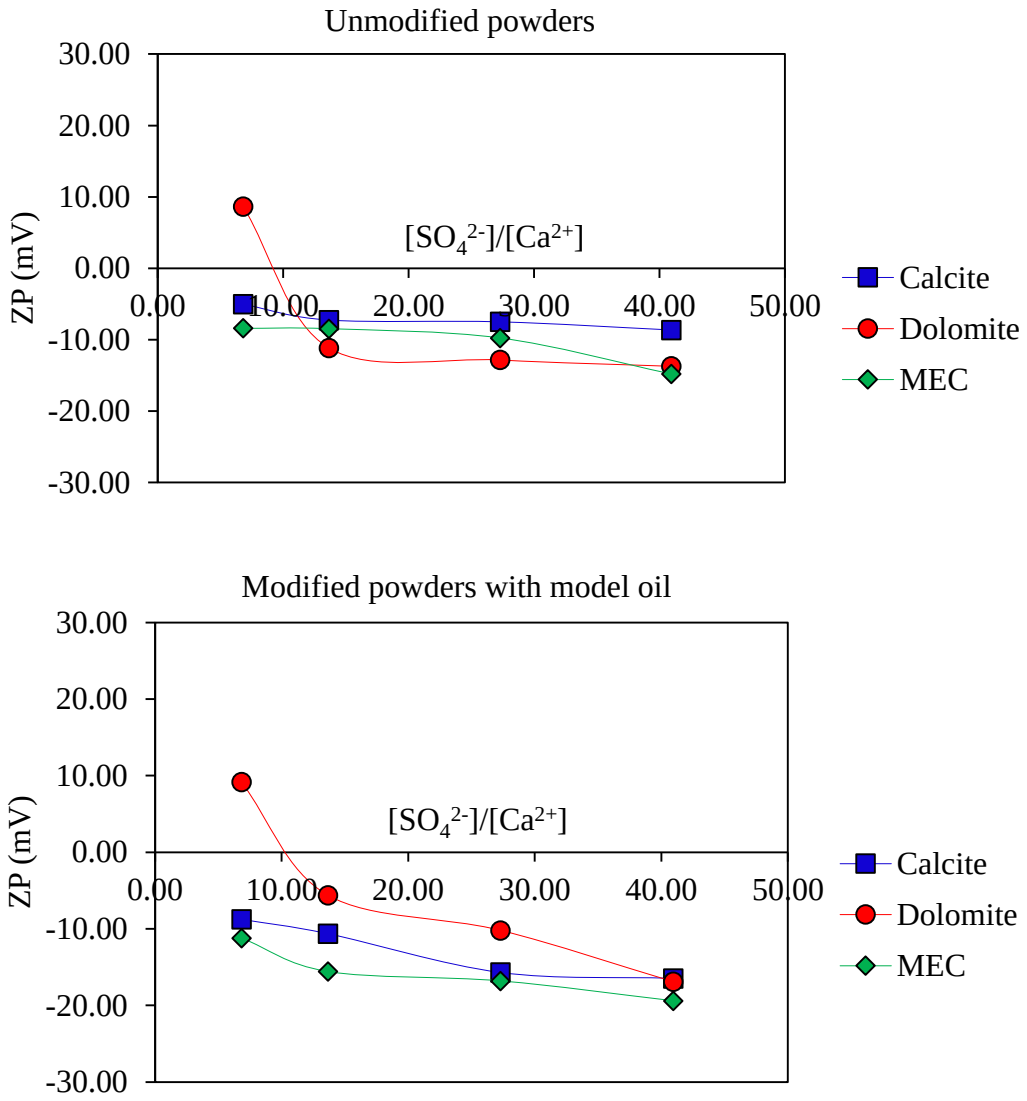

Figure 5.5: Relative effect of SO_4^{2-} ions in presence of Ca^{2+} ions on the zeta potential of unmodified (top) and modified (bottom) calcite, dolomite and Middle East Carbonate powders at an average unadjusted system pH=8.7, at 25 ºC and at 0.574 M constant ionic strength brine

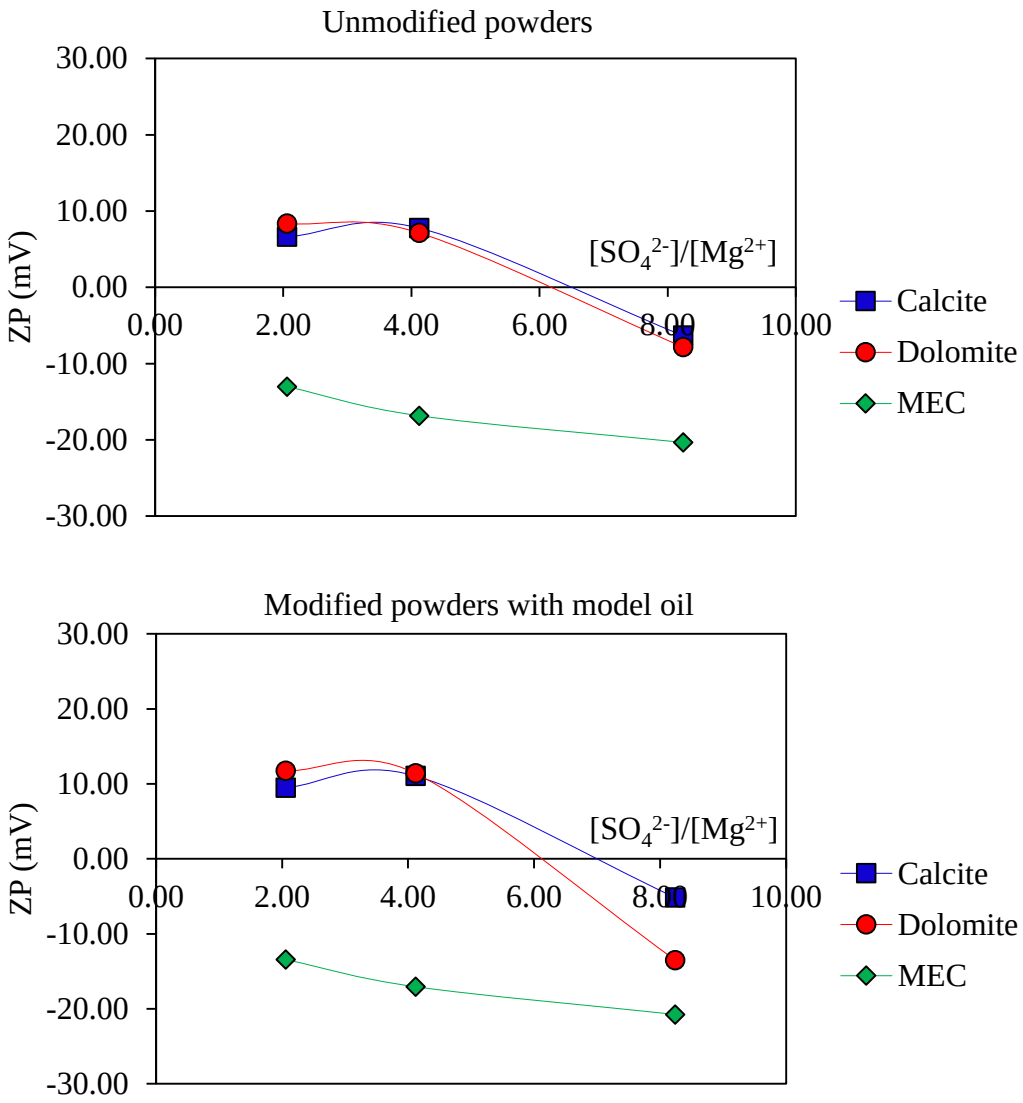

Figure 5.6: Relative effect of SO_4^{2-} ions in presence of Mg^{2+} ions on the zeta potential of unmodified (top) and modified (bottom) calcite, dolomite and Middle East Carbonate powders at an average unadjusted system pH=9.1, at 25 °C and at 0.574 M constant ionic strength brine

Out of the results present in this chapter, it can be concluded that the individual effect of potential determining ions in modifying carbonates surface charges, and thus altering the wettability, is affected by the presence of other potential determining ions, and the degree of effect depends on the relative concentration of each ion in the injected water. The effect of the magnesium ions was found to be dominant, either individually, or when present with other potential determining ions. Such strong effect would negatively affect the ability of other PDIs to adsorb on carbonate surfaces which is believed to help desorbing carboxylic material from the surface. On the other hand, this strong ability of magnesium ions to bring more positive charges could be beneficial if it could replace calcium ions with attached carboxylic material from carbonate surfaces.

CHAPTER 6

EFFECT OF MODIFIED ARABIAN GULF SEAWATER

In this chapter, a step forward towards investigating the relative effect of potential determining ions was taken by increasing the concentration of $Ca^{2+,}$ Mg^{2+} and SO_4^{2-} ions, but this time, all the three ions are present in the same brine. Formulated brines were made in an ionic composition equivalent to 50% diluted AGSW, and the ionic strength was kept constant by manipulating the concentration of NaCl salt. Formulated brines are shown in Table 6.1.

Zeta potential values of modified carbonates with model oil in AGSW and 50% diluted AGSW are shown in Figure 6.1. In Figure 6.2, zeta potential values in modified 50% diluted AGSW are shown when the concentrations of PDIS are increased. In addition to zeta potential measurements, modified carbonate chips with model oil were studied using AFM, SEM and EDS to evaluate the effect of varying the concentration of $Ca^{2+,}$ Mg^{2+} and SO_4^{2-} on the topology of these chips and to correlate any surface growth or modifications to the measured zeta potential values.

Table 6.1: Formulated brines for modified Arabian Gulf Seawater

Ions	AGSW	AGSW* (Twice diluted)	AGSW*2Ca	AGSW*4Ca	AGSW*2Mg	AGSW*4Mg	AGSW*2S	AGSW*4S
	ppm	ppm	Ppm	ppm	ppm	ppm	ppm	ppm
Na^{+}	18,043	9,022	9,022	8,400	7,550	4,400	8,550	6,850
Ca^{++}	652	326	652	1,304	326	326	326	326
Mg^{++}	2,159	1,080	1,080	1,080	2,159	4,318	1,080	1,080
Cl^{-}	31,808	15,904	14,900	13,500	12,000	4,300	13,500	9,500
$SO4^{--}$	4,450	2,225	2,225	2,225	2,225	2,225	4,450	8,900
HCO_3^{-}	173	87	87	87	87	87	87	87
TDS, ppm	57,285	28,643	27,965	26,595	24,347	15,656	27,992	26,742
Ionic Strength, M	1.15	0.573	0.575	0.574	0.574	0.575	0.575	0.574
	Salts needed, g/L							
NaHCO3	0.24	0.12	0.12	0.12	0.12	0.12	0.12	0.12
Na_2SO_4	6.58	3.29	3.29	3.29	3.29	3.29	6.58	13.16
NaCl	40.28	20.14	20.14	18.56	16.40	8.39	16.24	6.50
$CaCl_2*2H_2O$	2.39	1.20	2.39	4.78	1.20	1.20	1.20	1.20
$MgCl_2*6H_2O$	18.06	9.03	9.03	9.03	18.06	36.11	9.03	9.03

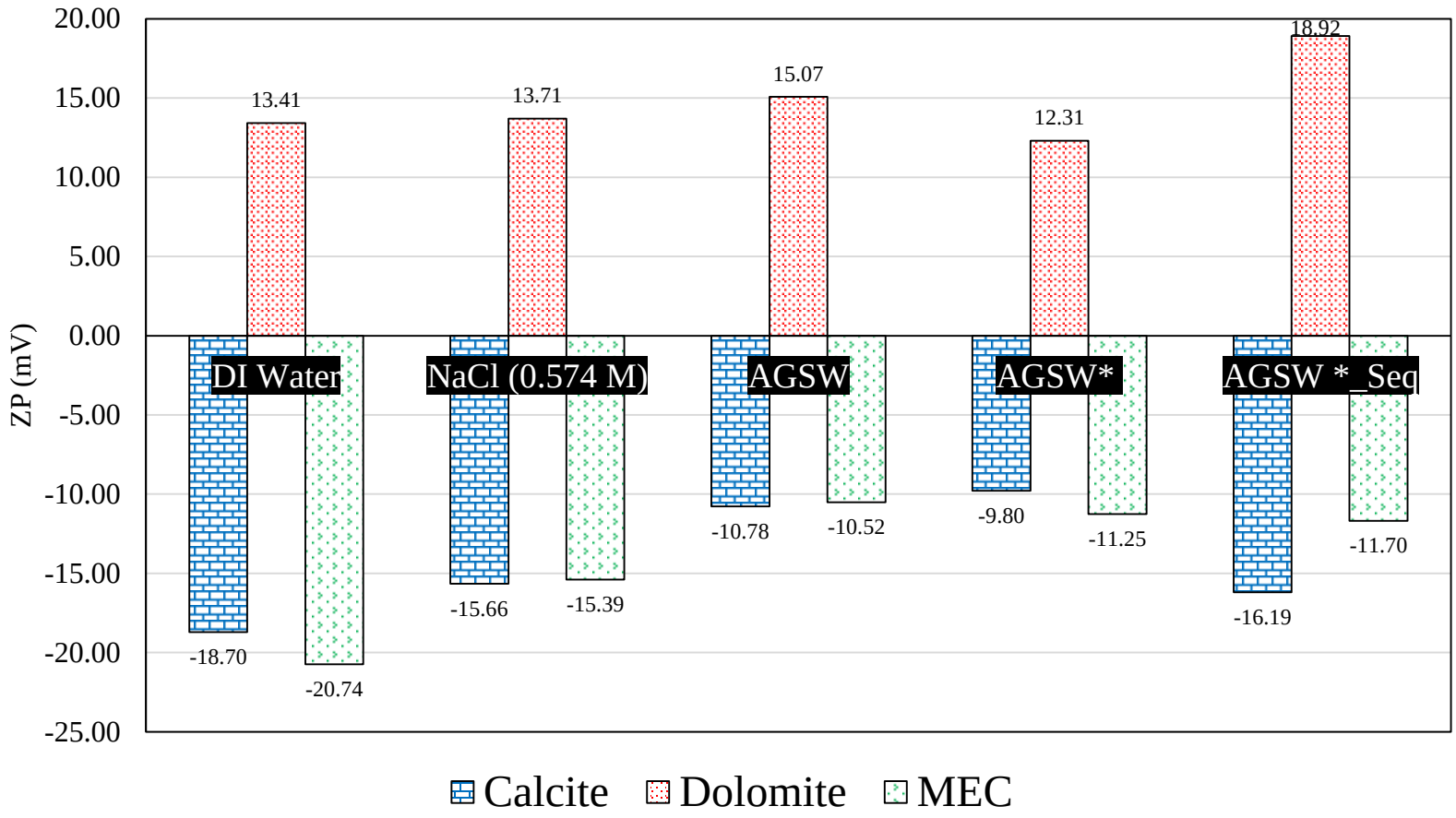

Figure 6.1: Comparison between zeta potential values of modified calcite, dolomite and Middle East Carbonate powders oil in deionized water, NaCl, Arabian Gulf Seawater and 50% diluted Arabian Gulf Seawater (AGSW*) and 50% diluted Arabian Gulf Seawater after primary conditioning with original Arabian Gulf Seawater (AGSW*-seq), all at initial unadjusted pH and at 25 ºC.

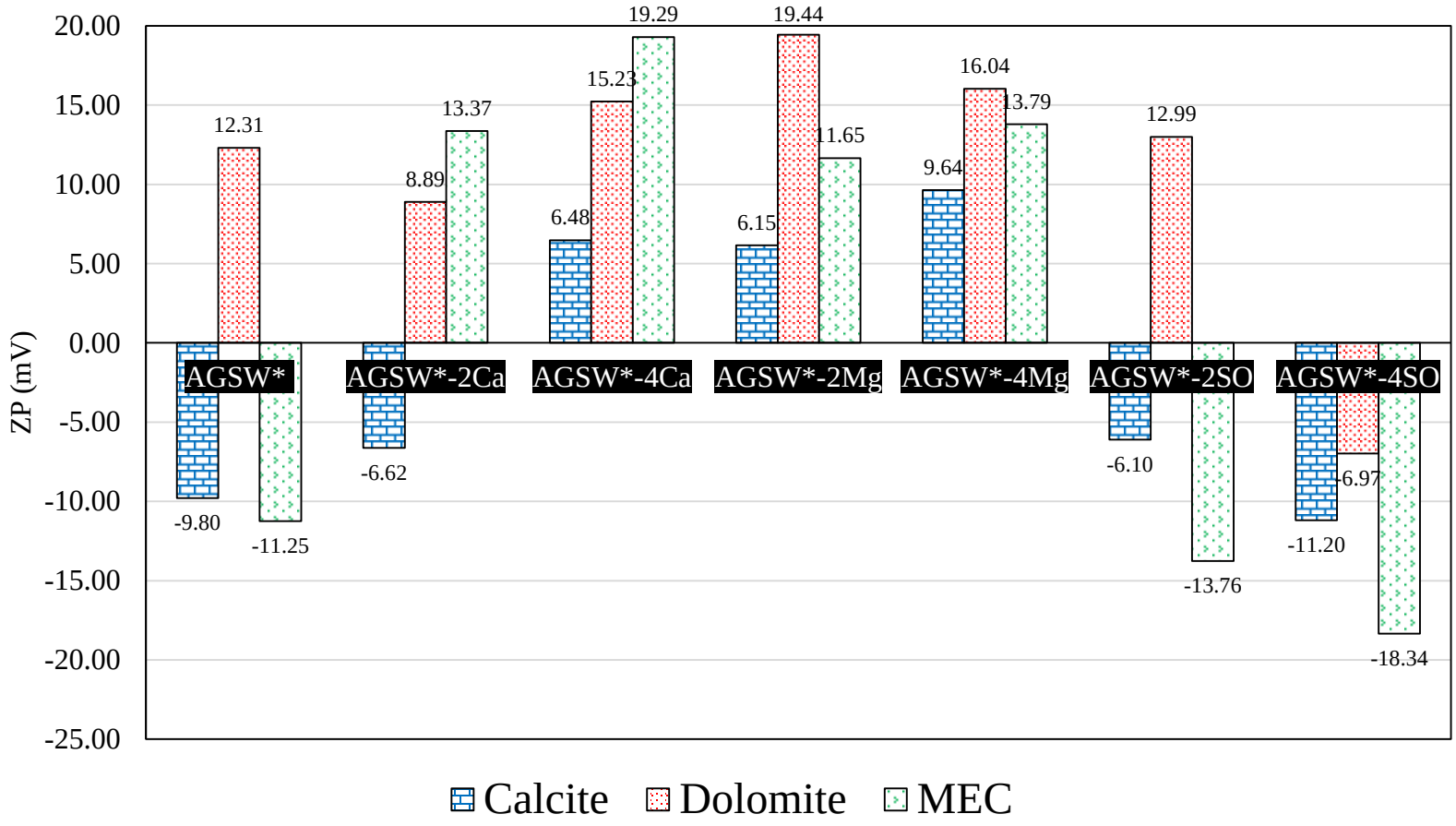

Figure 6.2: Effect of increasing PDIs concentrations of the 50% diluted Arabian Gulf Seawater on zeta potential of modified calcite, dolomite and Middle East Carbonate powders at initial unadjusted pH (~ pH 7.8) and at 25 ºC.

6.1 Surface Characterization of the Model Oil Adsorption

Modified chips with model oil from the three rock samples were characterized by SEM and EDS to confirm the adsorption of oil shown earlier by optical microscopic images in Figure 4.2b and Figure 4.3b for calcite and dolomite respectively. Results of SEM and EDS are shown in Figure 6.3 for modified calcite and Figure 6.4 for modified dolomite.

Adsorption of model oil can be indirectly confirmed from the EDS spectra. As it can be seen in both samples, the percentage of carbons on analyzed shiny deposits is very high compared to clear spots on other site of the rock where no deposits are found. The increase of carbon ions' concentration only comes from adsorbed stearic acid.

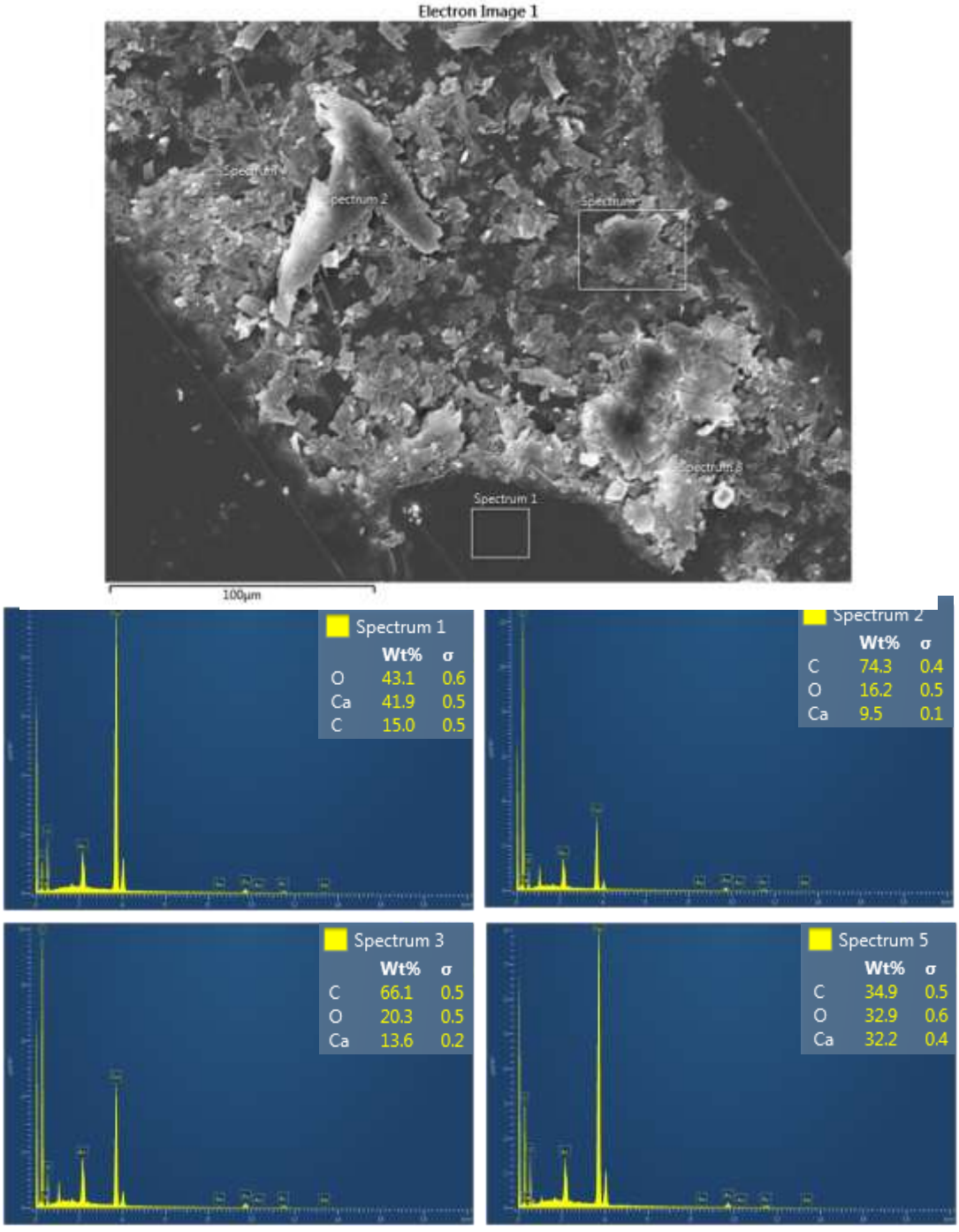

Figure 6.3: SEM image (top) and EDS spectra (bottom) of a modified calcite chip modified with model oil.

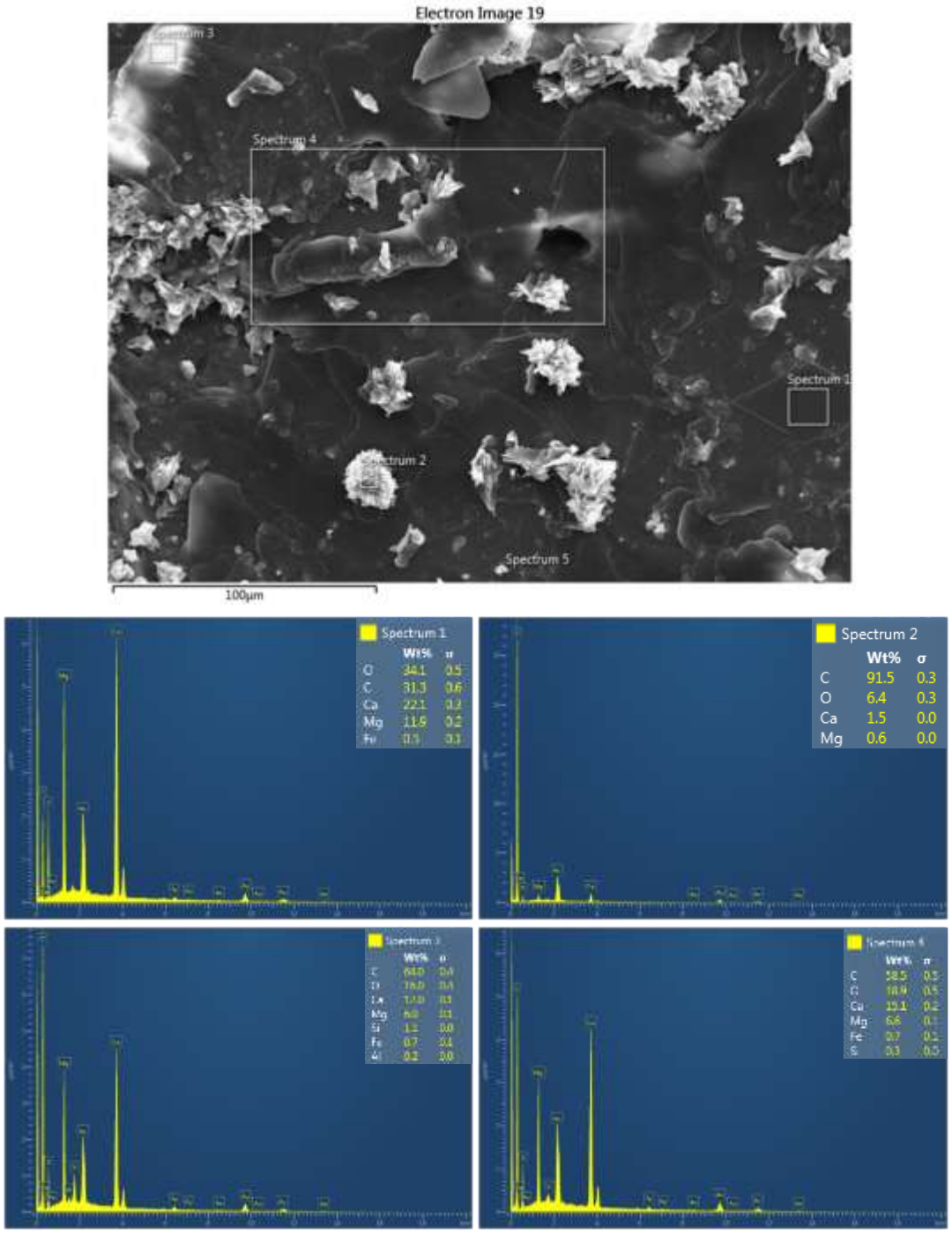

Figure 6.4: SEM image (top) and EDS spectra (bottom) of a modified dolomite chip modified with model oil.

6.2 Effect of Unmodified Arabian Gulf Seawater

On calcite, unmodified AGSW developed negative surface charges as shown in Figure 6.1, and as discussed in the previous chapter, this is mainly caused by adsorption of sulfate ions. From the optical microscopic and AFM images shown in Figure 6.5 and the SEM image shown in Figure 6.8, it can be clearly seen that very significant changes occurred on the calcite surface compared to the topology of the modified calcite surface shown in Figure 3.8. Three types of changes were found, and these are roughness on the original surface, development of small separated deposits and development of homogenous and flat crystals. Each one of these surface changes was analyzed by EDS to see what type of elements are present as shown in Figure 6.8. On the flat surface, all ions originally present on calcite lattice were detected. Although developed roughness can be attributed to adsorption of calcium ions, no solid conclusion can be made only from the EDS spectra. On the same spectrum, it was found that a very small percentage of sodium and chloride ions were detected which supports the previously discussed role of sodium chloride salt towards calcite surface charges. On crystals, the EDS spectra showed very high concentration of sodium and chloride ions and this indicates that sodium chloride crystals have precipitated on the calcite surface possibly as a result of exceeding solubility limits of this salt. Such precipitations are not welcomed during water flooding as that it would cause formation damage by blocking pore throats. From another EDS spectrum, sulfur, magnesium, sodium and chloride ions were detected and this supports previous conclusions made on adsorption of sulfate and magnesium ions which are most likely responsible for

the change of calcite surface structure as well as change in adsorbed carboxylic materials' shape.

To investigate the individual effect of the Ca^{2+}, Mg^{2+} and SO_4^{2-} ions present in the original AGSW on the observed changes on the calcite surface shown in Figure 6.5, $CaCl_2.2H_2O$, $MgCl_2.6H_2O$ and Na_2SO_4 salts were used to prepare three aqueous brines, each one contains one PDI at a concentration equivalent to its concentration at the AGSW. In each of these brines, modified and unmodified calcite chips were immersed for 24 hours, after which, it was allowed to dry at room temperate for 24 hours before been scanned by the optical microscope. Figure 6.6 compares the topology of calcite with and without model oil in AGSW and then in the three formulated brines. As it can be seen, significant dissolution were found on the calcite chips immersed in $MgCl_2.6H_2O$ and Na_2SO_4 while less degree of dissolution was found in $CaCl_2.2H_2O$. It is also noticed that the same changes occurred in the modified calcite chip which was immersed in AGSW were also noticed on the modified calcite chips immersed in $MgCl_2.6H_2O$ and Na_2SO_4. The negligible effect of $CaCl_2.2H_2O$ can be explained by the low concentration of Ca^{2+} ions in this brine compared to Mg^{2+} ions in $MgCl_2.6H_2O$. This results supports the previous conclusion on the effect of PDIs on the microscopic dissolution of the calcite. Another important notice is the curved shape of the rhombohedral shapes of calcite dissolution compared to the regular rhombohedral shape which were found in deionized water as shown in Figure 4.2. Same behavior of calcite dissolution were reported on $MgCl_2.2H_2O$ using AFM. [53, 54]

On dolomite, more positive charges were developed as shown in Figure 6.1. New surface roughness with scattered deposits and some crystals were seen on optical microscope and AFM images as shown in Figure 6.7. The EDS spectra shown in Figure 6.9 indicate that

no different ions other than those originally present in the dolomite lattice were detected. This doesn't mean that no adsorption of calcium and magnesium would have taken place. No significant clear oil deposits were found on the dolomite similar to those on the calcite, and this might indicate that oil is homogenously adsorbing on the dolomite surface and that the AGSW was not able to remove it.

On MEC, decrease in the magnitude of negative charges was found. From EDS spectra (Figure 6.10) some small percentages of magnesium ions was detected which indicates that some magnesium ions found a way to adsorb on MEC surface and it might be responsible for removing some oil by repacking calcium ions.

The EDS results discussed in this section confirms the previously suggested mechanism for oil recovery by AGSW from calcite which is adsorption of PDIs from injected water on the rock surface. It is very important to shed some light on the effect of sodium chloride salt towards carbonate surface charges based on EDS results discussed in this section. It can be concluded that both sodium and chloride ions can individually adsorb on calcite surfaces as it was found from the reported percentage of adsorbed ions on the EDS spectrum taken on modified calcite surfaces. It was also found from the microscopic images and the EDS spectra that sodium and chloride ions can deposit together in a form of sodium chloride precipitate. The individual adsorption of these two ions are very welcomed, especially for chloride ions, as it might have an effect similar to sulfate. On the other hand, deposition of sodium chloride as crystals is extremely not welcomed inside pores when water is injected. From either form of adsorptions, sodium chloride salt would have an effect on the surface charges of carbonate rocks, and this conclusion contradicts some reported conclusions on the innocent effect of sodium chloride salt. [4, 16, 31]

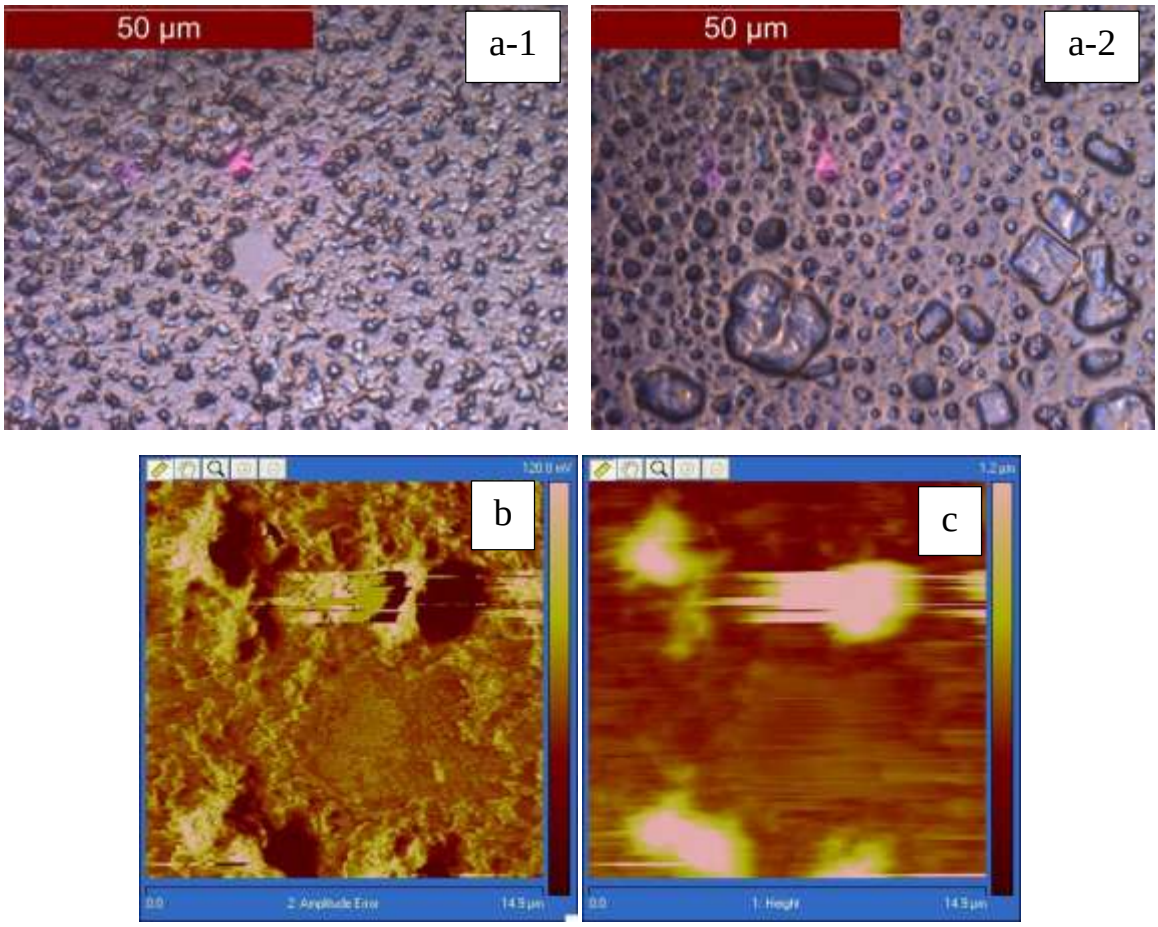

Figure 6.5: Microscopic surface images (a) and AFM deflection (b) and height (c) images for a modified calcite chip immersed in Arabian gulf Seawater showing shrinkage of adsorbed oil and development of rough surface.

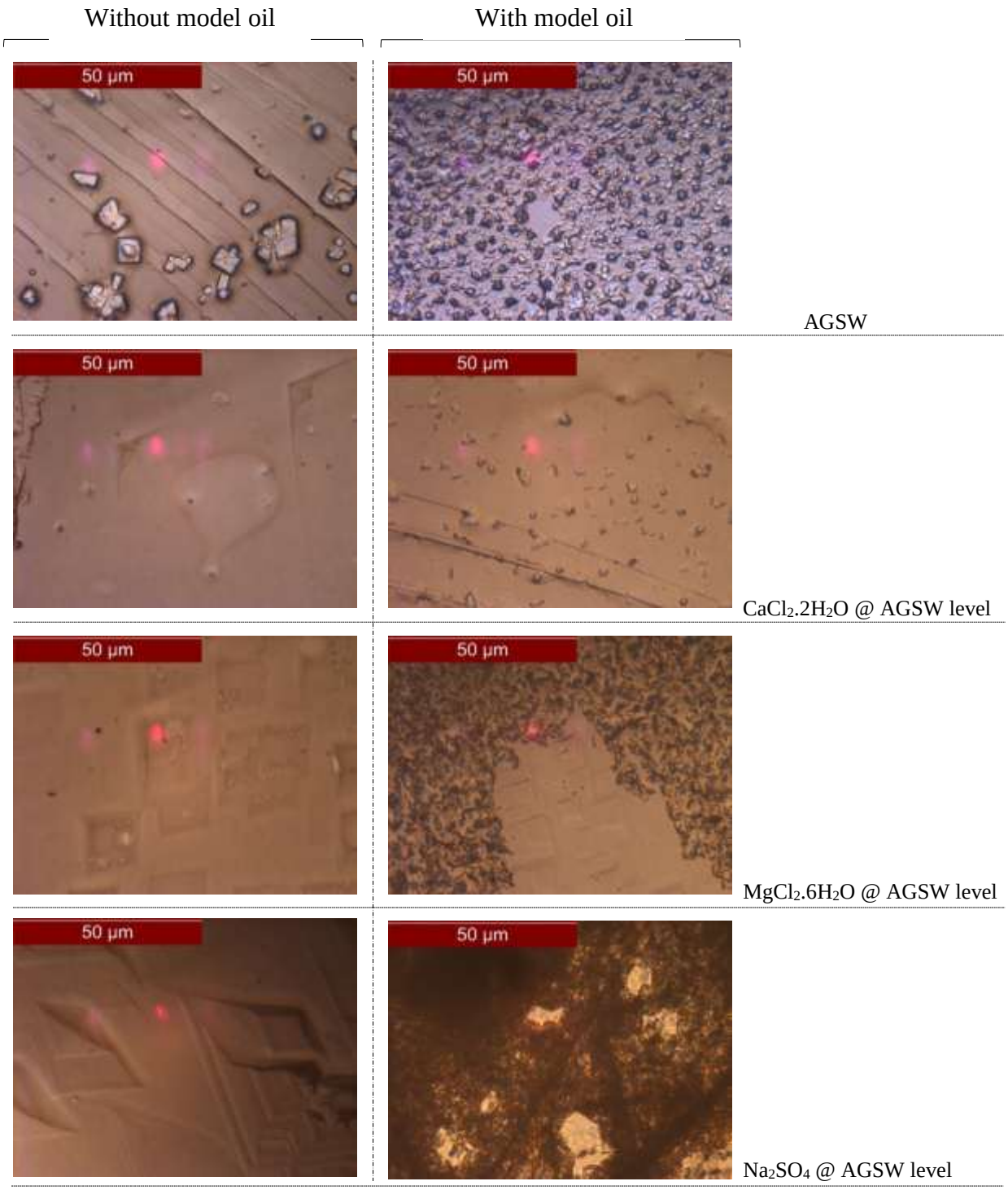

Figure 6.6: Individual effects of PDIs at Arabian Gulf Seawater salinity levels on the topology of modified and unmodified calcite chips.

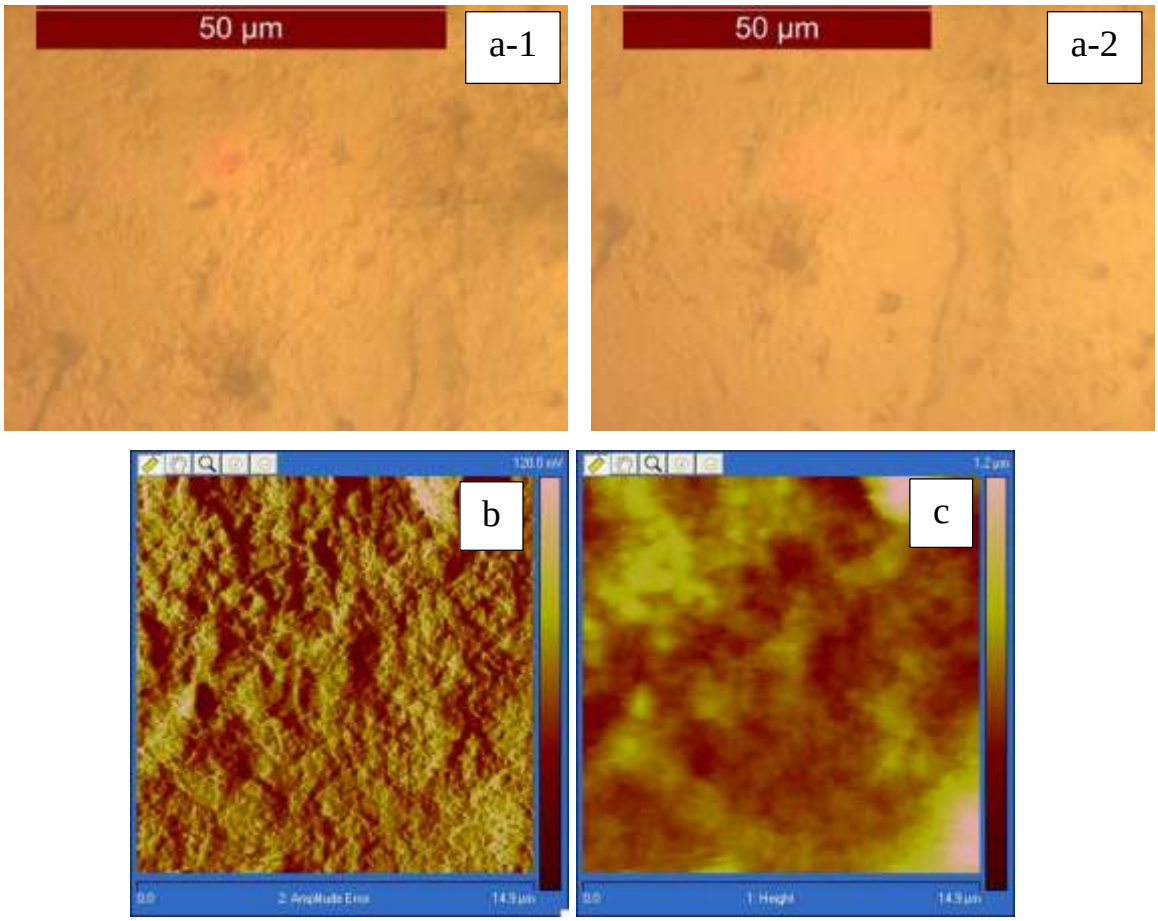

Figure 6.7: Microscopic surface images (a) and AFM deflection (b) and height (c) images for a modified dolomite chip immersed in Arabian Gulf Seawater

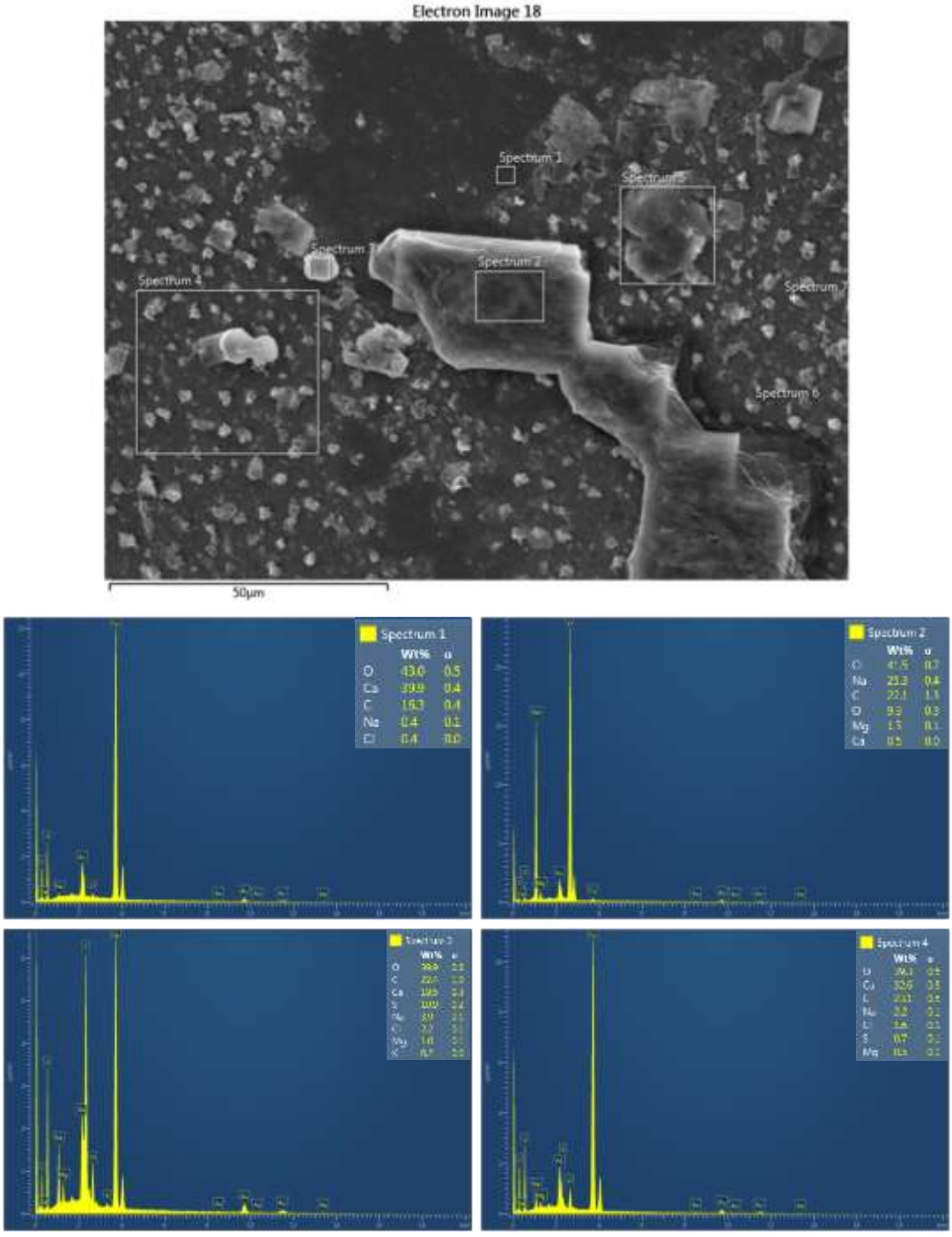

Figure 6.8: SEM image (top) and EDS spectra (bottom) of a modified calcite chip immersed in Arabian Gulf Seawater

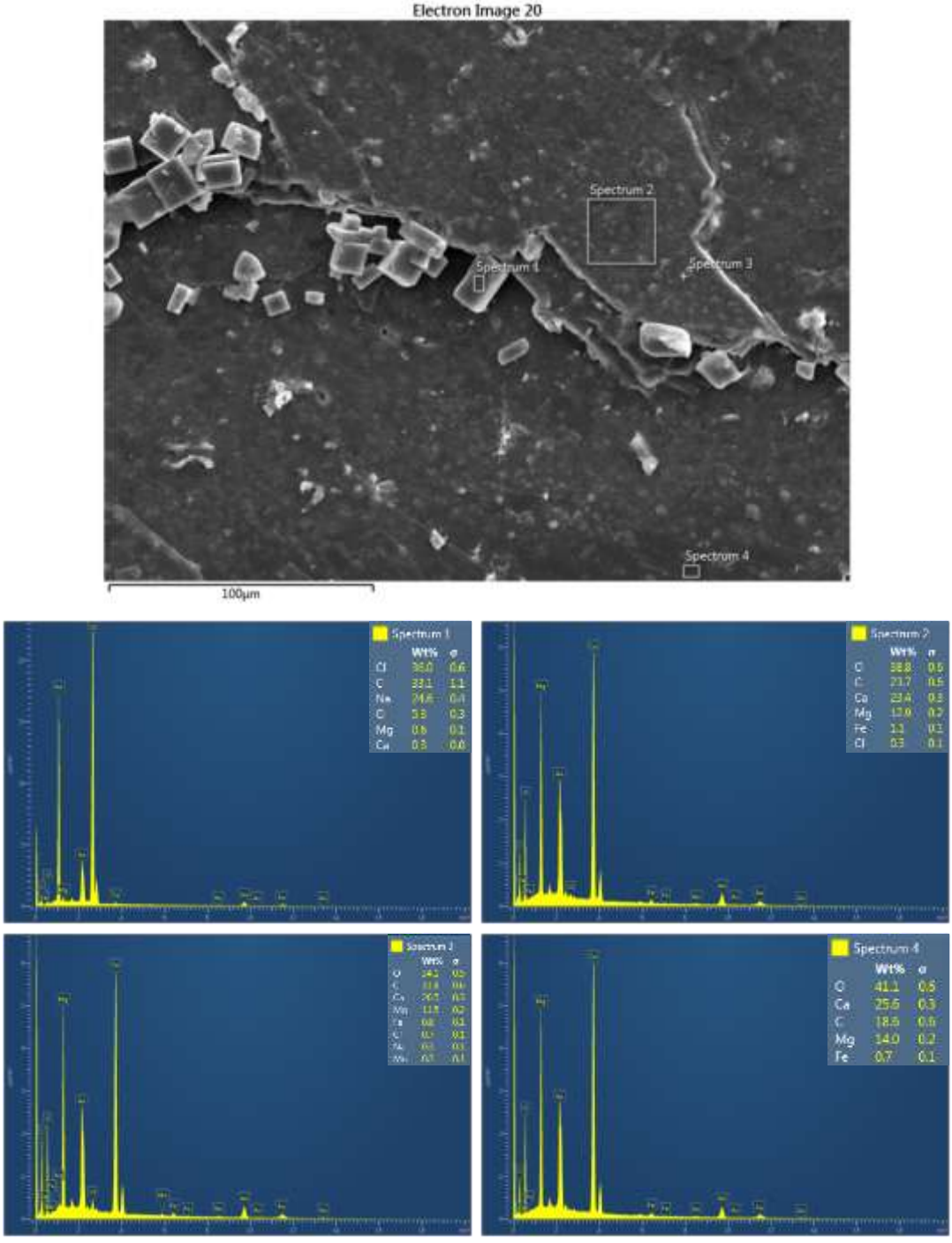

Figure 6.9: SEM image (top) and EDS spectra (bottom) for a modified dolomite chip immersed in Arabian Gulf Seawater

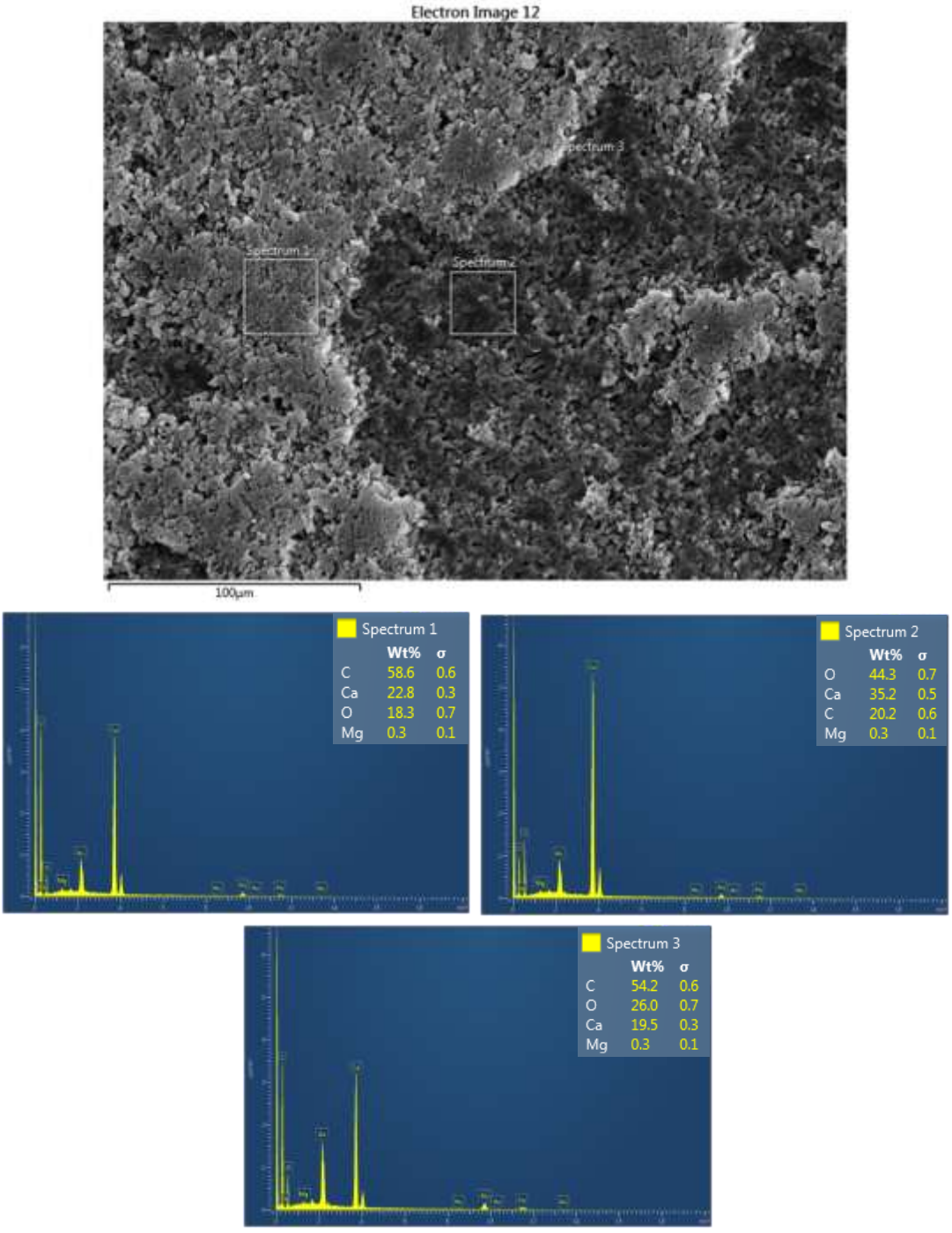

Figure 6.10: SEM image (top) and EDS spectra (bottom) of a modified Middle East Carbonate chip immersed in Arabian Gulf Seawater

6.3 Effect of Diluted Arabian Gulf Seawater

As shown in Figure 6.1, zeta potential measurements were conducted on carbonate powders been conditioned in 50% diluted AGSW (AGSW*) as well as when conditioned first in original AGSW before been conditioned in 50 % diluted AGSW (AGSW*-seq). Optical microscope, AFM images, SEM and EDS tests were only conducted for the chips which were conditioned in AGSW*.

From the optical microscope and the AFM images shown in Figure 6.11, surface roughness and separated black deposits were found. From the SEM image and the EDS spectra shown (Figure 6.12) magnesium, and sodium and chloride ions were detected, while high concentrations of carbon which indicates adsorption of oil was detected on separated surface deposits while no sodium chloride precipitates were found. Analysis of these results indicates that no adsorption of sulfate ions from 50% diluted AGSW took place and if some oil was removed, it would have been caused by either replacement of calcium ions by adsorbed magnesium or adsorption of chloride and sodium ions. However, such released oil would be negligible as a result of the small percentage of these adsorbed ions from the total bulk of rock surface elements as shown in the EDS spectra.

On the dolomite, no significant adsorption of ions other than those present in the rock lattice were detected on the newly developed rough surface based on EDS spectra shown in Figure 6.13. This does not exclude the possibility of having adsorption of positive ions. No significant removal of oil is expected based on the intensity of oil deposits shown in the SEM and optical microscopic images. Very few crystals of sodium chloride were detected

on the dolomite surface by SEM and optical images. On the MEC, scattered oil deposits were detected and no significant adsorption of sulfate or magnesium ions were detected by the EDS spectra shown in Figure 6.14.

Obtained results from all means of experiments on 50% diluted AGSW indicate that no significant release of adsorbed oil would be expected by direct use of 50% diluted AGSW compared to the unmodified AGSW. On the other hand, when 50% diluted AGSW is used after primary conditioning with unmodified AGSW, more oil is expected to be released, and in this case, the microscopic dissolution of carbonate surfaces would be responsible for the removal of adsorbed oil. In literature, some studies suggested the same conclusion on the inefficiency of diluted AGSW in removing more oil compared to using original unmodified AGSW. [7, 25] Jabbar et al [55] through contact angle measurements on calcite modified and conditioned with the same model oil and brines used in the current study, concluded that 50% diluted AGSW is not an efficient EOR fluid compared to the undiluted version of the same AGSW.

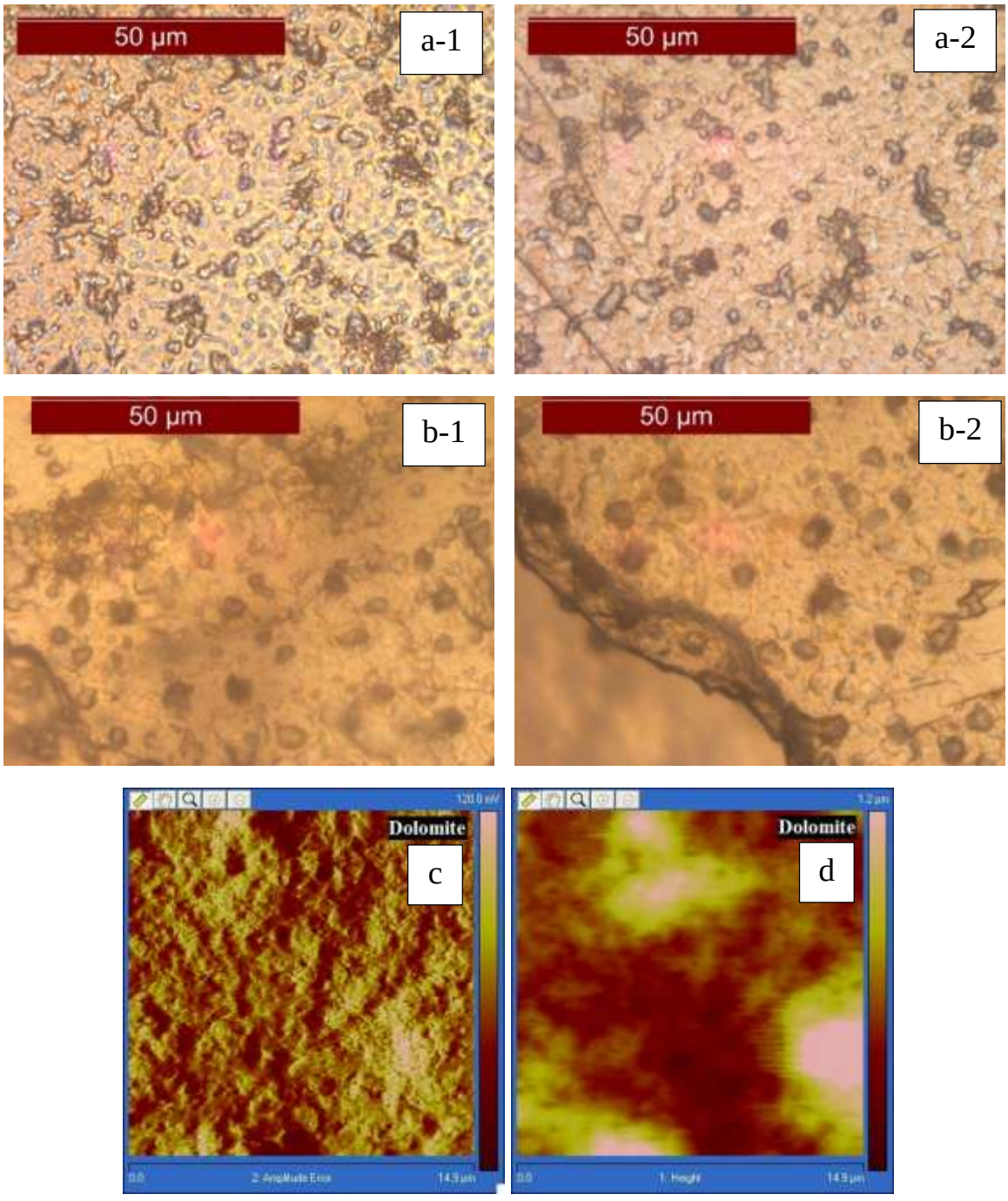

Figure 6.11: Microscopic surface images of calcite (a) and dolomite (b) and AFM deflection (c) and height (d) images for dolomite, all modified in model oil and immersed in 50% diluted Arabian Gulf Seawater

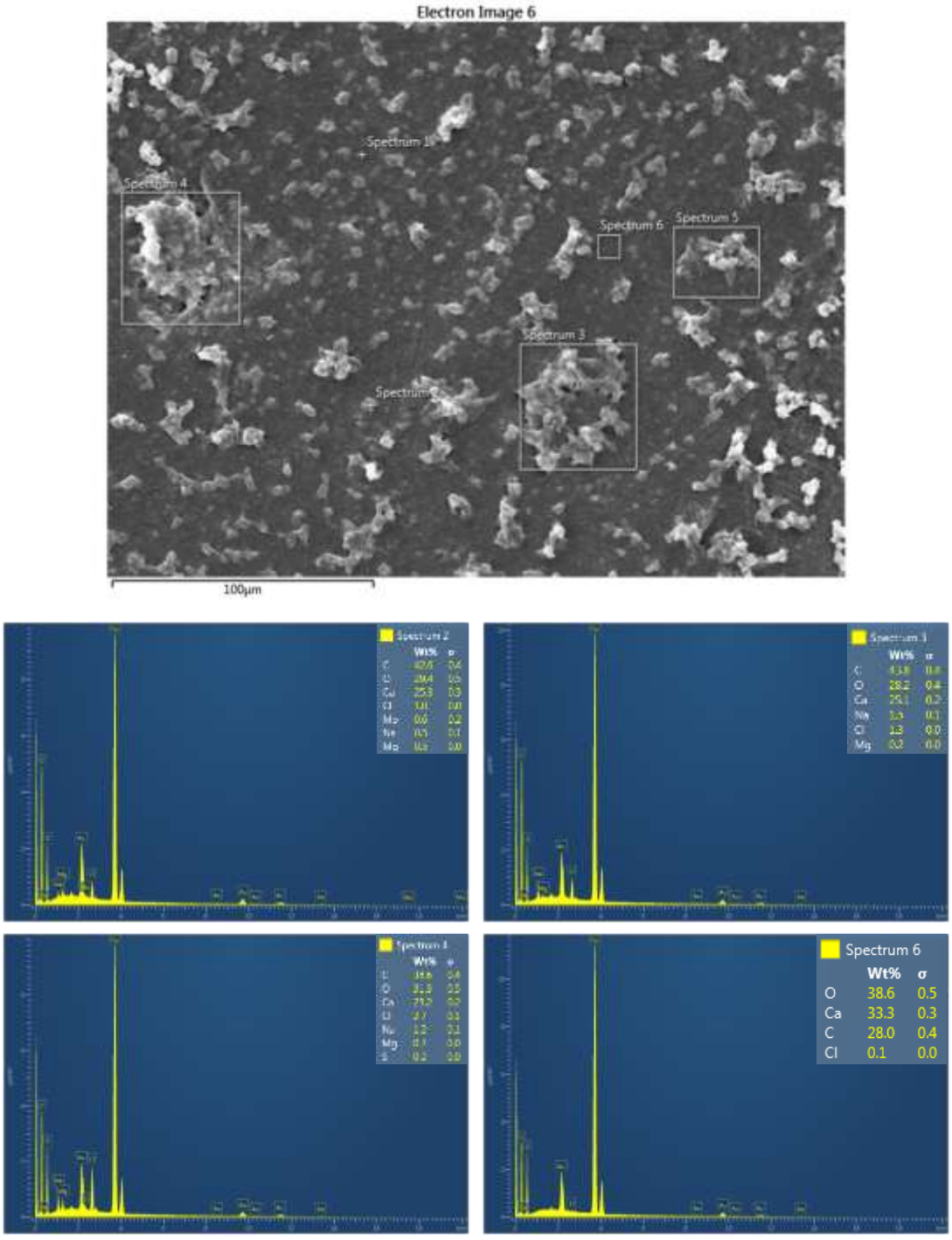

Figure 6.12: SEM image (top) and EDS spectra (bottom) of a modified calcite chip immersed in 50% diluted Arabian Gulf Seawater

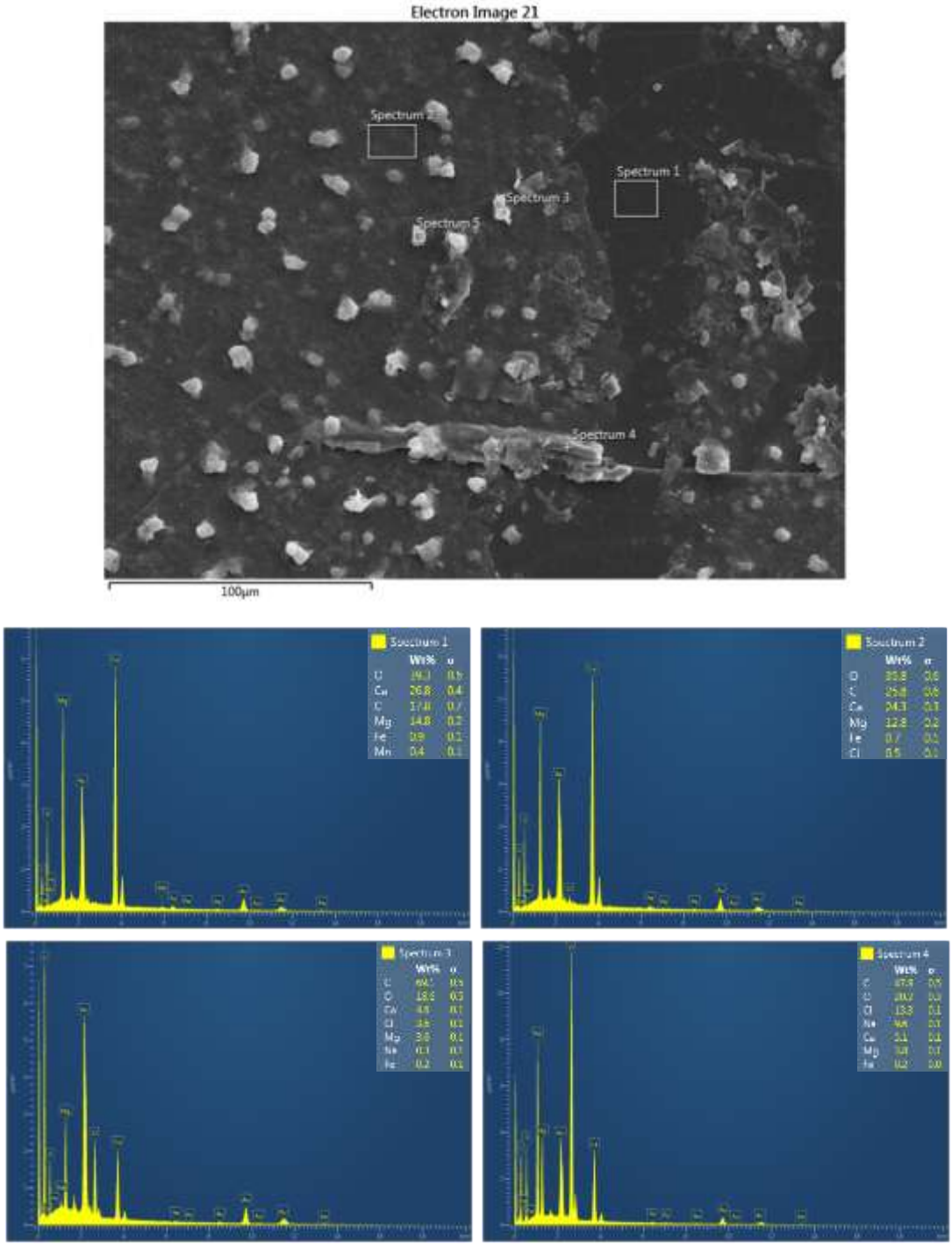

Figure 6.13: SEM image (top) and EDS spectra (bottom) of a modified dolomite chip immersed in 50% diluted Arabian Gulf Seawater

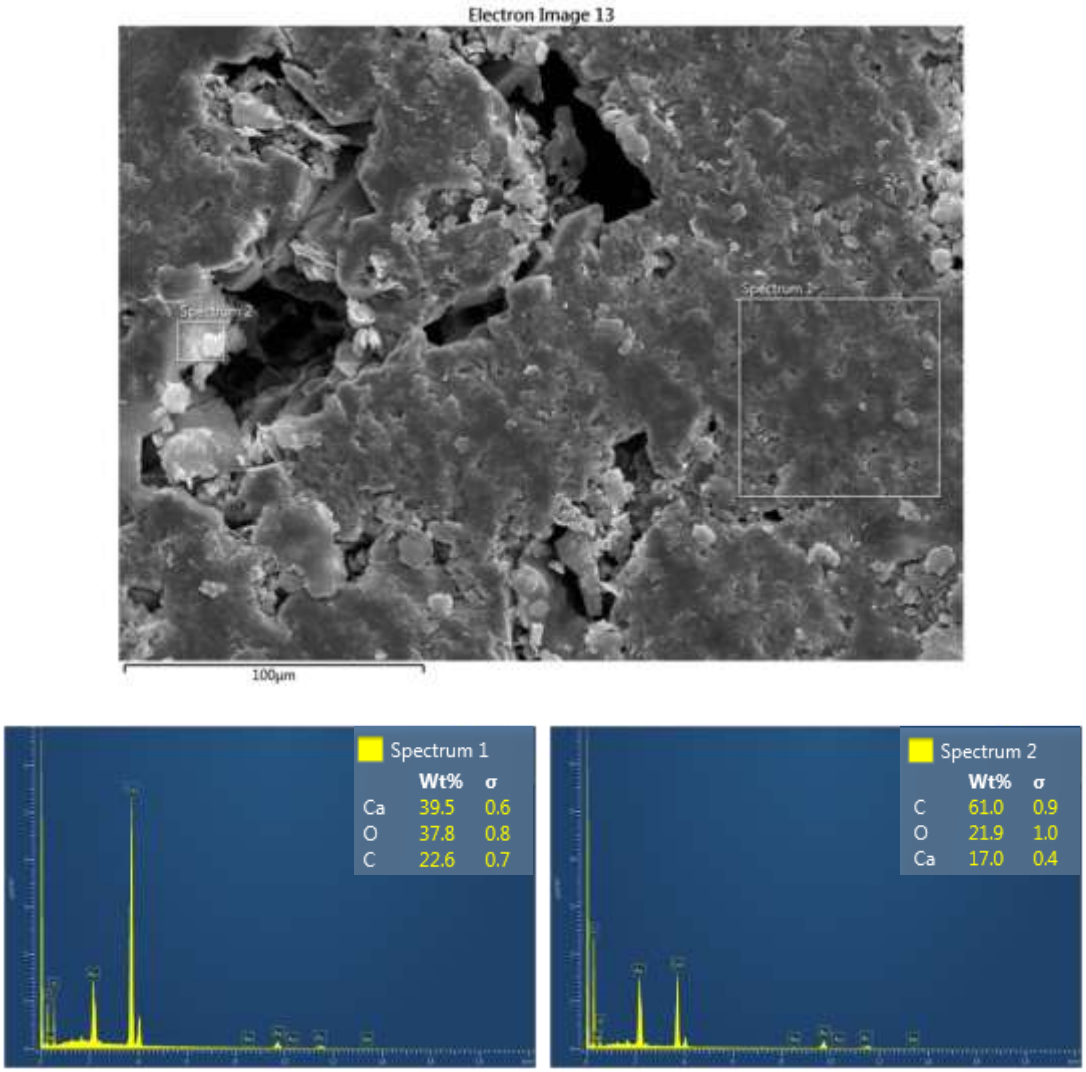

Figure 6.14: SEM image (top) and EDS spectra (bottom) of a modified MEC chip immersed in 50% diluted Arabian Gulf Seawater

6.4 Effect of Increasing Ca^{2+} Ions' Concentration

From zeta potential results, it can be seen that doubling the concentration of calcium ions will add more positive charges to all carbonate surfaces except on the calcite at lower calcium ions' concentration (Figure 6.2). From the optical and the AFM images of the calcite shown in Figure 6.15, it can be seen that the degree of surface roughness in modified calcite chip which was immersed in 50% AGSW, with increased calcium ions' concentration, was higher compared to when the chip was immersed in original AGSW (Figure 6.5). These kind of conditions would be caused by extensive adsorption of calcium and this would explain the increase in the magnitude of positive surface charges of all rock samples. From the EDS spectra shown in Figure 6.17, high concentration of calcium ions was found, however, no distinction can be made from these spectra between calcium ions originally on the surface and those possibly adsorbed from the brine. On oil deposits, small percentages of sulfur, magnesium, chloride and sodium ions were detected. These ions were not found on other analyzed areas of the rock surface, and this indicates that increasing calcium ions' concentration would affect adsorption of other PDIs. The same observations made on calcite were found on dolomite and MEC.

Jabbar et al [55] found that increasing calcium ions' concentration in 50% diluted AGSW doesn't decrease the oil wetness of modified calcite. In other studies, it was concluded that the presence of calcium ions is very important for adsorption of sulfate, and that the concentration ratio of calcium to sulfate should be as high as possible, but not to cause $CaSO_4$(s) precipitation. [26, 56]

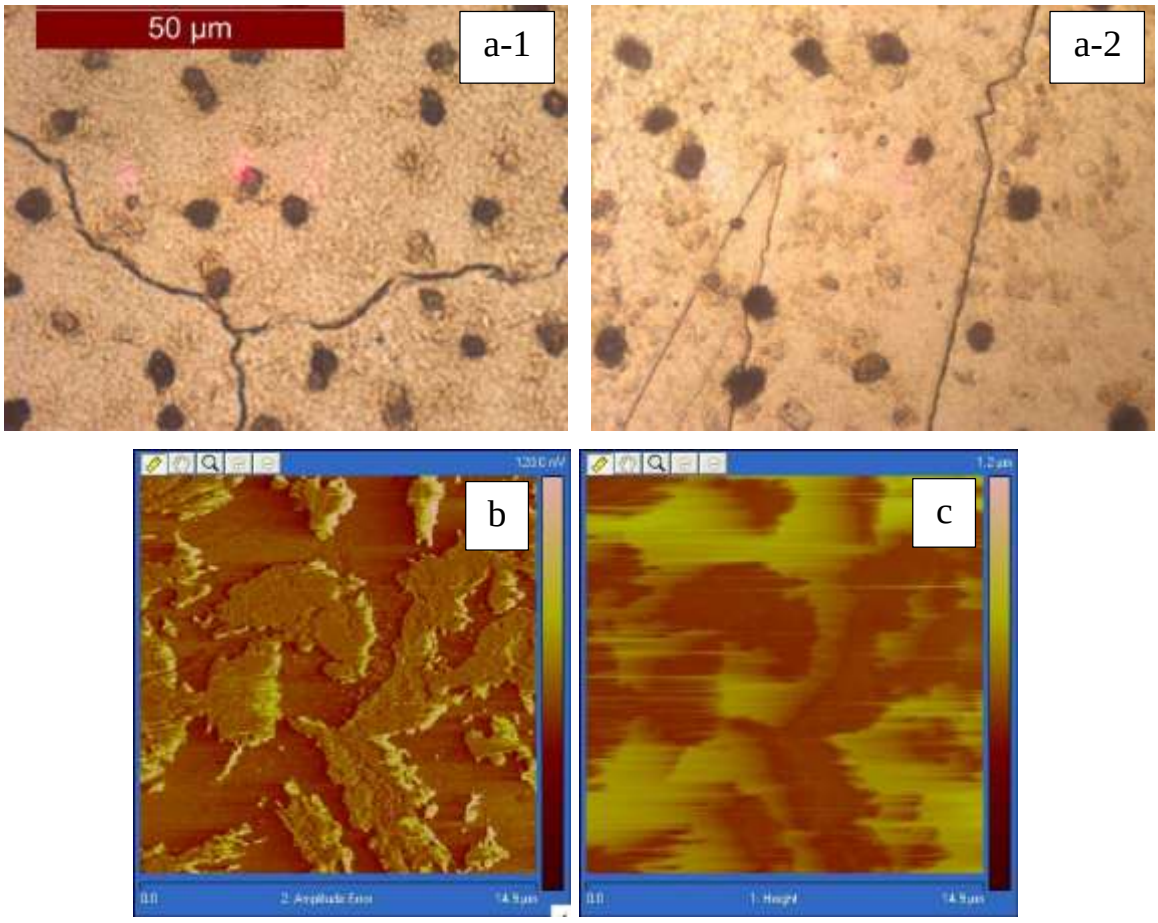

Figure 6.15 Microscopic surface images (a) and AFM deflection (b) and height (c) images for a modified calcite chip immersed in 50% diluted Arabian Gulf Seawater with doubled Ca^{2+} ions ' concentration (AGSW*-4Ca)

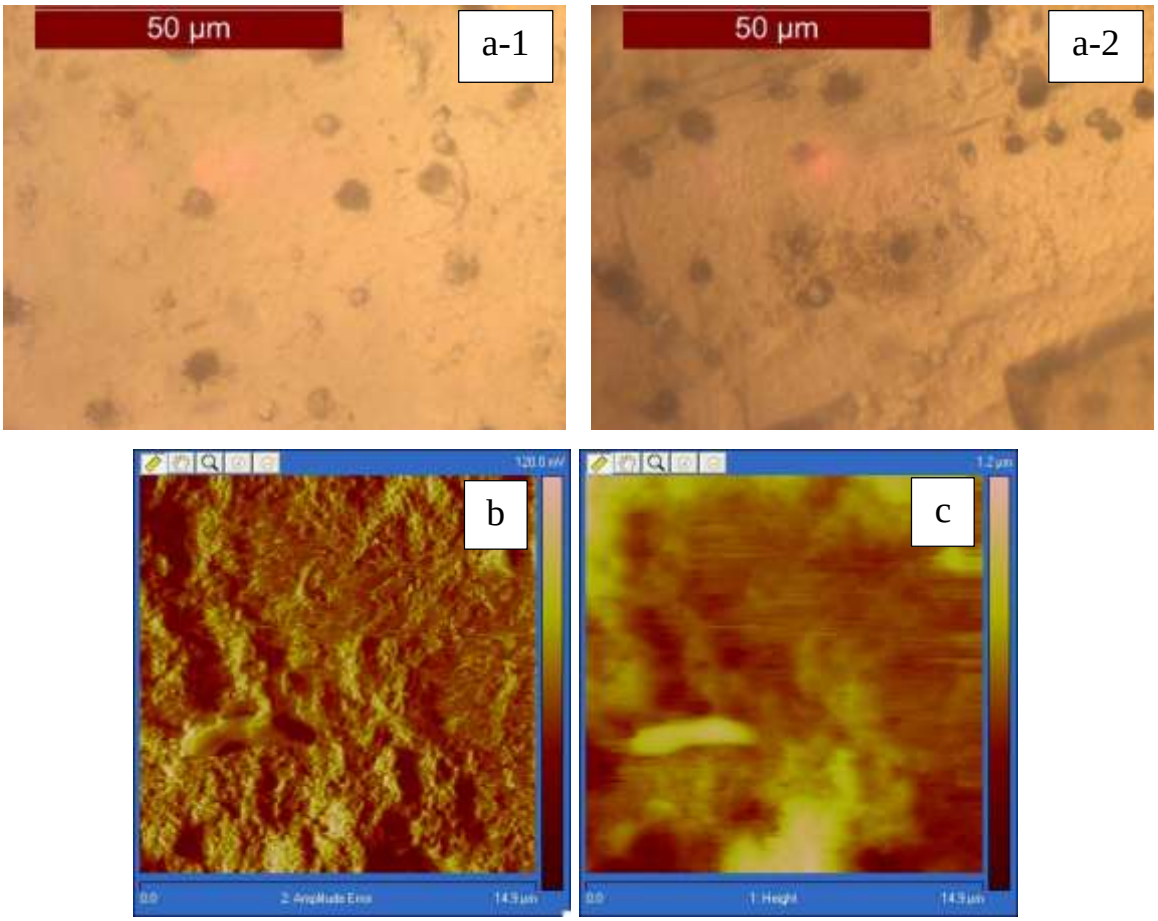

Figure 6.16: Microscopic surface images (a) and AFM deflection (b) and height (c) images for a modified dolomite chip immersed in 50% diluted Arabian Gulf Seawater with doubled Ca^{2+} ions ' concentration (AGSW*-4Ca)

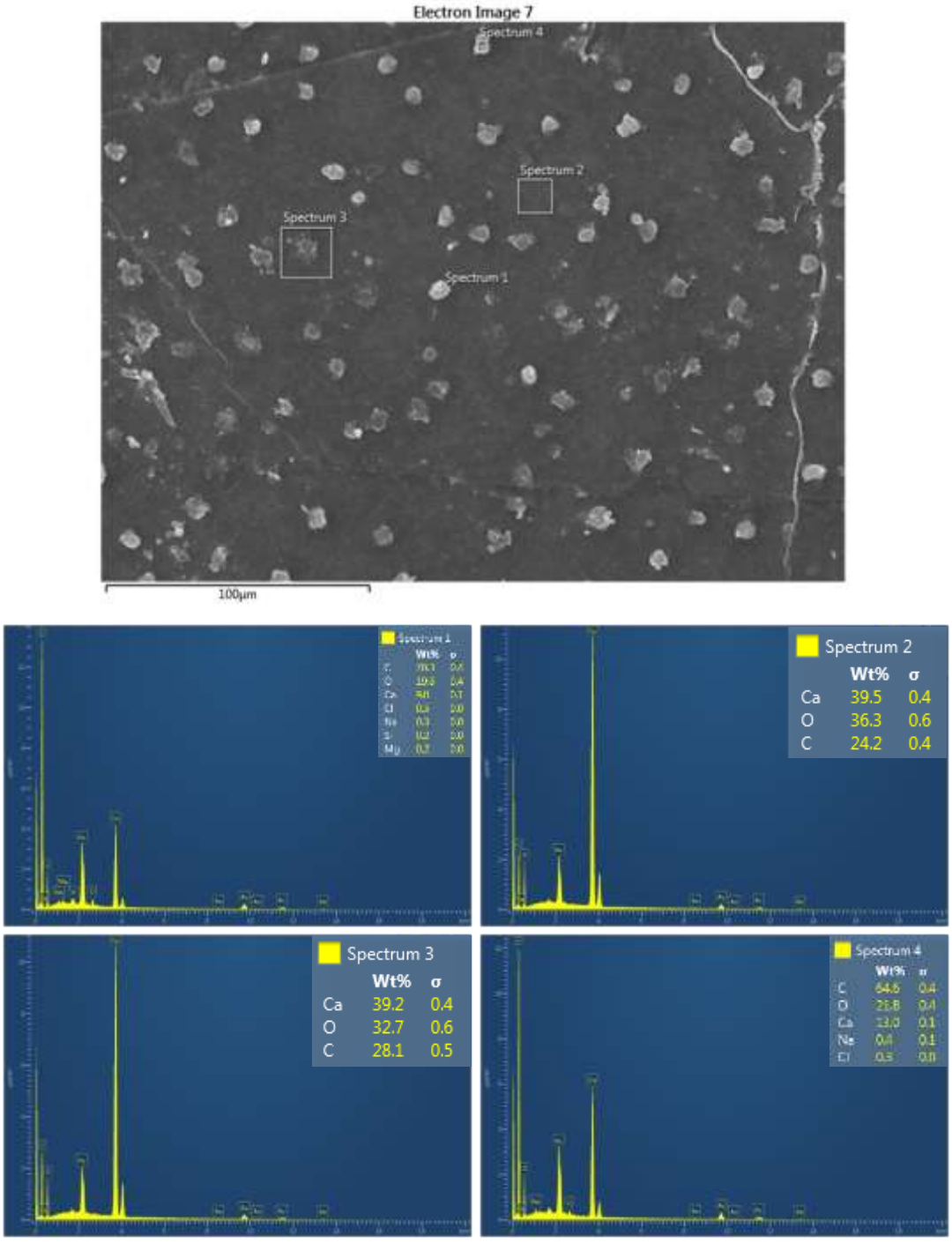

Figure 6.17: SEM image (top) and EDS spectra (bottom) of a modified calcite chip immersed in 50% diluted Arabian Gulf Seawater with doubled Ca^{2+} ions ' concentration (AGSW*-4Ca)

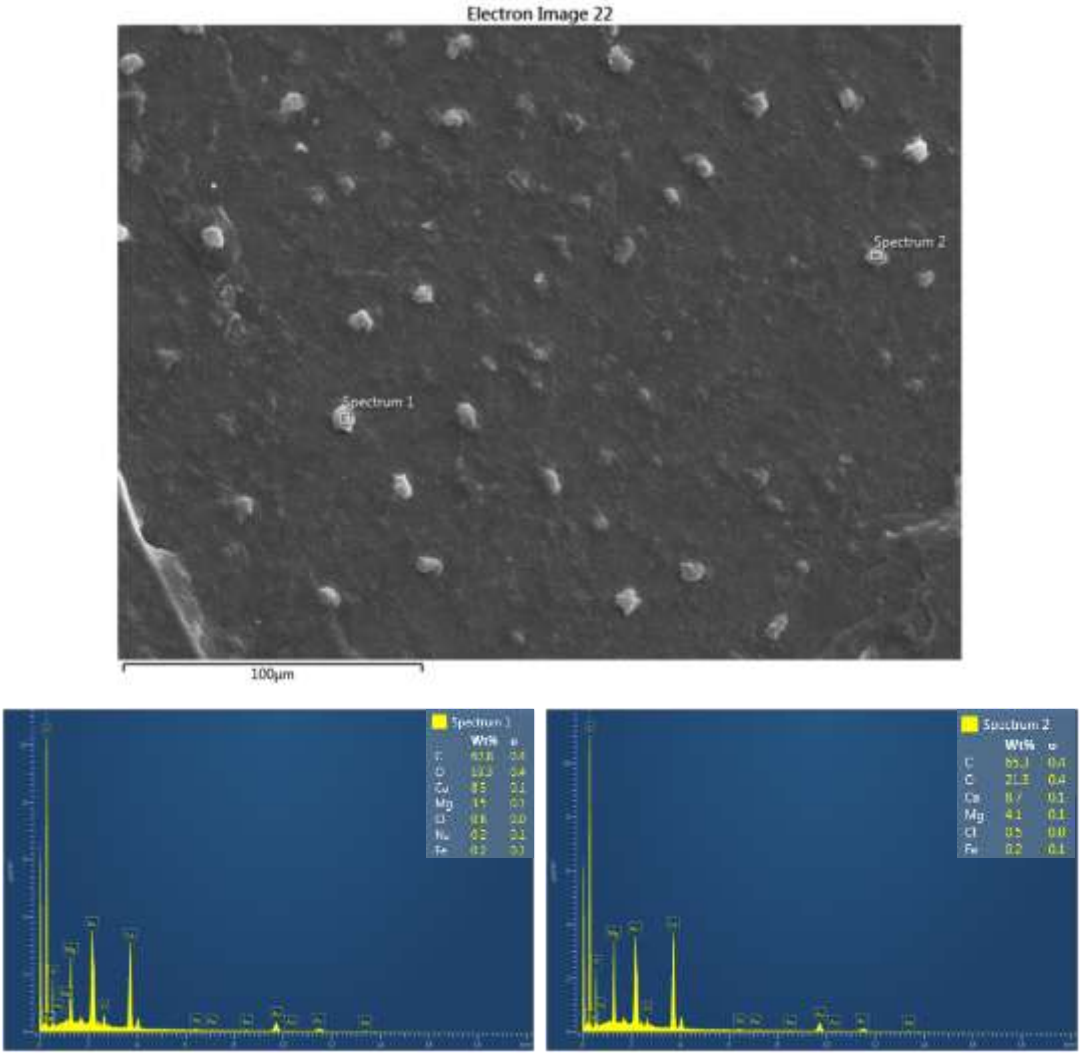

Figure 6.18: SEM image (top) and EDS spectra (bottom) of a modified dolomite chip immersed in 50% diluted Arabian Gulf Seawater with doubled Ca^{2+} ions ' concentration (AGSW*-4Ca)

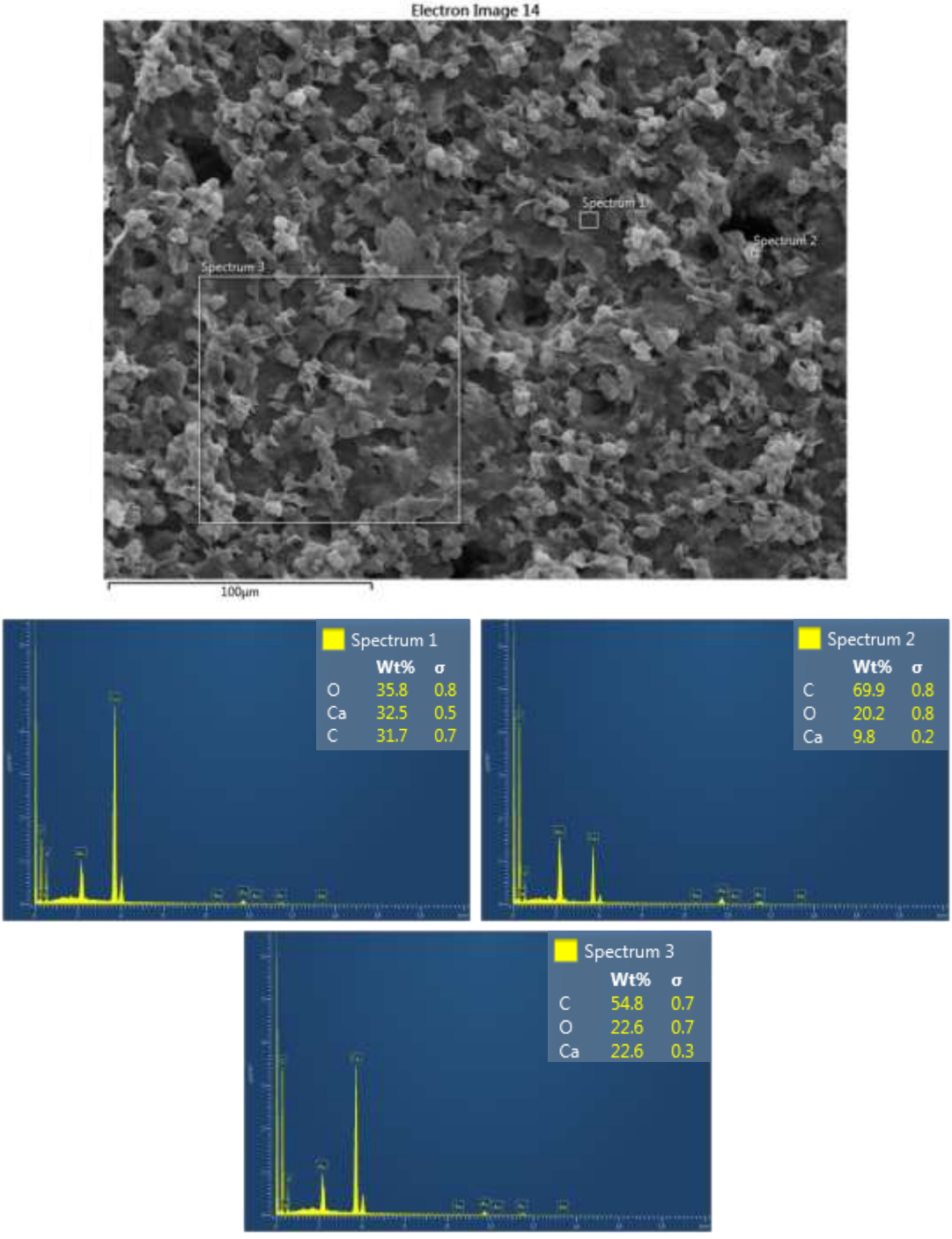

Figure 6.19: SEM image (top) and EDS spectra (bottom) of a modified Middle East Carbonate chip immersed in 50% diluted Arabian Gulf Seawater with doubled Ca^{2+} ions ' concentration (AGSW*-4Ca)

6.5 Effect of Increasing Mg^{2+} Ions' Concentration

Increasing magnesium ions' concentration, more positive surface charges were developed on all rock samples as shown in Figure 6.2. No significant changes in the surface roughness were found compared to what was found when calcium ions' concentration was increased as shown on the optical microscope and AFM images of calcite (Figure 6.20). Additionally, no significant sodium chloride crystals were found. On the EDS spectra, significant percentages of magnesium, sodium, chloride and sulfur ions were detected as shown in Figure 6.21. This might indicate that the presence of magnesium would increase the affinity of negative ions to adsorb on calcite surface. However, from previous zeta potential measurements no such observation was noted due to the high magnitude of developed positive surface charges by adsorption of magnesium which might masked the negative charges developed by possible adsorption of sulfate and chloride ions. On the MEC sample, magnesium, chloride and sodium ions were found as shown in Figure 6.23, while no adsorption of sulfur was detected on the EDS spectra.

No adsorption of sulfur or chloride ions was detected on the EDS spectra of the dolomite sample as shown in Figure 6.22. From the optical microscopic images shown in Figure 6.20, significant precipitations of sodium chloride crystals were detected. The intensity of oil deposits are much higher than what was found on the calcite chip. All these results indicate that on dolomite surfaces, no significant release of oil can be made by increasing the concentration of magnesium ions.

In the contact angle study conducted by Jabbar et al [55] it was found that increasing magnesium ions would alter modified calcite surface towards more water wet, in contrast to what was found when the calcium ions' concentration was increased. From analysis of produced water in the Ekofisk chalk oil field of Norway, which was subjected to months of north sea water injection, it was concluded that a slow dolomitization process occurred on the reservoir rock as a result of calcium ions dissolution and magnesium ions precipitation. [57] In addition to this positive role of magnesium ions, other researchers suggested that the presence of magnesium ions in the injected AGSW will control precipitation of $CaSO_4$(s) at high concentration ratios of calcium to sulfate when the water is injected at high temperatures. [4, 26]

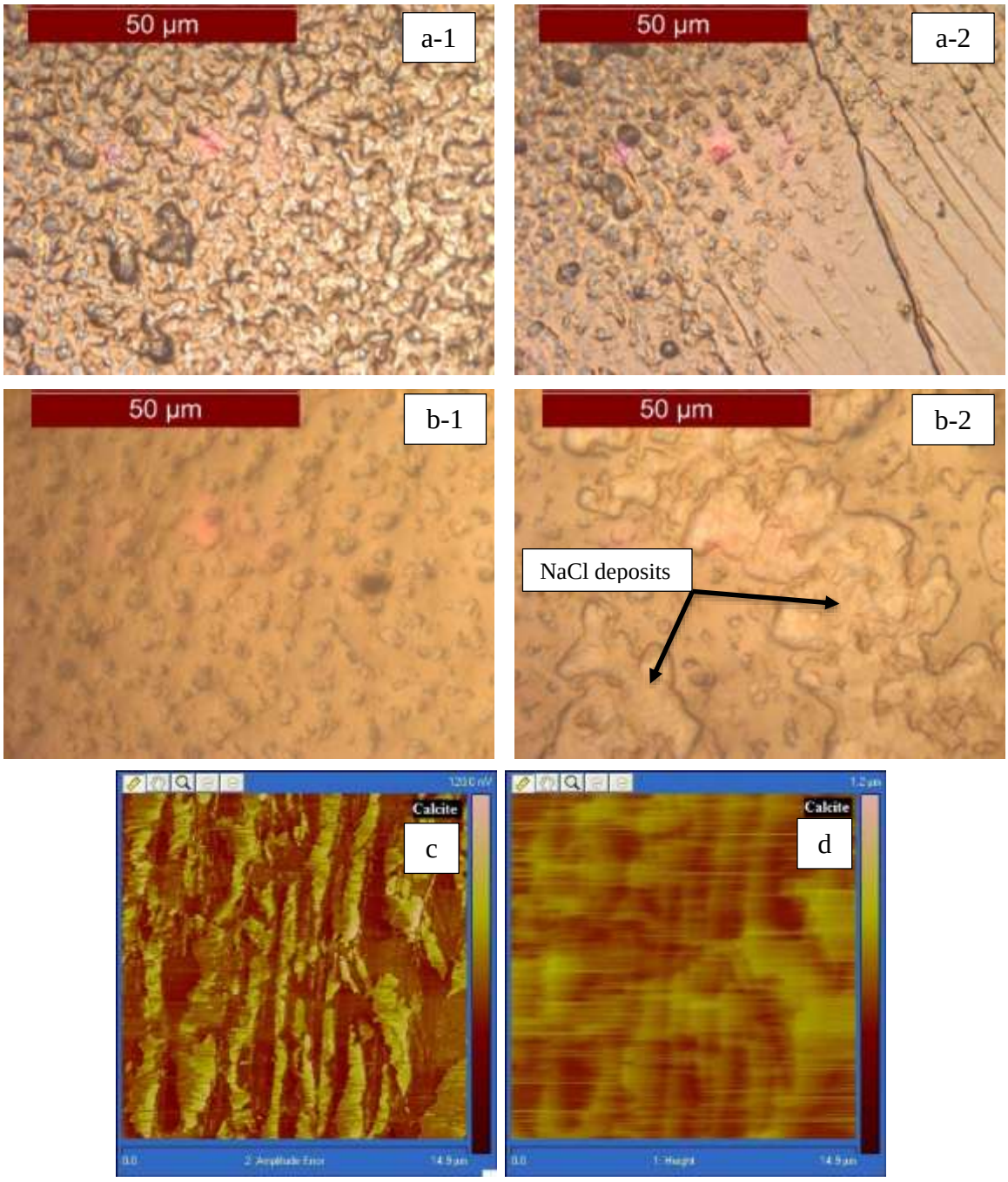

Figure 6.20: Microscopic surface images of calcite (a) and dolomite (b) and AFM deflection (c) and height (d) images of a calcite , all immersed in 50% diluted Arabian Gulf Seawater with doubled Mg^{2+} ions ' concentration (AGSW*-2Mg)

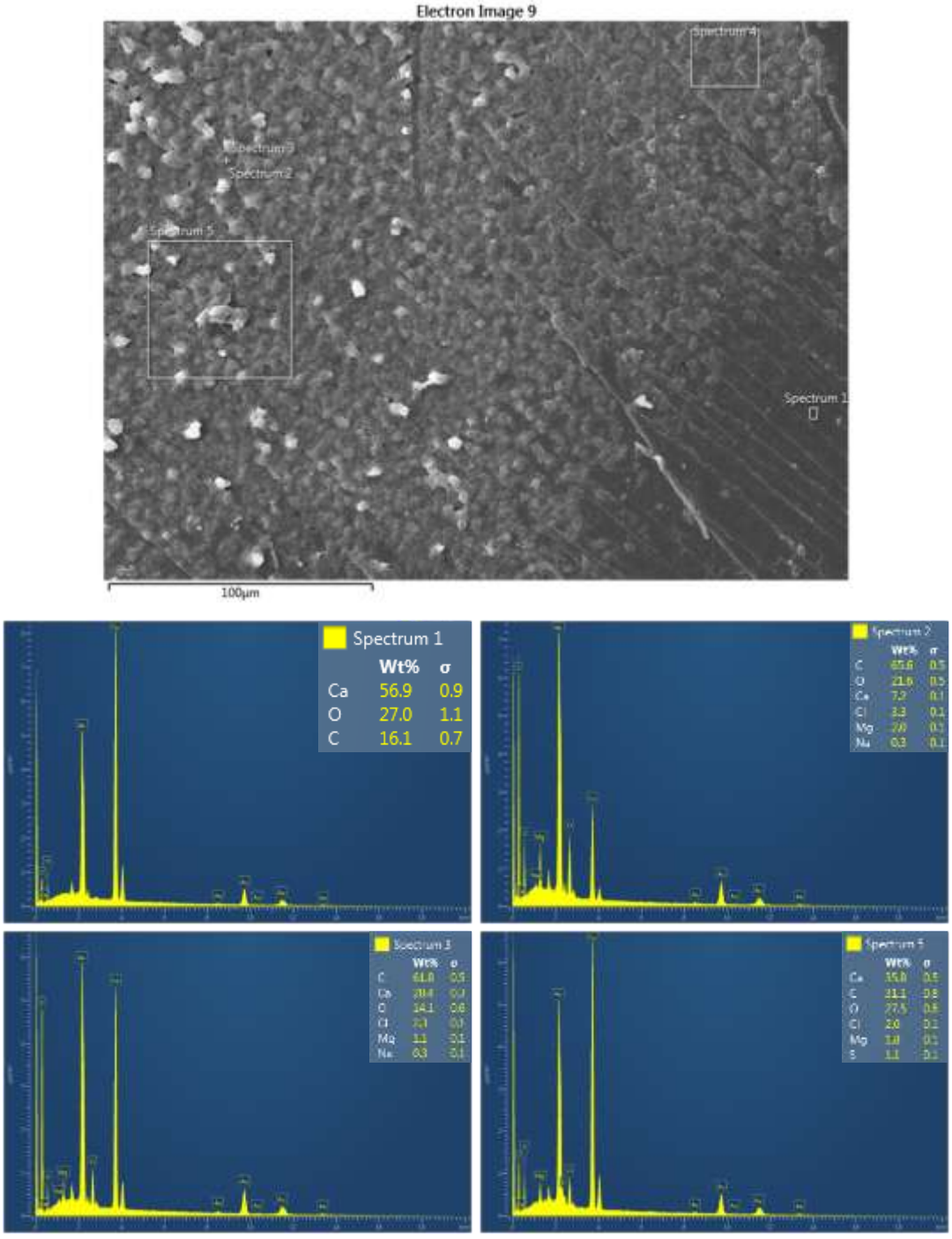

Figure 6.21: SEM image (top) and EDS spectra (bottom) of a modified calcite chip immersed in 50% diluted Arabian Gulf Seawater with doubled Mg^{2+} ions ' concentration (AGSW*-2Mg)

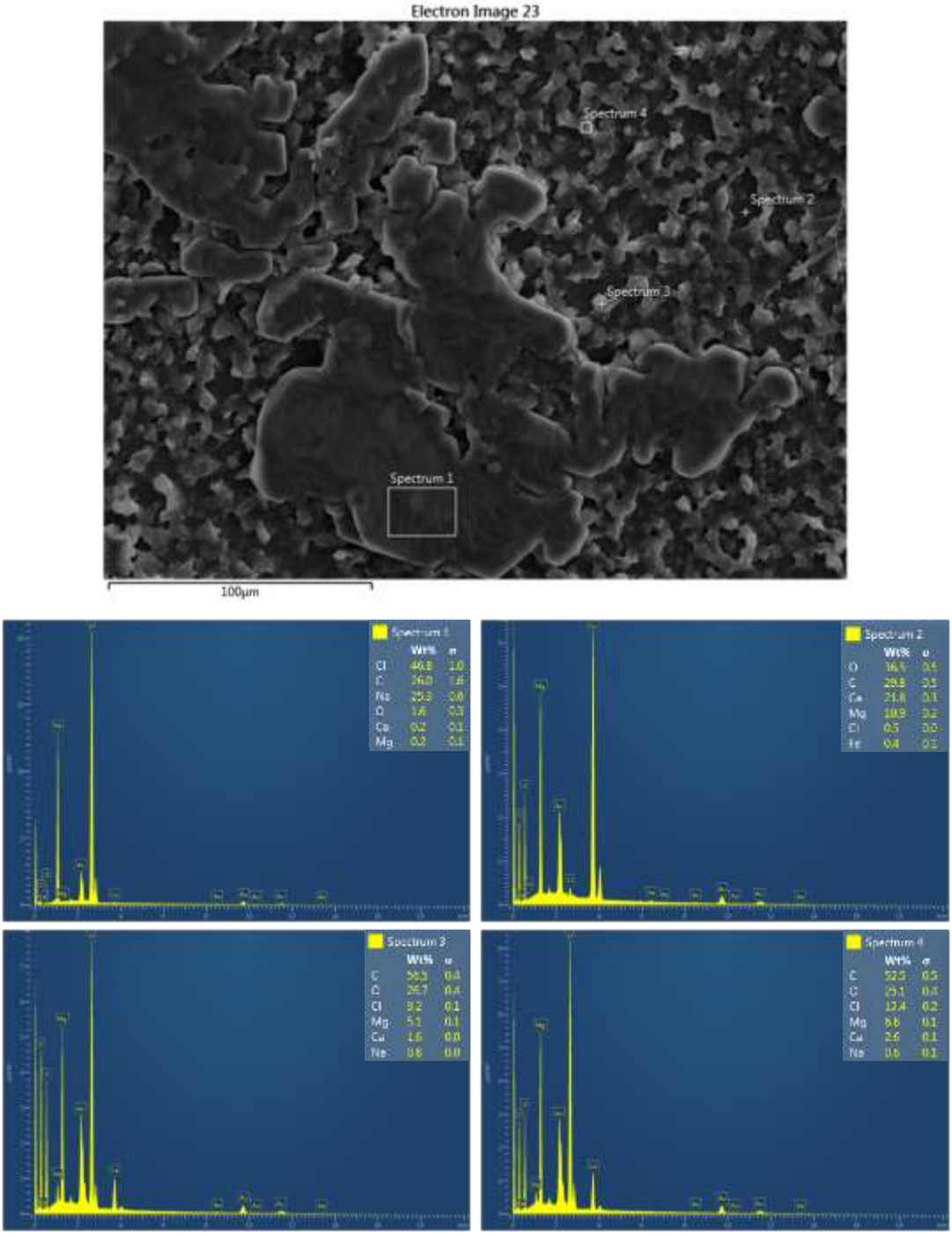

Figure 6.22: SEM image (top) and EDS spectra (bottom) for a modified dolomite chip immersed in 50% diluted Arabian Gulf Seawater with doubled Mg^{2+} ions ' concentration (AGSW*-2Mg)

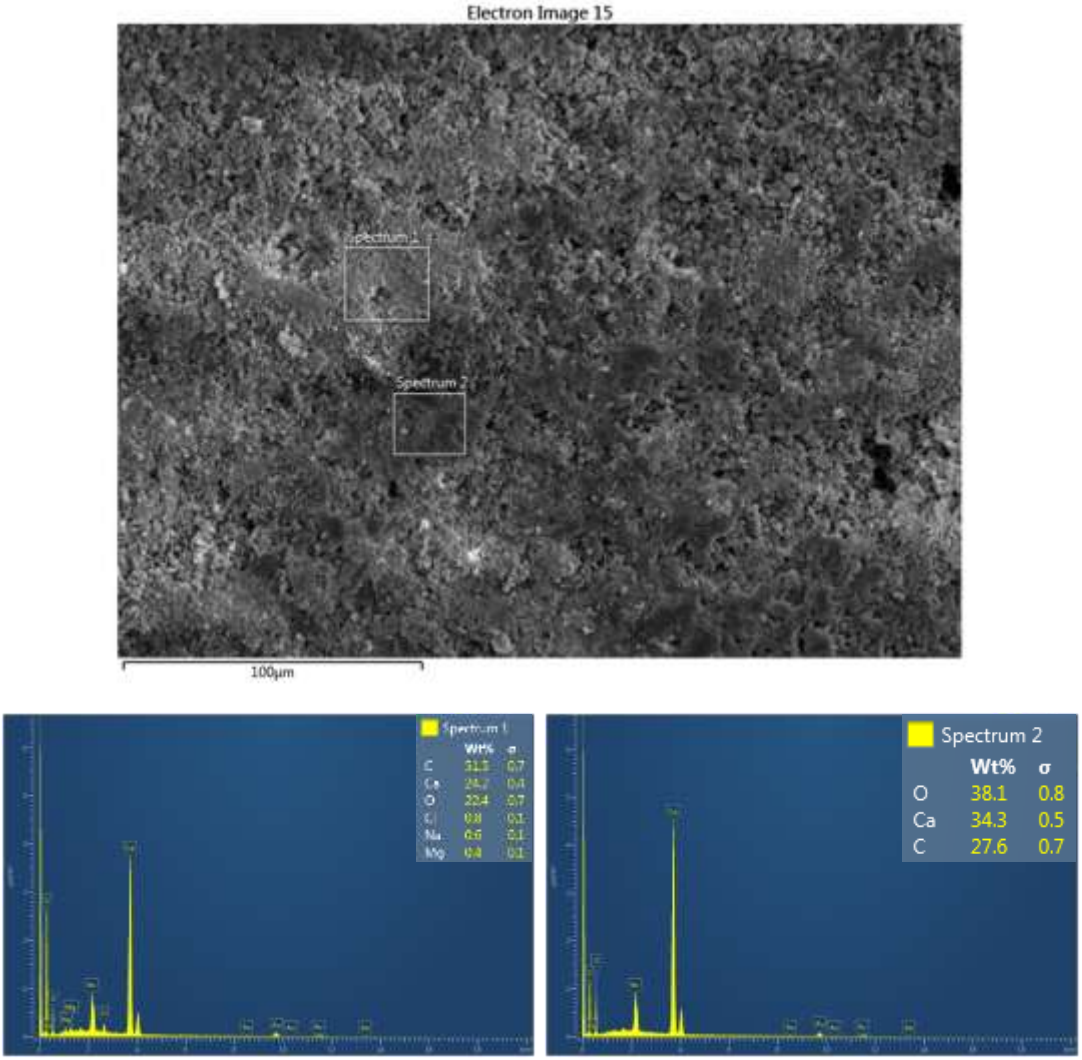

Figure 6.23: SEM image (top) and EDS spectra (bottom) of a modified Middle East Carbonate chip immersed in 50% diluted Arabian Gulf Seawater with doubled Mg^{2+} ions ' concentration (AGSW*-2Mg)

6.6 Effect of Increasing SO_4^{2-} Ions' Concentration

From zeta potential measurements shown in Figure 6.2, it can be seen that at two times or four times increased concentrations of sulfate ions in 50% diluted AGSW, calcite and MEC will always get negative surface charges even in presence of magnesium and calcium ions. On the other hand, negative surface charges were found in the dolomite sample only at high concentration of sulfate ions (AGSW*-4SO). These results are in line with the expected trend found on the relative effect of sulfate ions in the presence of calcium or magnesium discussed previously in chapter 5 for the relative effect of PDIs especially for the effect of magnesium ions on the development of negative surface charges by sulfate ions on the modified dolomite as shown in Figure 5.6.

From the optical microscope images of calcite (Figure 6.24) less oil deposits were seen while more crystals of precipitated sodium chloride were found. From the AFM deflection and height images, a lower degree of surface roughness was noticed comparison to when calcium ions' concentration was increased. From the EDS spectra shown in Figure 6.26, analysis of the surface areas where no deposits were present showed that no adsorption of ions other than those originally present in the calcite lattice were found. However, the high percentage of calcium ions might indicate some degree of adsorption of this ion from the brine. On other areas where different shapes of deposits are located, sodium, chloride, sulfur and magnesium ions were detected with large variation in each ion's percentage from one deposit to another. As it was found from the previous SEM images and EDS spectra on different spots on the calcite chip, it can be pointed out that when those ions adsorb on calcite, either individually or in form of precipitates, it will take place where oil

is located rather than anywhere else on the calcite surface, as it was found from the SEM and EDS tests.

It is very important to mention that although it is confirmed that some PDIs are able to find a place on the rock surface but no possible distinguish can be mad e with our current results between whether these PDIs have adsorbed or precipitated on the rock surface. However, our current finding can shed some light on the physical aspects of sulfate adsorption during smart water flooding and this would add more features to the commonly agreed role of sulfate ions. On MEC, no other ions than those present on the rock lattice were detected on the EDS spectra shown in Figure 6.28.

On the dolomite, more scattered oil deposits and larger sodium chloride precipitates in addition to relatively small precipitated crystals were all seen on the optical microscope images (Figure 6.25b). From the SEM image and the EDS spectra shown in Figure 6.27 large precipitates were confirmed to be sodium chloride while very high percentage of sulfur was detected on the smaller crystals. From the intensity of oil despite, as well as the positive zeta potential, this high percentage of sulfur indicates that these crystals are either precipitates of sulfate-based inorganic scales or some organic sulfate complexes been deposited on the calcite surface. From the analysis of the relatively clear dolomite surface on the same chips, no other ions than those present in the dolomite lattice were found which confirms that no individual adsorption of sulfate is expected.

Although sulfate was found to be the super PDI among all other ions, severe problems could happen due to presence of sulfate with high concentration, such as reservoir souring and scaling. [4] Another mechanism related to the role of sulfate ions was reported by Zahid

et al [58] after core flooding experiments on core samples from a Middle East reservoir. It was concluded that when high salinity brines that contain sulfate ions come in contact with oil at high pressure and temperature, it will decrease the viscosity of that oil and it will develop some emulsions between the brine and oil. They concluded that the viscosity reduction and the developed emulsions are believed to be responsible for the improved recovery of oil.

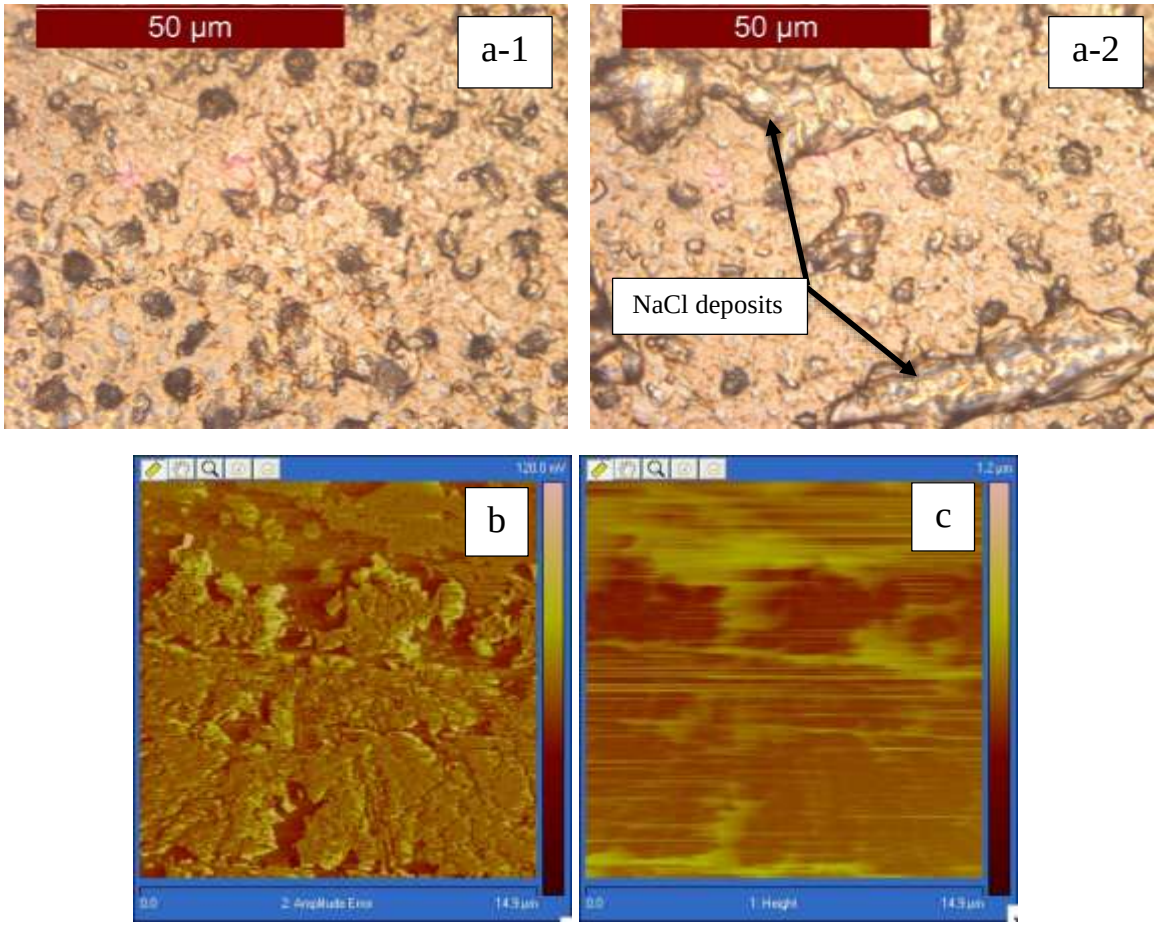

Figure 6.24: Microscopic surface images (a) and AFM deflection (b) and height (c) images for a modified calcite chip immersed in 50% diluted Arabian Gulf Seawater with doubled $SO4^{2-}$ ions ' concentration (AGSW*-2SO)

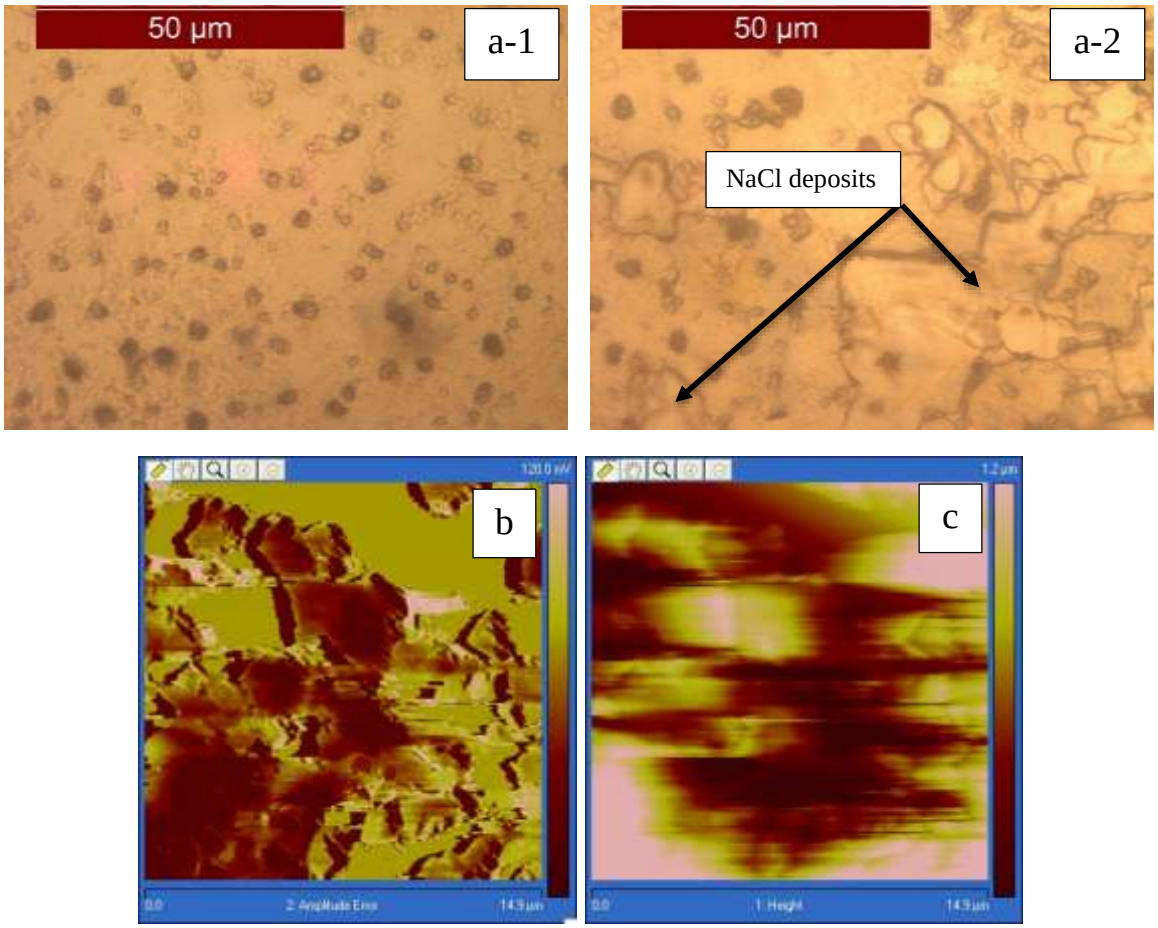

Figure 6.25: Microscopic surface images (a) and AFM deflection (b) and height (c) images for a modified dolomite chip immersed in 50% diluted Arabian Gulf Seawater with doubled $SO4^{2-}$ ions ' concentration (AGSW*-2SO)

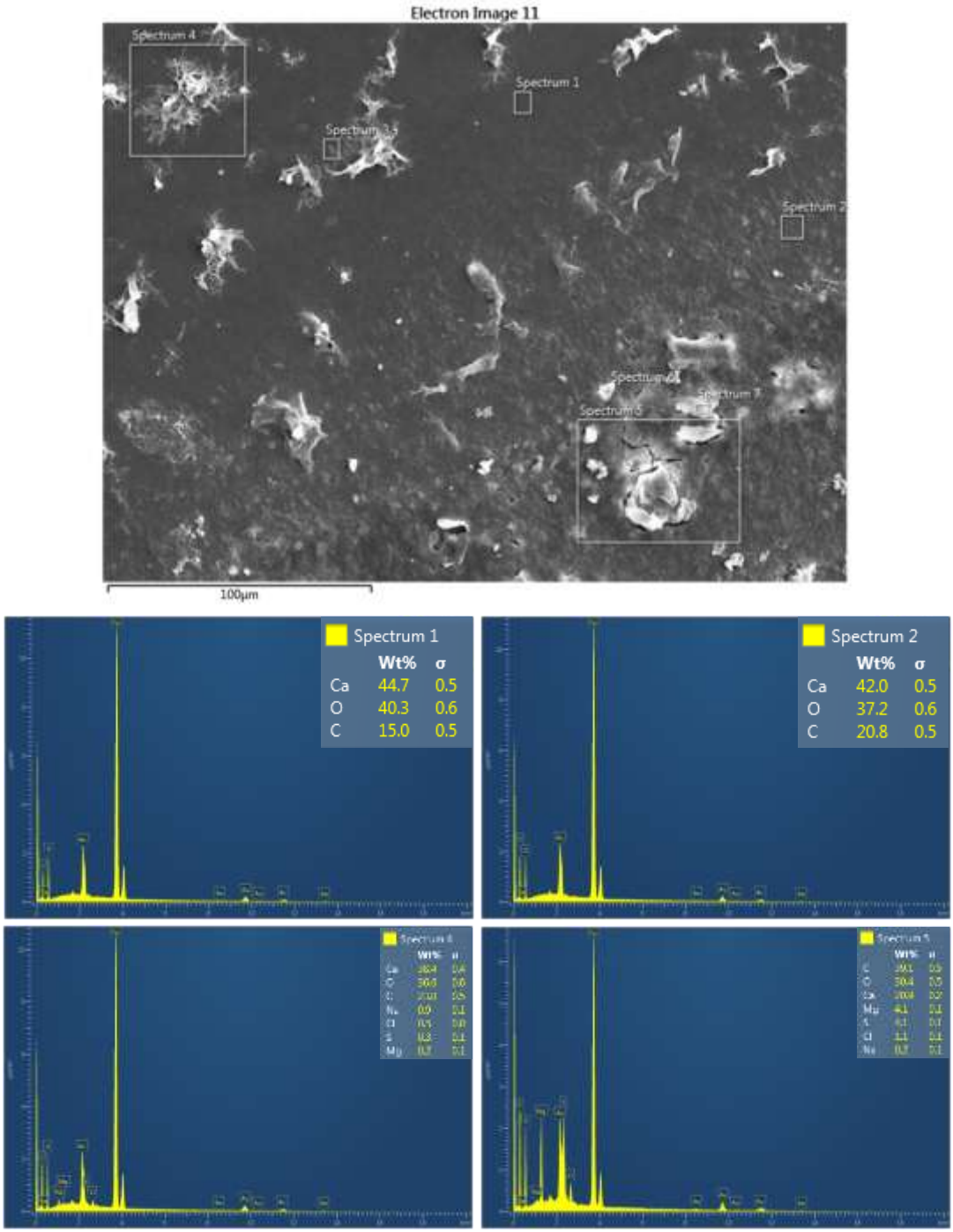

Figure 6.26: SEM image (top) and EDS spectra (bottom) of a modified calcite chip immersed in 50% diluted Arabian Gulf Seawater with doubled $SO4^{2-}$ ions ' concentration (AGSW*-2SO)

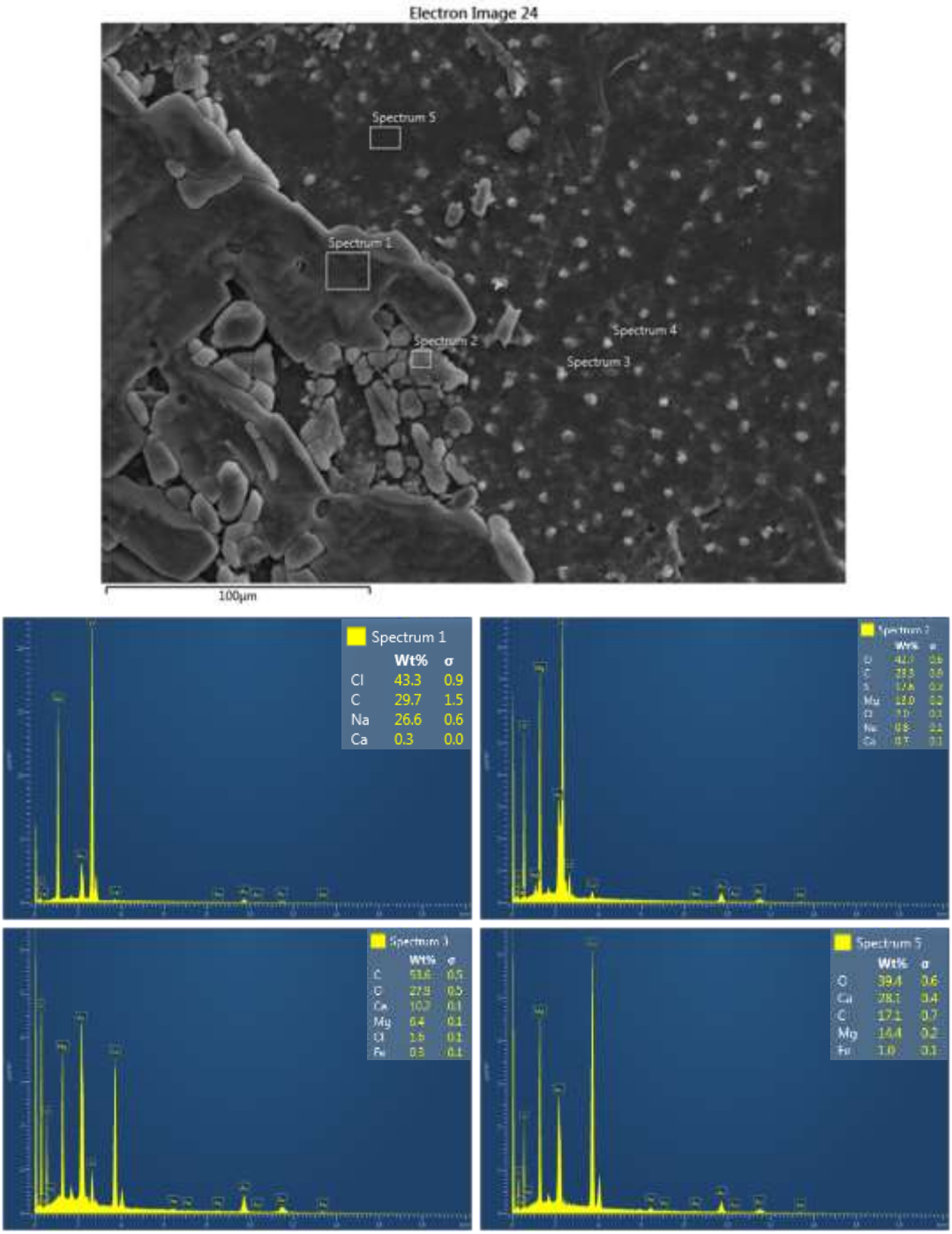

Figure 6.27: SEM image (top) and EDS spectra (bottom) of a modified dolomite chip immersed in 50% diluted Arabian Gulf Seawater with doubled $SO4^{2-}$ ions ' concentration (AGSW*-2SO)

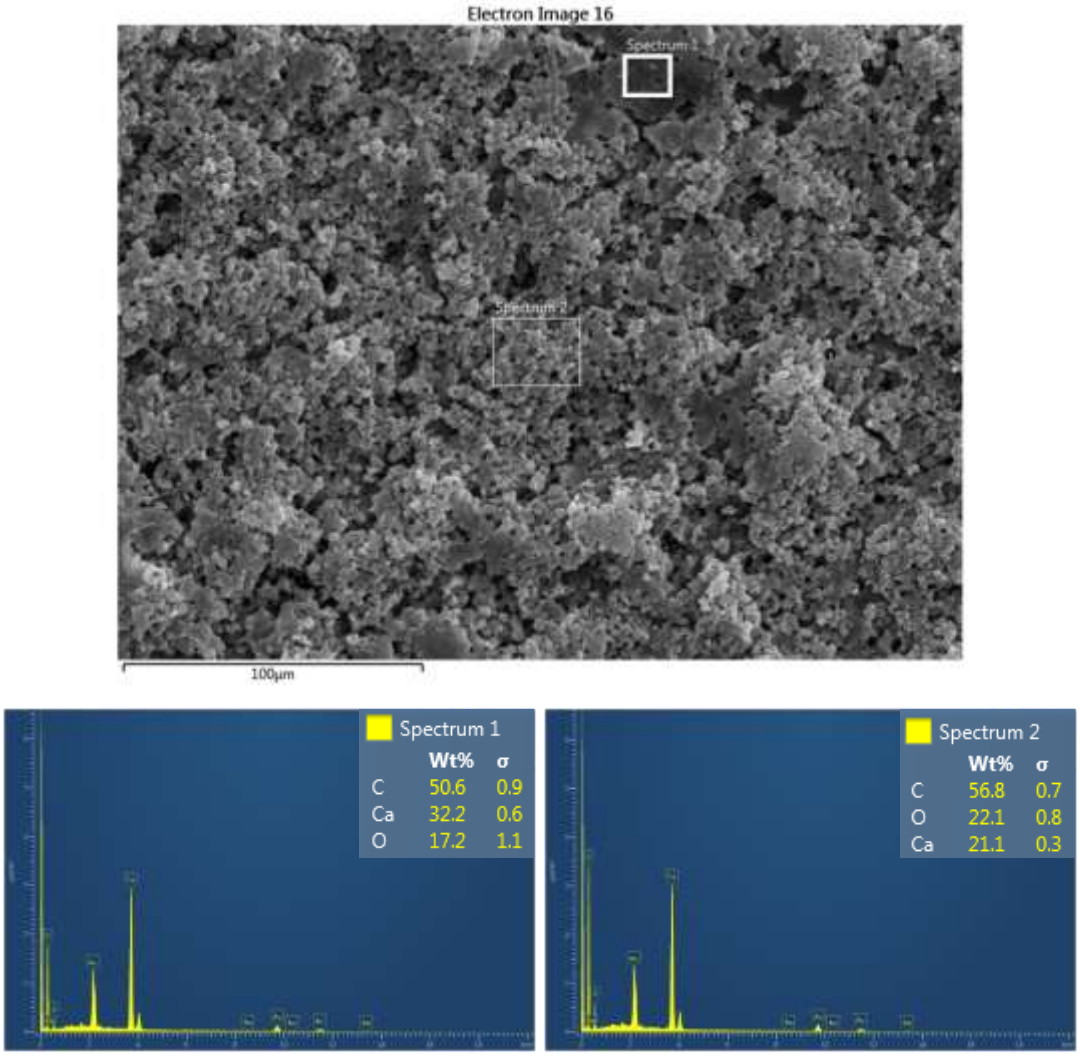

Figure 6.28: SEM image (top) and EDS spectra (bottom) of a modified Middle East Carbonate chip immersed in 50% diluted Arabian Gulf Seawater with doubled $SO4^{2-}$ ions ' concentration (AGSW*-2SO)

CHAPTER 7

ZETA POTENTIAL MEASUREMENTS FOR THE SEQUENTIAL DILUTION OF THE ARABIAN GULF SEAWATER

On the basis of the fundamental understanding and knowledge developed throughout the experimental work of the current study, an attempt is made in this chapter to provide detailed interpretation of one of the incremental oil recovery by sequential dilution of the seawater. [5, 59, 60] The reported incremental oil recovery was observed on a real carbonate reservoir core samples (80% calcite, 13% dolomite and less than 1% quartz) was observed when the injected AGSW water was sequentially diluted two times and up to 20 times, after which, no more oil was recovered as shown in Figure 7.2. Laboratory findings were verified by a small scale field test. [22]

To see how the sequentially injection of AGSW could affect surface charges of calcite, dolomite and MEC, modified powders with model oil from each rock sample was conditioned first with brine representing AGSW (AGSW).

To measure the zeta potential of carbonate powders been contacted with sequentially diluted AGSW, settled powder on the bottom of the conditioning tube that contained original AGSW were centrifuged for 1 hour and the maximum possible volume of separated brine was drained using a syringe needle and on powder left, 50% diluted AGSW

was added. The resultant mixture was conditioned on shaker for 24 hours for another zeta potential measurements. These procedures were followed on 10 times, 20 times and 100 times diluted brines from AGSW as depicted in below Figure 7.1. Zeta potential results of this part, at initial unadjusted system pHs (Table 7.1), are shown in Figure 7.3.

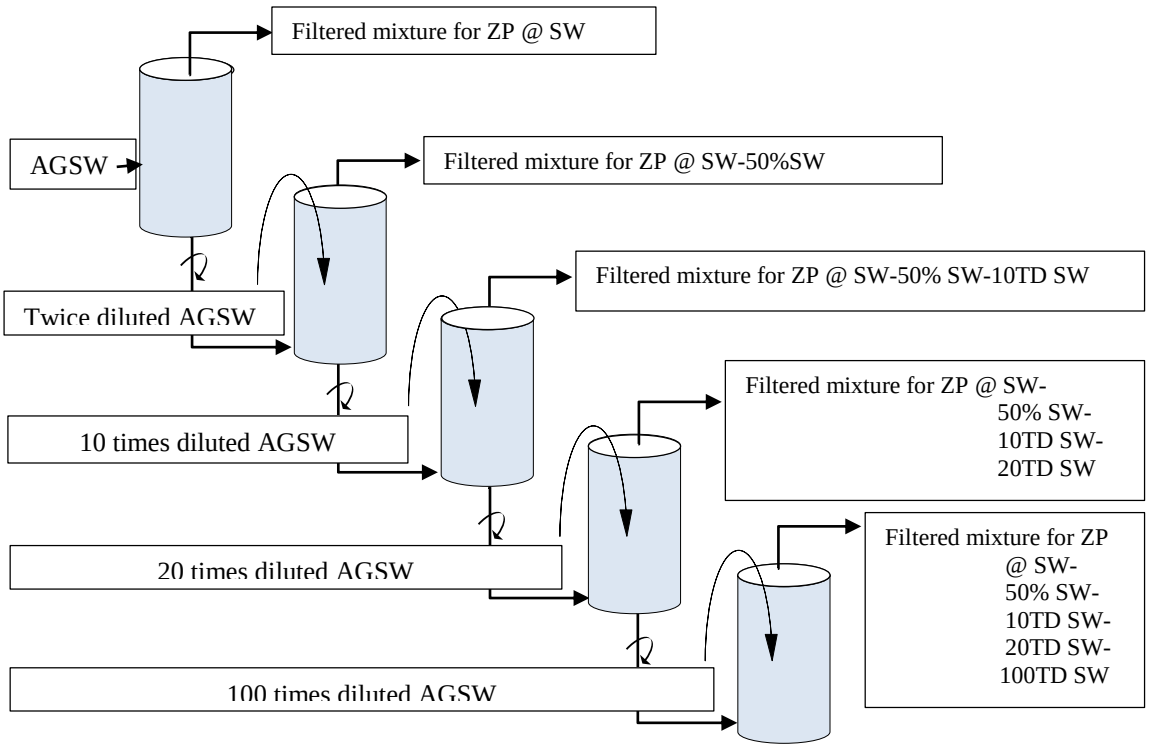

Figure 7.1: Illustration of the experimental procedures for zeta potential measurements of modified calcite, dolomite and Middle East Carbonate powders in sequentially diluted Arabian Gulf Seawater at initial unadjusted pH.

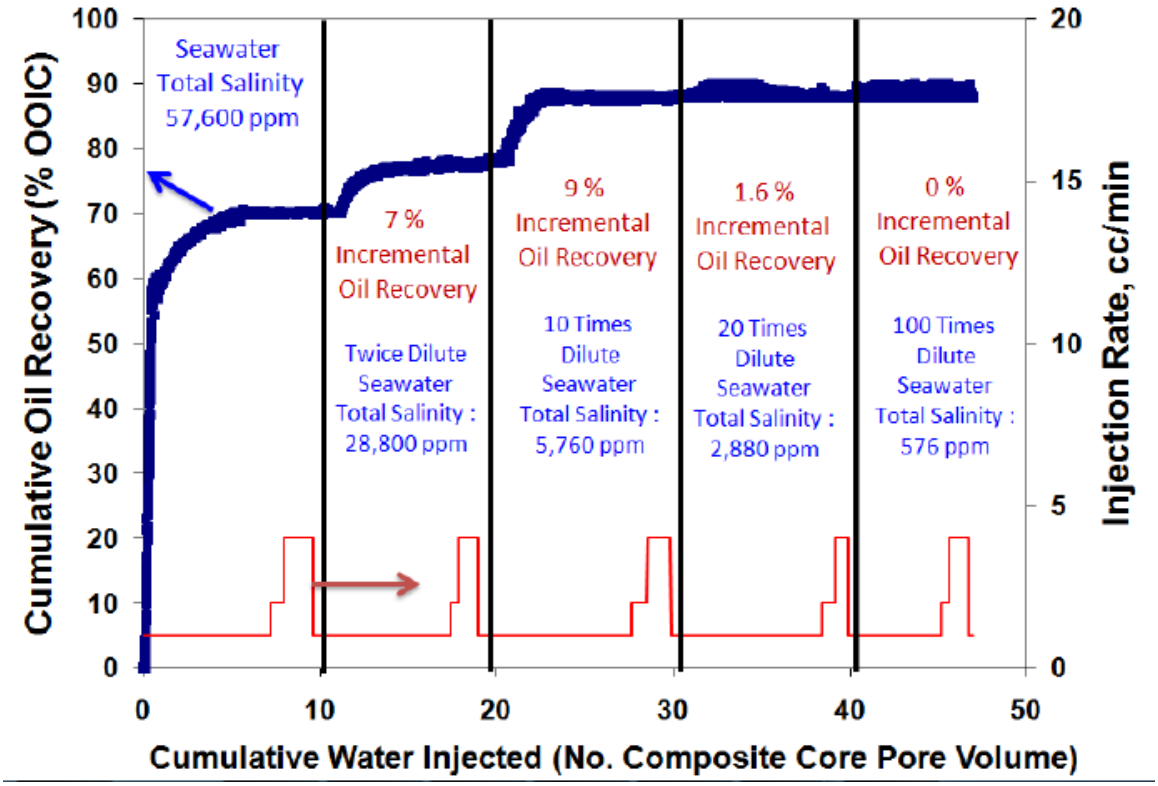

Figure 7.2: Incremental recovery reported Al-Yousef et al. (CSUG/SPE 137634).

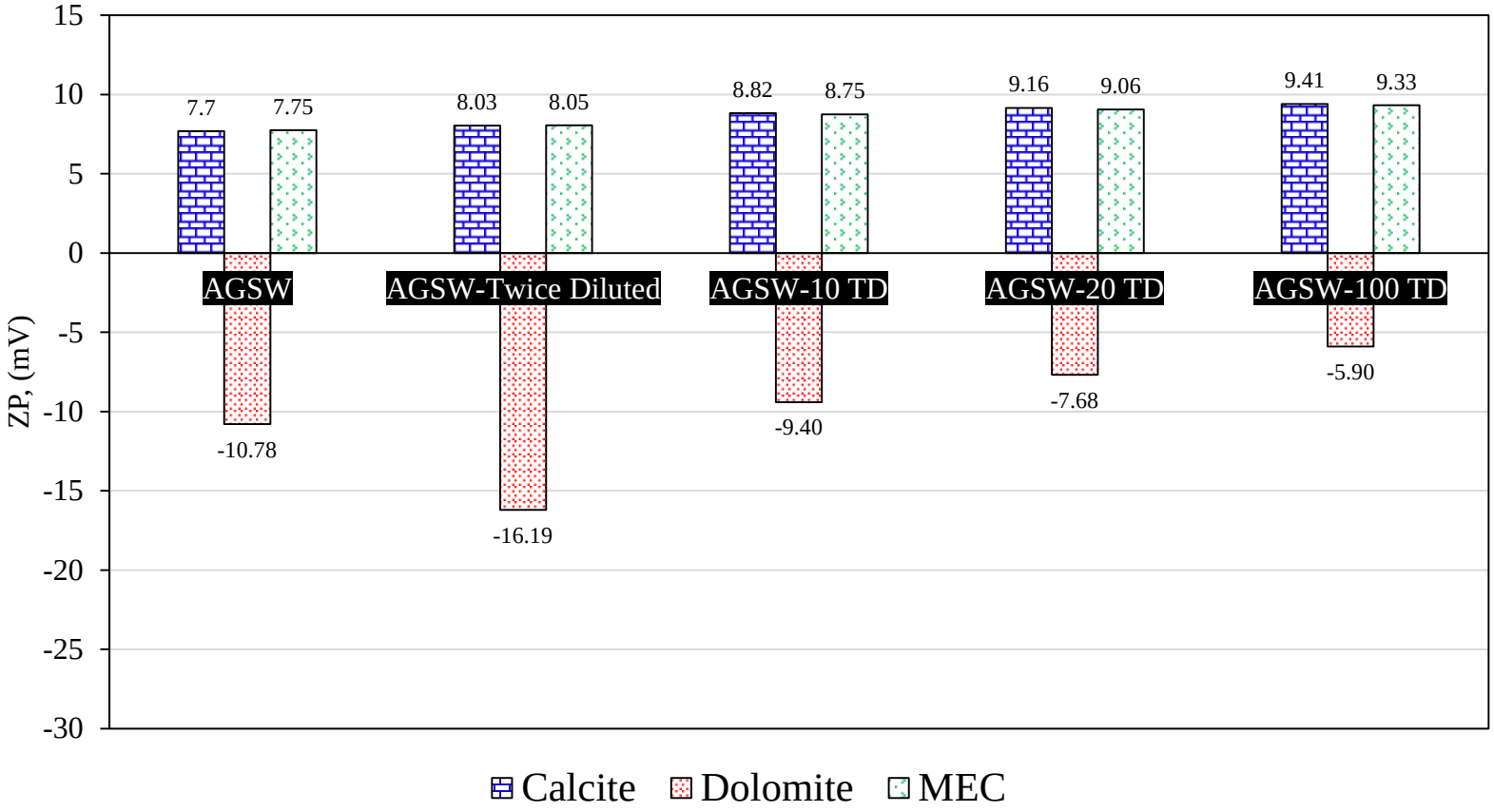

Figure 7.3: Effect of sequentially diluted Arabian Gulf Seawater on zeta potential of modified calcite, dolomite and Middle East Carbonate powders with model oil 25 ºC and at initial unadjusted pH (Table 7.1 summarizes the pH values)

Table 7.1: Initial unadjusted pH values during zeta potential measurements for the sequential dilution of the Arabian Gulf Seawater

Brine	Calcite	Dolomite	MEC
AGSW	pH 7.70	pH 7.75	pH 7.70
AGSW-twice diluted	pH 8.03	pH 8.05	pH 7.95
AGSW-10TD	pH 8.82	pH 8.75	pH 8.52
AGSW-20TD	pH 9.16	pH 9.06	pH 8.90
AGSW-100TD	pH 9.41	pH 9.33	pH 9.31

From the calculated zeta potential values, it can be seen that for the dolomite, additional positive surface charges more than those developed after primary conditioning with AGSW were developed when 50% diluted AGSW was sequentially used. When 10 times diluted AGSW was used after 50% diluted AGSW, the magnitude of positive surface charges decreased to a value less than what was found on primary AGSW. Further slight decrease was also found when 20 times diluted AGSW was used and another slighter decrease was noticed in 100 times diluted AGSW. The same trend of zeta potential values, but in the direction of the opposite sign, was found on modified calcite, but this time, higher decrease in the magnitude of negative surface charges continued up to the stage of using 100 times diluted AGSW. The same trend was also found in modified MEC, but the magnitude of increase or decrease in the negative charges was not as high as what was found in modified calcite.

When comparing the trend of incremental recovery reported by Yousef et al. [5, 59, 60], Figure 7.2, with the observed trend of zeta potential values shown in Figure 7.3, a correlation between zeta potential values and reported incremental oil recoveries, can be made as follows:

I. Phase A: Incremental recovery during primary AGSW injection

In this phase, a plateau of 70% of oil recovery was reported after injection of about 6 pore volumes of AGSW as can be seen from Figure 7.2. From zeta potential, comparison between values of surface charges obtained in deionized water and those obtained in AGSW (Figure 7.3) indicates that in AGSW good negative charges are maintained in calcite and MEC, while slight increase in the magnitude of positive charges took place on dolomite.

Table 7.2: Comparison between zeta potential values of modified carbonates in deionized water and Arabian Gulf Seawater at initial unadjusted pH

	Modified calcite	Modified MEC	Modified dolomite
Deionized water	-18.70	-20.74	13.41
AGSW	-10.78	-10.52	15.07

The negative surface charges found on calcite and MEC in AGSW can be attributed to the presence of sulfate ions on each sample's surface. This is supported by the previously obtained results for the individual and relative effect of sulfate ions as discussed in the previous two chapters. For the decrease in the magnitude of the negative charges (from -18.7 to -10.78) which is observed on the AGSW compared to deionized water, two mechanisms might be responsible, and these can be either adsorption of positive ions, such as calcium or magnesium, or it can be the compression of electric double layers due to the high ionic strength in AGSW. On dolomite, however, no significant effect of sulfate ions is expected due to the relative effect of magnesium ions on adsorption of sulfate which was

discussed in the previous chapter while the slight increase in the positive charges can be attributed to the possible adsorption of positive ions such as calcium and magnesium.

Based on the above discussion, elaboration on the mechanism of wettability alteration, reported by Yousef et al. [5, 59, 60] for the observed recovery can be made. During AGSW injection, adsorbed oil on calcite site was mainly removed by the adsorption of sulfate with very weak possibility of recovering oil by replacement of positive surface ions with attached oil by magnesium ions coming from the injected AGSW. This is due to the initial high concentration of positive ions on pore space surfaces possibly adsorbed during aging of cores with formation water which has very high concentration of cations as shown in Table 3.8. At this phase, if some oil was originally on dolomite sites, it is not expected to be recovered as a result of the weak ability of sulfate ions to be adsorbed on the dolomite surfaces due to the presence of positive cations on the solution.

II. Phase B: Incremental recovery during 50% diluted AGSW

As shown in Figure 7.2, a plateau of 70% recovery was achieved after injecting 6 pore volumes, and after injection of up to 10 pore volumes, no more oil was recovered. At the end of this stage, it is expected that a condition of chemical equilibrium was achieved among all system components. When twice diluted AGSW was injected, this condition of equilibrium was distorted and another phase of ions interactions took place in the system, which resulted in additional 7% of oil recovery. The most logical recovery mechanism during this phase could be the microscopic dissolution of rock surfaces, from both, calcite and dolomite by which the retained oil was released. When twice diluted AGSW was

injected, a transfer of ions from rock surfaces to the bulk of solution took place in order to equilibrate concentrations of ions on the system and due to this process some positive surface ions with attached oil would have left the rock surface which resulted in the 7% incremental recovery. Only by this mechanism, decreased negative charges on calcite surface and decreased positive changes on dolomite surfaces can be explained.

III. Phase C: Incremental recovery during 10 times, and 20 times diluted AGSW

Incremental recovery reported in this phase can be attributed to the state of chemical unequilibrium which continued due to injection of AGSW that contains less ions than what was present in the pore space system. No more oil will be released when a state of chemical equilibrium is achieved such as when 100 times diluted AGSW was injected. This explains why no more oil was recovered at this stage of injection.

Based on these explanations made in this section, it can be pointed out that more than one chemical process can be responsible for the wettability alteration of carbonate rocks by smart water flooding.

CHAPTER 8

CONCLUSIONS AND RECOMMENDATIONS

8.1 Conclusions

Through comprehensive zeta potential measurements coupled with microscopic surface characterization techniques on typical carbonate rocks, the level of understanding about the recovery mechanism during smart water flooding was improved. This was achieved by conducting laboratory experiments on these rock samples on selected fixed conditions and varied major conditions which have direct impact of the role of potential determining ions present in injection water from AGSW. The following conclusions can be made from the interpretation of the obtained results:

- Adsorption of carboxylic materials from oil on carbonate rocks decreases the magnitude of positive surface charges or increases the magnitude of negative surface charges.
- Carboxylic materials adsorb stronger on dolomite surfaces than on calcite surfaces.
- Zeta potential of calcite in deionized water is negative due to the preferential dissolution of calcium ions from the surface lattice while in dolomite no significant surface dissolution was seen. Therefore, dolomite surfaces possess positive surface charges in deionized water.

- In addition to hydrogen and hydroxide ions, calcium, magnesium and sulfate ions are confirmed to be regarded as potential determining ions toward carbonate rocks which are able to modify or alter original surface charges.
- Adsorption of magnesium ions on carbonate surfaces can develop more positive charges compared to adsorption of calcium ions while strong negative charges can be developed by adsorption of sulfate which have very high affinity towards carbonate surfaces.
- Co-adsorption of potential determining ions can happen on the same carbonate surface with varied relative effect based on the relative concentration between adsorbed ions.
- Adsorption of sulfate ions adds more negative surface charges to both calcite and dolomite surfaces; and this is believed to be able to partially displace adsorbed carboxylic materials.
- Adsorption of magnesium ions will significantly decrease negative surface charges developed by adsorbed sulfate ions, compared to adsorption of calcium ions. However, the affinity of other potential determining ions to adsorb on carbonate surfaces increases more in the presence of magnesium than in the presence of calcium ions.
- Arabian Gulf Seawater adds more negative charges to carbonate surfaces compared to diluted seawater; and this it attributed to the higher concentration of sulfate ions in the seawater.
- When diluted Arabian seawater was used after primary conditioning of the carbonate particles by original Arabian Gulf seawater, the magnitude of negative

charges in the calcite, MEC and the positive charges in the dolomite has increased compared to when the diluted seawater is directly used. By such sequential conditioning, adsorbed carboxylic materials are believed to be released by the induced dissolution of the carbonates minerals rather than ions exchange/adsorption.

- The efficiency of diluted Arabian Gulf seawater in altering the surface charges of carbonate surfaces can be improved by increasing the concentration of magnesium and sulfate ions. This should be supported by a detailed solubility calculation to prevent scale precipitation inside the reservoir.

8.2 Recommendations

- Similar set of experiments should be conducted to study the zeta potential of other types of carbonate minerals, such like magnesite, anhydrite, gypsum, etc.
- Other types of carboxylic acids or other crude oil compounds (asphaltene, resins) should be studied.
- Surface growth and modified surface structures should be characterized by a high resolution technique that enables detecting organic and inorganic compounds.
- Detailed solubility study should be conducted to assess the possibility of scale precipitation when PDIs are increased/decreased.

APPENDIX:

TABULATED ZETA POTENTIAL MEASUREMENTS

A. Effect of pH and Deionized Water

Table A.1: Measured zeta potential values of unmodified calcite, dolomite and Middle East Carbonate suspensions in deionized water (correspondes to Figure 4.1)

Unmodified Powders					
Calcite		Dolomite		MEC	
pH	ZP (mV)	pH	ZP	pH	ZP
4.00	5.37	3.80	34.83	4.00	3.48
6.00	-1.96	5.60	31.13	6.15	-4.71
8.00	-6.45	6.50	27.57	7.30	-10.40
9.50	-12.51	9.65	16.59	9.60	-14.58
10.50	-18.00	10.57	8.95	10.50	-16.38
11.50	-24.88	11.53	1.92	11.55	-16.20

Table A.2: Measured zeta potential values of modified calcite, dolomite and Middle East Carbonate suspensions in deionized water (correspondes to Figure 4.1)

Modified Powders					
Calcite		Dolomite		MEC	
pH	ZP (mV)	pH	ZP	pH	ZP
3.20	8.30	3.60	32.95	4.00	-7.31
4.20	5.65	5.12	26.88	5.80	-11.00
6.00	-4.19	6.15	21.70	7.05	-14.80
8.00	-11.22	7.70	17.75	9.40	-20.74
9.53	-18.70	9.63	13.41	10.55	-21.88
10.45	-20.83	10.50	8.92	11.50	-21.33
		11.50	-4.73		

B. Individual Effects of PDIs

Table A.3: Measured zeta potential values of unmodified calcite, dolomite and Middle East Carbonate suspensions as function of increased Ca^{2+} ions' concentration (correspondes to Figure 4.9)

Unmodified Powders			
$[Ca^{2+}]$, (ppm)	Calcite (mV)	Dolomite (mv)	MEC (mv)
326	-10.11	12.23	10.23
652	-8.69	13.56	13.47
1,304	9.38	15.64	14.67
1,956	9.95	19.20	18.43

Table A.4: Measured zeta potential values of modified calcite, dolomite and Middle East Carbonate suspensions as function of increased Ca^{2+} ions' concentration (correspondes to Figure 4.9)

Unmodified Powders			
$[Ca^{2+}]$, (ppm)	Calcite (mV)	Dolomite (mv)	MEC (mv)
326	-7.36	11.01	-9.34
652	-5.98	10.43	-4.33
1,304	9.82	13.34	16.45
1,956	12.05	20.11	19.13

Table A.5: Measured zeta potential values of unmodified calcite, dolomite and Middle East Carbonate suspensions as function of increased Mg^{2+} ions' concentration (correspondes to Figure 4.10)

Unmodified Powders			
$[Mg^{2+}]$, (ppm)	Calcite (mV)	Dolomite (mv)	MEC (mv)
1,080	8.32	11.23	8.62
2,159	11.60	13.34	17.28
4,318	14.16	17.24	19.42
6,477	16.14	18.52	22.45

Table A.6: Measured zeta potential values of modified calcite, dolomite and Middle East Carbonate suspensions as function of increased Mg^{2+} ions' concentration (correspondes to Figure 4.10)

Modified Powders			
$[Mg^{2+}]$, (ppm)	Calcite (mV)	Dolomite (mv)	MEC (mv)
1,080	7.26	13.88	-8.92
2,159	9.04	14.58	9.91
4,318	13.73	15.88	16.66
6,477	16.64	22.78	19.83

Table A7: Measured zeta potential values of unmodified calcite, dolomite and Middle East Carbonate suspensions as function of increased SO_4^{2-} ions' concentration (correspondes to Figure 4.11)

Unmodified Powders			
$[SO_4^{2-}]$, (ppm)	Calcite (mV)	Dolomite (mv)	MEC (mv)
2,225	-11.20	10.30	-11.52
4,450	-12.43	-8.29	-15.56
8,900	-15.11	-10.69	-16.68
13,350	-17.56	-10.93	-19.91

Table A.7: Measured zeta potential values of modified calcite, dolomite and Middle East Carbonate suspensions as function of increased SO_4^{2-} ions' concentration (correspondes to Figure 4.11)

Modified Powders			
$[SO_4^{2-}]$, (ppm)	Calcite (mV)	Dolomite (mv)	MEC (mv)
2,225	-9.43	-4.54	-9.77
4,450	-12.13	-7.85	-14.90
8,900	-13.62	-11.31	-15.85
13,350	-15.49	-14.80	-20.39

C. Relative Effects of PDIs

Table A.8: Relative effect of Ca^{2+} to Mg^{2+} ions on measured zeta potential values of unmodified calcite, dolomite and Middle East Carbonate (correspondes to Figure 5.1)

Unmodified Powders					
$[Ca^{2+}]$, ppm	$[Mg^{2+}]$, ppm	$[Ca^{2+}]/[Mg^{2+}]$ ratio	Calcite (mV)	Dolomite (mv)	MEC (mv)
326	1,080	0.30	8.51	12.33	8.48
652	1,080	0.60	9.58	12.91	9.89
1,304	1,080	1.21	9.80	14.47	12.70
1,956	1,080	1.81	13.35	16.45	17.00

Table A.9: Relative effect of Ca^{2+} to Mg^{2+} ions on measured zeta potential values of modified calcite, dolomite and Middle East Carbonate (correspondes to Figure 5.1)

Modified Powders					
$[Ca^{2+}]$, ppm	$[Mg^{2+}]$, ppm	$[Ca^{2+}]/[Mg^{2+}]$ ratio	Calcite (mV)	Dolomite (mv)	MEC (mv)
326	1,080	0.30	10.47	9.22	9.93
652	1,080	0.60	10.21	13.98	16.15
1,304	1,080	1.21	8.25	16.01	17.22
1,956	1,080	1.81	11.44	17.84	19.97

Table A.10: Relative effect of Ca^{2+} to SO_4^{2-} ions on measured zeta potential values of unmodified calcite, dolomite and Middle East Carbonate (correspondes to Figure 5.2)

Unmodified Powders					
$[Ca^{2+}]$, ppm	$[SO_4^{2-}]$, ppm	$[Ca^{2+}]/[SO_4^{2-}]$ ratio	Calcite (mV)	Dolomite (mv)	MEC (mv)
326	2,225	0.15	-5.05	8.64	-8.41
652	2,225	0.29	-3.83	13.10	-8.72
1,304	2,225	0.59	10.76	13.38	-5.42
1,956	2,225	0.88	11.30	14.83	-4.64

Table A.11: Relative effect of Ca^{2+} to SO_4^{2-} ions on measured zeta potential values of modified calcite, dolomite and Middle East Carbonate (correspondes to Figure 5.2)

Modified Powders					
$[Ca^{2+}]$, ppm	$[SO_4^{2-}]$, ppm	$[Ca^{2+}]/[SO_4^{2-}]$ ratio	Calcite (mV)	Dolomite (mv)	MEC (mv)
326	2,225	0.15	-8.76	9.16	-11.20
652	2,225	0.29	-4.72	13.98	-6.65
1,304	2,225	0.59	11.64	14.33	-5.88
1,956	2,225	0.88	14.23	17.84	-5.47

Table A.12: Relative effect of Mg^{2+} to Ca^{2+} ions on measured zeta potential values of unmodified calcite, dolomite and Middle East Carbonate (correspondes to Figure 5.3)

Unmodified Powders					
$[Mg^{2+}]$, ppm	$[Ca^{2+}]$, ppm	$[Mg^{2+}]/[Ca^{2+}]$ ratio	Calcite (mV)	Dolomite (mv)	MEC (mv)
1,080	326	3.31	6.57	12.33	8.48
2,159	326	6.62	7.42	12.90	8.63
4,318	326	13.25	12.42	16.99	9.19
6,477	326	19.87	12.87	19.37	11.73

Table A.13: Relative effect of Mg^{2+} to Ca^{2+} ions on measured zeta potential values of modified calcite, dolomite and Middle East Carbonate (correspondes to Figure 5.3)

Modified Powders					
$[Mg^{2+}]$, ppm	$[Ca^{2+}]$, ppm	$[Mg^{2+}]/[Ca^{2+}]$ ratio	Calcite (mV)	Dolomite (mv)	MEC (mv)
1,080	326	3.31	10.47	9.22	9.93
2,159	326	6.62	13.33	14.41	11.12
4,318	326	13.25	14.83	14.87	13.95
6,477	326	19.87	17.29	16.79	16.32

Table A.14: Relative effect of Mg^{2+} to SO_4^{2-} ions on measured zeta potential values of unmodified calcite, dolomite and Middle East Carbonate (correspondes to Figure 5.4)

Unmodified Powders					
$[Mg^{2+}]$, ppm	$[SO_4^{2-}]$, ppm	$[Mg^{2+}]/[SO_4^{2-}]$ ratio	Calcite (mV)	Dolomite (mv)	MEC (mv)
1,080	2,225	0.49	6.63	8.36	-13.02
2,159	2,225	0.97	8.42	14.65	-9.98
4,318	2,225	1.94	11.02	17.50	9.85

Table A.15: Relative effect of Mg^{2+} to SO_4^{2-} ions on measured zeta potential values of modified calcite, dolomite and Middle East Carbonate (correspondes to Figure 5.4)

Modified Powders					
$[Mg^{2+}]$, ppm	$[SO_4^{2-}]$, ppm	$[Mg^{2+}]/[SO_4^{2-}]$ ratio	Calcite (mV)	Dolomite (mv)	MEC (mv)
1,080	2,225	0.49	9.50	11.74	-13.44
2,159	2,225	0.97	12.37	15.79	-9.16
4,318	2,225	1.94	14.23	15.56	6.14

Table A.16: Relative effect of SO_4^{2-} to Ca^{2+} ions on measured zeta potential values of unmodified calcite, dolomite and Middle East Carbonate (correspondes to Figure 5.5)

Unmodified Powders					
$[SO_4^{2-}]$, ppm	$[Ca^{2+}]$, ppm	$[SO_4^{2-}]/[Ca^{2+}]$ ratio	Calcite (mV)	Dolomite (mv)	MEC (mv)
2,225	326	6.83	-5.05	8.64	-8.41
4,450	326	13.65	-7.25	-11.16	-8.46
8,900	326	27.30	-7.50	-12.85	-9.76
13,350	326	40.95	-8.64	-13.73	-14.80

Table A.17: Relative effect of SO_4^{2-} to Ca^{2+} ions on measured zeta potential values of modified calcite, dolomite and Middle East Carbonate (correspondes to Figure 5.5)

Modified Powders					
$[SO_4^{2-}]$, ppm	$[Ca^{2+}]$, ppm	$[SO_4^{2-}]/[Ca^{2+}]$ ratio	Calcite (mV)	Dolomite (mv)	MEC (mv)
2,225	326	6.83	-8.76	9.16	-11.20
4,450	326	13.65	-10.63	-5.60	-15.57
8,900	326	27.30	-15.70	-10.20	-16.80
13,350	326	40.95	-16.46	-16.90	-19.39

Table A.18: Relative effect of SO_4^{2-} to Mg^{2+} ions on measured zeta potential values of unmodified calcite, dolomite and Middle East Carbonate (correspondes to Figure 5.6)

Unmodified Powders					
$[SO_4^{2-}]$, ppm	$[Mg^{2+}]$, ppm	$[SO_4^{2-}]/[Mg^{2+}]$ ratio	Calcite (mV)	Dolomite (mv)	MEC (mv)
2,225	1,080	2.06	6.63	8.36	-13.02
4,450	1,080	4.12	7.77	7.14	-16.83
8,900	1,080	8.24	-6.34	-7.83	-20.33

Table A.19: Relative effect of SO_4^{2-} to Mg^{2+} ions on measured zeta potential values of modified calcite, dolomite and Middle East Carbonate (correspondes to Figure 5.6)

Modified Powders					
$[SO_4^{2-}]$, ppm	$[Mg^{2+}]$, ppm	$[SO_4^{2-}]/[Mg^{2+}]$ ratio	Calcite (mV)	Dolomite (mv)	MEC (mv)
2,225	1,080	2.06	9.50	11.74	-13.44
4,450	1,080	4.12	11.05	11.39	-17.06
8,900	1,080	8.24	-5.17	-13.50	-20.75

D. Effect of Modified Arabian Gulf Seawater

Table A.20: Effect of modified Arabian Gulf Seawater on zeta potential of modified calcite, dolomite and Middle East Carbonate (correspondes to Figure 6.1 and Figure 6.2)

Modified Powders			
Brine	Calcite (mv)	Dolomite (mv)	MEC (mv)
DI Water	-18.70	13.41	-20.74
NaCl (0.574 M)	-15.66	13.71	-15.39
AGSW	-10.78	15.07	-10.52
AGSW* (50% diluted)	-9.80	12.31	-11.25
AGSW*-2Ca	-6.62	8.89	13.37
AGSW*-4Ca	6.48	15.23	19.29
AGSW*-2Mg	6.15	19.44	11.65
AGSW*-4Mg	9.64	16.04	13.79
AGSW*-2SO	-6.10	12.99	-13.76
AGSW*-4SO	-11.20	-6.97	-18.34

E. Effect of Sequentially Diluted Arabian Gulf Seawater

Table A.21: Effect of sequentially diluted Arabian Gulf Seawater on zeta potential of modified calcite, dolomite and Middle East Carbonate (correspondes to Figure 7.3)

Brine	Calcite (mv)	Dolomite (mv)	MEC (mv)
AGSW	-10.78	15.07	-10.52
AGSW-Twice Diluted	-16.19	18.92	-11.70
AGSW-10 TD	-9.40	12.95	-11.14
AGSW-20 TD	-7.68	10.97	-10.12
AGSW-100 TD	-5.90	10.81	-10.48

REFERENCES

[1] Tiab, D, Donaldson, E 2004, *Petrophysics (Second Edition): Theory and Practice of Measuring Reservoir Rock and Fluid Transport Properties,* Gulf Publishing Company, Houston, Texas, USA.

[2] Akbar, M et al. 2001, 'A Snapshot of Carbonate Reservoir Evaluation', *Schlumberger Oilfiled Review*, Winter 2000/2001.

[3] Strand, S, Austad, T, Puntervold, T, Hognesen, E, Olsen, M, Barstad, M 2008, '"Smart Water" for Oil Recovery from Fractured Limestone: A Preliminary Study', *Energy & Fuels,* vol. 22, no. 5, pp. 3126-3133.

[4] Strand, S, Hognesen, E, Austad, T 2006, 'Wettability alteration of carbonates: Effects of potential determining ions (Ca^{2+} and SO_4^{2-}) and temperature' *Colloids and Surfaces A: Physicochemical and Engineering Aspects,* vol. 275, no. 1-3, pp. 1-10.

[5] Yousef, A, Al-Saleh, S, Al-Jawfi, M 2012, 'Improved/Enhanced Oil Recovery from Carbonate Reservoirs by Tuning Injection Water Salinity and Ionic Content', *Paper SPE 154076 presented at the SPE Improved Oil Recovery Symposium,* SPE, 14-18 April, Tulsa, Oklahoma, USA.

[6] Legens, C, Toulhoat, H, Cuiec, L, Villieras, F, Palermo, T 1999, 'Wettability Change Related to Adsorption of Organic Acids on Calcite: Experimental and Ab Initio Computational Studies', *SPE Journal,* vol. 4, no. 4, pp. 328-333.

[7] Jafar, S, Austad, T, Strand, S 2012, 'Water-Based Enhanced Oil recovery (EOR) by "Smart Water" in Carbonate Reservoirs', *Paper SPE 154570 presented at the SPE EOR Conference at Oil and Gas West Asia*, SPE, 16-18 April, Muscat, Oman.

[8] Hirasaki, G, Zhang, D 2004, 'Surface Chemistry of Oil Recovery From Fractured, Oil-Wet, Carbonate Formations', *SPE Journal,* vol. 9, no. 2, pp. 151-162.

[9] Zhang, P, Tweheyo, M, Austad, T 2006, 'Wettability Alteration and Improved Oil Recovery in Chalk: The Effect of Calcium in the Presence of Sulfate', *Energy&Fuels,* vol. 20, no. 5, pp. 2056-2062.

[10] Alotaibi, M, Nasr-El-Din, H, Fletcher, J 2011, 'Electrokinetics of Limestone and Dolomite Rock Particles', *SPE Reservoir Evaluation & Engineering,* vol. 14, no. 5, pp. 594-603.

[11] Thomas, M, Clouse, J, Longo J 1993, 'Adsorption of organic compounds on carbonate minerals: 1. Model compounds and their influence on mineral wettability' *Chemical Geology*, vol. 109, no. 1-4, pp. 201-213.

[12] Zhang, P, Austad, T 2005, 'The Relative Effects of Acid Number and Temperature on Chalk Wettability' *Paper SPE 92999 presented at the SPE International Symposium on Oilfield Chemistry,* SPE, 2-4 February, The Woodlands, Texas.

[13] Hiorth, A, Cathles, L, Madland, M 2010, 'The Impact of Pore Water Chemistry on Carbonate Surface Charges and Oil Wettability', *Transport in Porous Media,* vol. 85, no. 1, pp. 1-21.

[14] Nasralla, R, Nasr-El-Din, H 2011, 'Impact of Electrical Surface Charges and Cation Exchange on Oil Recovery by Low Salinity Water', *Paper SPE 147937 presented at the SPE Asia Pacific Oil and Gas Conference and Exhibition*, SPE, 20-22 September, Jakarta, Indonesia.

[15] Buckley, J, Takamura, K, Morrow, N 1989, 'Influence of Electrical Surface Charges on the Wetting Properties of Crude Oils', *SPE Reservoir Engineering*, vol. 4, no. 3, pp. 332-340.

[16] Zhang, P, Austad, T 2006, 'Wettability and oil recovery from carbonates: Effects of temperature and potential determining ions', *Colloids and Surfaces A: Physicochemical and Engineering Aspects,* vol. 279, no. 1-3, pp. 179-187.

[17] Alotaibi, M, Nasr-El-Din, H 2009, 'Chemistry of Injection Water and its Impact on Oil Recovery in Carbonate and Clastic Formations', *Paper SPE 121565 presented at the SPE International Symposium on Oilfield Chemistry*, SPE, 20-22 April, The Woodlands. Texas.

[18] Webb, K, Black, C, Al-Ajeel, H 2004, 'Low Salinity Oil Recovery - Log-Inject-Log', *Paper SPE 89379 presented at the SPE/DOE Symposium on Improved Oil Recovery*, SPE, 17-21 April, Tulsa, Oklahoma.

[19] McGuire, P, Chatham, J, Paskvan, F, Sommer, D, Carini, F 2005, 'Low Salinity Oil Recovery: An Exciting New EOR Opportunity for Alaska's North Slope', *Paper SPE 93903 presented at the SPE Western Regional Meeting*, SPE, 30 March-1 April, Irvine, California.

[20] Seccomble, J, Lager, A, Webb, K, Jerauld, G 2008, 'Improving Wateflood Recovery: LoSal™ EOR Field Evaluation', *Paper SPE 113480 presented at the SPE Symposium on Improved Oil Recovery*, SPE, 20-23 April, Tulsa, Oklahoma, USA.

[21] Abdulla, F, Hashem, H, Abdulraheem, B, Al-Nnaqi, M, Al-Qattan, A, Jhon, H, Cunningham, P, Briggs, P, Thawer, R, 2013, 'First EOR Trial using Low Salinity Water Injection in the Greater Burgan Field, Kuwait', *Paper SPE 164341 presented at the SPE Middle East Oil and Gas Show and Conference*, SPE 10-13 March, Manama, Bahrain.

[22] Yousef, A, Liu, J, Blanchard, G, Al-Saleh, S, Al-Zahrani, T, Al-Zahrani, R, Tammar, H, Al-Mulhim, N 2012, 'Smart Waterflooding: Industry's First Field Test in Carbonate Reservoirs', *Paper SPE 159526 presented at the SPE Annual Technical Conference and Exhibition*, SPE, 8-10 October, San Antonio, Texas, USA.

[23] Austad, T 2008, ' "Smart Water" for Enhanced Recovery: A Comparison of Mechanisms in Carbonates and Sandstone', *A Presntation in Force seminar on Low Salinity*, 15th May, NPD Norway.

[24] RezaeiDoust, A, Puntervold, T, Austad, T 2011, 'Chemical Verification of the EOR Mechanism by Using Low Saline/Smart Water in Sandstone', *Energy&Fuels*, vol. 25, no. 5, pp. 2151-2162.

[25] Zahid, A, Shapiro, A, Skauge, A 2012, 'Experimental Studies of Low Salinity Water Flooding Carbonate: A New Promising Approach', *Paper SPE 155625 presented at the SPE EOR Conference at Oil and Gas West Asia*, SPE, 16-18 April, Muscat, Oman.

[26] Zhang, P, Tweheyo, M, Austad, T 2007, 'Wettability alteration and improved oil recovery by spontaneous imbibition of seawater into chalk: Impact of the potential determining ions Ca^{2+}, Mg^{2+}, and SO_4^{2-}', *Colloids and Surfaces A: Physicochemical and Engineering Aspects*, vol. 301, no. 1-3, pp. 199-208.

[27] Hiemenz, PC 1977, *Principles of Colloid and Surface Chemistry*, Marcel Dekker Inc., New York, USA.

[28] Evertee, DH, 1994, *Basic Principles of Colloid Science*, Royal Society of Chemistry, London, UK.

[29] Rodríguez, K, Araujo, M 2006, 'Temperature and pressure effects on zeta potential values of reservoir minerals', *Journal of Colloid and Interface Science*, vol. 300, no. 2, pp. 788-794.

[30] Cicerone, D, Regazzoni, A, Blesa, M 1992, 'Electrokinetic properties of the calcite/water interface in the presence of magnesium and organic matter', *Journal of Colloid and Interface Science*, vol. 154, no. 2, pp. 423-433.

[31] Pierre, A, Lamarche, J, Mercier, R, Foissy, A, Persello, J 1990, 'Calcium as Potential Determining Ion in Aqueous Calcium Suspensions', *Journal of Dispersion Science and Technology*, vol. 11, no. 6, pp. 611-635.

[32] Legens, C, Toulhoat, H, Cuiec, L, Villieras, F, Palermo, T 1999, 'Wettability Change Related to Adsorption of Organic Acids on Calcite: Experimental and Ab Initio Computational Studies', *Paper SPE 49319 presented at the SPE Annual Technical Conference and Exhibition*, SPE, 27-30 September, New Orleans, Louisiana.

[33] Gomari, K, Karoussi, O, Hamouda, A 2006, 'Mechanistic Study of Interaction Between Water and Carbonate Rocks for Enhancing Oil Recovery', *Paper SPE 99628 presented at the SPE Europec/EAGE Annual Conference and Exhibition*, SPE, 12-15 June, Vienna, Austria.

[34] Alotaibi, M, Nasr-El-Din, H 2011, 'Electrokinetics of Limestone Particles and Crude-Oil Droplets in Saline Solutions', *SPE Reservoir Evaluation & Engineering*, vol. 14, no. 5, pp. 604-611.

[35] Basu, S, Sharma, M 1999, 'Investigating the Role of Crude Oil Components on Wettability Alteration Using Atomic Force Microscopy', *SPE Journal*, vol. 4, no. 3, pp. 235-241.

[36] Kumar, K, Dao, E, Mohanty, K 2005, 'Atomic Force Microscopy Study of Wettability Alteration', *Paper SPE 93009 presented at the SPE International Symposium on Oilfield Chemistry*, SPE, 2-4 February, The Woodlands, Texas.

[37] Karoussi, O, Hamouda, A 2007, 'Macroscopic and nanoscale study of wettability alteration of oil-wet calcite surface in presence of magnesium and sulfate ions', *Journal of Colloid and Interface Science*, vol. 317, pp. 26-34.

[38] Heryanto, R, Hasan, M, Abdullah, E, Kumoro, A 2007, 'Solubility of Stearic Acid in Various Organic Solvents and Its Prediction using Non-ideal Solution Models', *ScienceAsia*, vol. pp. 469-472.

[39] ASTM Standard D974-12, 2012, "Standard Test Method for Acid and Base Number by Color-Indicator Titration," ASTM International, West Conshohocken, AP, 2012, DOI: 10.1520/D0974-12, www.astm.org.

[40] Lindlof, J, Stoffer, K 1983, 'A Case Study of Seawater Injection Incompatibility', *Journal of Petroleum Technology*, vol. 35, no. 7, pp. 1256 - 1262.

[41] Lindlof, J, Stoffer, K 1983, 'A Case Study of Seawater Injection Incompatibility', *Journal of Petroleum Technology*, vol. 35, no. 7, pp. 1256 - 1262.

[42] Brookhaven Instruments, 2002, '*Instruction Manauls for Zeta Potential Analyzer*', Brookaaven Instruments Corporation, New York, USA.

[43] Somasundaran, P, Agar, G 1967, 'The zero point of charge of calcite', *Journal of Colloid and Interface Science*, vol. 24, no. 4, pp. 433-440.

[44] Siffert, D, Fimbel, P 1984, 'Parameters affecting the sign and magnitude of the eletrokinetic potential of calcite', *Colloids and Surfaces*, vol. 11, no. 3-4, pp. 377-389.

[45] Vdović, N, Bišćan, J 1998, 'Electrokinetics of natural and synthetic calcite suspensions', *Colloids and Surfaces A: Physicochemical and Engineering Aspects*, vol. 137, no. 1-3, pp. 7-14.

[46] Karoussi, O, Skovbjerg, L, Hassenkam, T, Stipp, S, Hamouda, A 2008, 'AFM study of calcite surface exposed to stearic and heptanoic acids', *Colloids and Surfaces A: Physicochemical and Engineering Aspects*, vol. 325, no. 3, pp. 107-114.

[47] Smith, M, Knauss, K, Higgins, S 2013, 'Effects of crystal orientation on the dissolution of calcite by chemical and microscopic analysis', *Chemical Geology*, vol. 360–361, pp. 10-21.

[48] Abdallah, W, Gmira, A 2013, 'Wettability Assessment and Surface Compositional Analysis of Aged Calcite Treated with Dynamic Water', *Energy&Fuels*, vol. 28, no. 3, pp. 1652-1663.

[49] Pokrovsky, O, Schott, J, Thomas, F 1999, 'Dolomite surface speciation and reactivity in aquatic systems', *Geochimica et Cosmochimica Acta*, vol. 63, no. 19–20, pp. 3133-3143.

[50] Marouf, R, Khelifa, K, Schott, J, Khelifa, A 2009, 'Zeta potential study of thermally treated dolomite samples in electrolyte solutions', *Microporous and Mesoporous Materials*, vol. 122, no. 1–3, pp. 99-104.

[51] Johnston, DL 1969, *The Flotation of Apatite and Dolomite in Orthophoshate Soltuion*, in *Department of Mineral Engineering*, PhD Dissertation, The University of British Columbia, Vancouver, Canada.

[52] Gomari, K, Hamouda, A, Denoyel, R 2006, 'Influence of sulfate ions on the interaction between fatty acids and calcite surface', *Colloids and Surfaces A: Physicochemical and Engineering Aspects*, vol. 287, no. 1–3, pp. 29-35.

[53] Karoussi, O, Hamouda, A 2007, 'Macroscopic and nanoscale study of wettability alteration of oil-wet calcite surface in presence of magnesium and sulfate ions', *Journal of Colloid and Interface Science*, vol. 317, pp. 26-34.

[54] Arvidson, R, Collier, M, Davis, K, Vinson, M, Amonette, J, Luttuge, A 2006, 'Magnesium inhibition of calcite dissolution kinetics', *Geochimica et Cosmochimica Acta*, vol. 70, no. 3, pp. 583-594.

[55] Jabbar, M, Al-Hashim, H, Abdallah, W 2013, 'Effect of Brine Composition on Wettability Alteration of Carbonate Rocks in the Presence of Polar Compounds', *Paper SPE 168067 presented at the SPE Saudi Arabia Section Technical Symposium and Exhibition*, SPE, 19-22 May, Al-Khobar, Saudi Arabia.

[56] Austad, T., et al. 2005. *Seawater as IOR Fluid in Fractured Chalk*. Paper SPE 93000 presented at the SPE International Symposium on Oilfield Chemistry, 2-4 February, The Woodlands, Texas.

[57] Petrovich, R, Hamouda, A 1998, 'Dolomitization of Ekofisk Oil Field Reservoir Chalk by Injected Seawater', *Proceedings of the 9th International Symposium on Water-Rock Interaction*s, March 30th-April 3rd, Taupo, New Zeland.

[58] Zahid, A, Stenby, E, Shapiro, A 2012, 'Smart Waterflooding (High Sal/Low Sal) in Carbonate Reservoirs', *Paper SPE 154508 presented at the SPE Europec/EAGE Annual Conference*, SPE, 4-7 June, Copenhagen, Denmark.

[59] Yousef, A, Al-Saleh, S, Al-Kaabi, A, Al-Jawfi, M 2010, 'Laboratory Investigation of Novel Oil Recovery Method for Carbonate Reservoirs', *Paper SPE 137634 presented at the Canadian Unconventional Resources and International Petroleum Conference*, SPE, 19-21 October, Calgary, Alberta, Canada.

[60] Yousef, A, Al-Salehsalah, S, Al-Jawfi, M 2011, 'New Recovery Method for Carbonate Reservoirs through Tuning the Injection Water Salinity: Smart WaterFlooding', *Paper SPE 143550 presented at the SPE EUROPEC/EAGE Annual Conference and Exhibition*, SPE, 23-26 May, Vienna, Austria.

VITAE

Name:	Ahmed Amara Musa Kasha
Nationality:	Sudanese
Date of Birth:	21st of March 1987
Email :	musakasha@yahoo.com
Address:	Jabra North, Block 11, House No. 255 Khartoum, Sudan.

Academic Background:

- M.Sc. in Petroleum Engineering
  King Fahd University of Petroleum & Minerals, May 2014
  Dhahran, Saudi Arabia.

- B.Sc. in Petroleum Engineering
  University of Khartoum, August 2009
  Khartoum, Sudan.

Published Papers:

- Hassan B. Nimir, Kamal Abdalaziz and **Ahmed A. Kasha**. 2013, "*Rheological Properties of Guar Gum for Potential Use in Enhanced Oil Recovery in Sudanese Oil Fields*". University of Khartoum Engineering Journal Vol. 3 Issue 1, pp 39-45.
  http://ejournals.uofk.edu/index.php/engineering/article/view/348